Résumé

Ce mémoire traite du développement de récepteurs et de techniques d'estimation de canal pour les systèmes mobiles sans fil de type DS-CDMA multi-porteuse. Deux problèmes principaux doivent être pris en compte dans ce cas. Premièrement, l'Interférence d'Accès Multiple (IAM) causée par d'autres utilisateurs. Deuxièmement, les propriétés des canaux de propagation dans les systèmes radio mobiles.
Ainsi, dans la première partie du manuscrit, nous proposons deux structures adaptatives (dites détection séparée et détection jointe) pour la mise en œuvre de récepteurs minimisant l'erreur quadratique moyenne (MMSE), fondés sur un Algorithme de Projection Affine (APA). Ces récepteurs permettent de supprimer les IAM, notamment lorsque le canal d'évanouissement est invariant dans le temps. Cependant, comme ces récepteurs nécessitent les séquences d'apprentissage de chaque utilisateur actif, nous développons ensuite deux récepteurs adaptatifs dits aveugles, fondés sur un algorithme de type projection affine. Dans ce cas, seule la séquence d'étalement de l'utilisateur désiré est nécessaire. Quand les séquences d'étalement de tous les utilisateurs sont disponibles, un récepteur reposant sur le décorrélateur est aussi proposé et permet d'éliminer les IAM, sans qu'une période pour l'adaptation soit nécessaire.
Dans la seconde partie, comme la mise en œuvre de récepteurs exige l'estimation du canal, nous proposons plusieurs algorithmes pour l'estimation des canaux d'évanouissement de Rayleigh, variables dans le temps et produits dans les systèmes multi-porteuses. A cette fin, les canaux sont approximés par des processus autorégressifs (AR) d'ordre supérieur à deux. Le premier algorithme repose sur deux filtres de Kalman interactifs pour l'estimation conjointe du canal et de ses paramètres AR. Puis, pour nous affranchir des hypothèses de gaussianité nécessaires à la mise en œuvre d'un filtre optimal de Kalman, nous étudions la pertinence d'une structure fondée sur deux filtres H_∞ interactifs. Enfin, l'estimation de canal peut être vue telle un problème d'estimation fondée sur un modèle à erreur-sur-les-variables (EIV). Les paramètres AR du canal et les variances de processus générateur et du bruit d'observation dans la représentation de l'espace d'état du système sont dans ce cas estimés conjointement à partir du noyau des matrices d'autocorrélation appropriées.

Mot clés: DS-CDMA multi-porteuse, développement de récepteurs, filtrage adaptatif, canaux d'évanouissement de Rayleigh, estimation du canal, processus AR, filtrage de Kalman, filtrage H_∞, erreur-sur-les-variables.

Abstract

This dissertation deals with the development of receivers and channel estimation techniques for multi-carrier DS-CDMA mobile wireless systems. Two major problems should be taken into account in that case. Firstly, the Multiple Access Interference (MAI) caused by other users. Secondly, the multi-path fading of mobile wireless channels.
In the first part of the dissertation, we propose two adaptive structures (called separate and joint detection) to design Minimum Mean Square Error (MMSE) receivers, based on the Affine Projection Algorithm (APA). These receivers are able to suppress the MAI, particularly when the fading channel is time-invariant. However, as they require a training sequence for every active user, we then propose two blind adaptive multiuser receiver structures based on a blind APA-like multiuser detector. In that case, only the knowledge of the spreading code of the desired user is required. When the spreading codes of all users are available, a decorrelating detector based receiver is proposed and is able to completely eliminate the MAI without any training.
In the second part, as receiver design usually requires the estimation of the channel, we propose several training-based algorithms for the estimation of time-varying Rayleigh fading channels in multi-carrier systems. For this purpose, the fading channels are approximated by autoregressive (AR) processes whose order is higher than two. The first algorithm makes it possible to jointly estimate the channel and its AR parameters based on two-cross-coupled Kalman filters. Nevertheless, this filtering is based on restrictive Gaussian assumptions. To relax them, we investigate the relevance of a structure based on two-cross-coupled H_∞ filters. This method consists in minimizing the influence of the disturbances such as the additive noise on the estimation error. Finally, we propose to view the channel estimation as an Errors-In-Variables (EIV) issue. In that case, the channel AR parameters and the variances of both the driving process and the measurement noise in the state-space representation of the system are estimated from the null space of suitable correlation matrices.

Keywords: multi-carrier DS-CDMA, receiver design, adaptive filtering, Rayleigh fading channels, channel estimation, AR processes, Kalman filtering, H_∞ filtering, errors-in-variables.

Ali JAMOOS Contribution à la mise en œuvre de récepteurs et de techniques d'estimation de canal pour les systèmes mobiles DS-CDMA multi-porteuse 2007

Numéro d'ordre : 3382

THÈSE

PRÉSENTÉE À

L'UNIVERSITÉ BORDEAUX 1

ÉCOLE DOCTORALE DES SCIENCES PHYSIQUES ET DE L'INGÉNIEUR

PAR ALI JAMOOS

POUR OBTENIR LE GRADE DE

DOCTEUR

SPÉCIALITÉ : AUTOMATIQUE, PRODUCTIQUE, SIGNAL ET IMAGE

Contributions on Receiver Design and Channel Estimation for Multi-Carrier DS-CDMA Mobile Systems

---

Soutenue le 15 juin 2007

Après avis de :

MM.	NICOLAI CHRISTOV	Professeur à l'Université de Lille	*Rapporteurs*
	HANNA ABDEL NOUR	Professeur à l'Université Al-Quds, Jérusalem	

Devant la commission d'examen formée de :

MM.	MOHAMED NAJIM	Professeur à l'ENSEIRB, Bordeaux	
	NICOLAI CHRISTOV	Professeur à l'Université de Lille	
	HANNA ABDEL NOUR	Professeur à l'Université Al-Quds, Jérusalem	
	PIERRE BAYLOU	Professeur à l'ENSEIRB, Bordeaux	*Président*
	NASSER HAMAD	Professeur à l'Université Arab American, Jenin	
	ERIC GRIVEL	Maître de Conférences à l'ENSEIRB, Bordeaux	*Rapporteur de séance*

Equipe Signal et Image, Dpt LAPS IMS UMR CNRS 5218, Université Bordeaux 1
École Nationale Supérieure d'Electronique, Informatique et Radiocommunications de Bordeaux (ENSEIRB)
351 cours de la Libération - 33405 TALENCE cedex - France

– 2007 –

Dedication

I dedicate this work to my parents,
to my wife Intesar
and to my children Hasan and Hamzah

Acknowledgements

I would like to sincerely thank all of those who helped me during the period of this work.

Firstly, I would like to thank Prof. Mohamed Najim for giving me the opportunity to join his group and for his continuous support.

I would like to express my sincere gratitude to Dr. Eric Grivel for his guidance, encouragement, advices and insightful comments.

I would like to thank the reading committee: Prof. Nicolai Christov and Dr. Hanna Abdel Nour for the careful reading of this thesis and for their helpful comments. I would also like to thank the examination committee: Prof. Pierre Baylou and Dr. Nasser Hamad for agreeing to be on the board of examiners.

I would like to thank Prof. Roberto Guidorzi for the fruitful collaboration, helpful suggestions and insightful comments.

I would like to thank the members of our group for their support, advices and helpful suggestions. More particularly, I would like to thank David Labarre, William Bobillet and Julie Grolleau for the fruitful collaboration and the helpful discussions.

I would like to thank the Master students: Walid Hassasneh, Hutaf Ruwished and Ahmad Abdo at the faculty of enginnering/Al-Quds university for the research work they have carried out with me.

I would like to thank the Palestinian, Syrian and Arab friends in Bordeaux: Iyad saadeddin, Ismail Haj-Taha, Abdelrahman Meero, Saed Raji, Amer Shaban, Omar Abu-Sammour, Jamal Al-Sadi, Faisal Al-Mallouhi, Zakwan Qurit, Shadi Junid, Khalil Al-Rifai, Amjad Al-Halak, Mohammad Balousha, Bashar Jubeh. Thank you all for your support, for the nice activities and the nice memories we have in Bordeaux. Your friendship has made our life abroad a lot easier. I would also like to thank my friends in Palestine and all over the world for their concern.

I would like to thank the French Government and the consulate of France in Jerusalem for offering me a four year scholarship. More particularly, I would like to thank Mme Christine Laoue at the CROUS of Bordeaux.

My deep gratitude goes to my beloved family in Palestine, especially my parents for the endless support they have provided me with during my whole life.

At last but not least, I am deeply grateful to my wife Intesar for her advices, support and patience.

Abstract

This dissertation deals with the development of receivers and channel estimation techniques for multi-carrier DS-CDMA mobile wireless systems. Two major problems should be taken into account in that case. Firstly, the Multiple Access Interference (MAI) caused by other users. Secondly, the multi-path fading of mobile wireless channels.
In the first part of the dissertation, we propose two adaptive structures (called separate and joint detection) to design Minimum Mean Square Error (MMSE) receivers, based on the Affine Projection Algorithm (APA). These receivers are able to suppress the MAI, particularly when the fading channel is time-invariant. However, as they require a training sequence for every active user, we then propose two blind adaptive multiuser receiver structures based on a blind APA-like multiuser detector. In that case, only the knowledge of the spreading code of the desired user is required. When the spreading codes of all users are available, a decorrelating detector based receiver is proposed and is able to completely eliminate the MAI without any training.
In the second part, as receiver design usually requires the estimation of the channel, we propose several training-based algorithms for the estimation of time-varying Rayleigh fading channels in multi-carrier systems. For this purpose, the fading channels are approximated by autoregressive (AR) processes whose order is higher than two. The first algorithm makes it possible to jointly estimate the channel and its AR parameters based on two-cross-coupled Kalman filters. Nevertheless, this filtering is based on restrictive Gaussian assumptions. To relax them, we investigate the relevance of a structure based on two-cross-coupled H_∞ filters. This method consists in minimizing the influence of the disturbances such as the additive noise on the estimation error. Finally, we propose to view the channel estimation as an Errors-In-Variables (EIV) issue. In that case, the channel AR parameters and the variances of both the driving process and the measurement noise in the state-space representation of the system are estimated from the null space of suitable correlation matrices.

Keywords: multi-carrier DS-CDMA, receiver design, adaptive filtering, Rayleigh fading channels, channel estimation, AR processes, Kalman filtering, H_∞ filtering, errors-in-variables.

Résumé

Ce mémoire traite du développement de récepteurs et de techniques d'estimation de canal pour les systèmes mobiles sans fil de type DS-CDMA multi-porteuse. Deux problèmes principaux doivent être pris en compte dans ce cas. Premièrement, l'Interférence d'Accès Multiple (IAM) causée par d'autres utilisateurs. Deuxièmement, les propriétés des canaux de propagation dans les systèmes radio mobiles.

Ainsi, dans la première partie du manuscrit, nous proposons deux structures adaptatives (dites détection séparée et détection jointe) pour la mise en œuvre de récepteurs minimisant l'erreur quadratique moyenne (MMSE), fondés sur un Algorithme de Projection Affine (APA). Ces récepteurs permettent de supprimer les IAM, notamment lorsque le canal d'évanouissement est invariant dans le temps. Cependant, comme ces récepteurs nécessitent les séquences d'apprentissage de chaque utilisateur actif, nous développons ensuite deux récepteurs adaptatifs dits aveugles, fondés sur un algorithme de type projection affine. Dans ce cas, seule la séquence d'étalement de l'utilisateur désiré est nécessaire. Quand les séquences d'étalement de tous les utilisateurs sont disponibles, un récepteur reposant sur le décorrélateur est aussi proposé et permet d'éliminer les IAM, sans qu'une période pour l'adaptation soit nécessaire.

Dans la seconde partie, comme la mise en œuvre de récepteurs exige l'estimation du canal, nous proposons plusieurs algorithmes pour l'estimation des canaux d'évanouissement de Rayleigh, variables dans le temps et produits dans les systèmes multi-porteuses. A cette fin, les canaux sont approximés par des processus autorégressifs (AR) d'ordre supérieur à deux. Le premier algorithme repose sur deux filtres de Kalman interactifs pour l'estimation conjointe du canal et de ses paramètres AR. Puis, pour nous affranchir des hypothèses de gaussianité nécessaires à la mise en œuvre d'un filtre optimal de Kalman, nous étudions la pertinence d'une structure fondée sur deux filtres H_∞ interactifs. Enfin, l'estimation de canal peut être vue telle un problème d'estimation fondée sur un modèle à erreur-sur-les-variables (EIV). Les paramètres AR du canal et les variances de processus générateur et du bruit d'observation dans la représentation de l'espace d'état du système sont dans ce cas estimés conjointement à partir du noyau des matrices d'autocorrélation appropriées.

Mot clés: DS-CDMA multi-porteuse, développement de récepteurs, filtrage adaptatif, canaux d'évanouissement de Rayleigh, estimation du canal, processus AR, filtrage de Kalman, filtrage H_∞, erreur-sur-les-variables.

Contents

Introduction

Multi-Carrier Direct-Sequence Code Division Multiple Access (MC-DS-CDMA) is a multiplexing technique that combines the advantages of both multi-carrier modulation and DS-CDMA [Har97]. Among them, high system flexibility, high data rate transmission, high bandwidth efficiency and fading resilience can be pointed out. Adopted as an option for the down-link transmission in the CDMA2000 third Generation (3G) cellular standard [CDM01], MC-DS-CDMA is also one of the potential candidates for the future fourth Generation (4G) broadband wireless systems [Han03]. When designing receivers for MC-DS-CDMA mobile wireless systems, two main problems must be taken into account. Firstly, the Multiple Access Interference (MAI) caused by other active users greatly limits the system capacity, especially when the received signal power of the desired user is less than that of other users (i.e. the "near-far" problem). Secondly, the multi-path fading of mobile radio channels which highly degrades the system Bit Error Rate (BER) performance. More particularly, due to user mobility, each carrier is subject to Doppler shifts resulting in time-varying fading. Thus, the estimation of the fading process over each carrier is essential to achieve optimal diversity combining and coherent symbol detection at the receiver.

Therefore, in this dissertation, our objective is twofold. Firstly, we aim at designing new receivers for MC-DS-CDMA systems that are able to suppress the MAI and to mitigate the near-far problem. Secondly, as receiver design usually requires the explicit channel estimation, we intend to develop new techniques to estimate time-varying fading channels.

In the first chapter, we provide a general presentation of MC-DS-CDMA mobile wireless systems in Rayleigh fading channels. Among the various combinations of DS-CDMA and multi-carrier transmission, we focus our attention on the time-domain spreading based MC-DS-CDMA scheme proposed by Kondo *et al.* [Kon96]. It should be noted that this scheme is different from the so-called MC-CDMA which is based on frequency-domain spreading [Har97]. Once the MC-DS-CDMA transmitter model is detailed, the channel model is introduced. By suitably choosing the number of carriers and their spacing, each

carrier is assumed to undergo independent frequency non-selective fading. In addition, we study time-varying fading channels which is not the case in [Kon96], where the fading channels are assumed to be time-invariant. The time-variation of the fading process over each carrier is usually modeled by a zero-mean Wide Sense Stationary (WSS) complex Gaussian process. In addition, according to the Jakes model [Jak74], its theoretical Power Spectral Density (PSD) is band-limited, U-shaped and exhibits twin peaks at $\pm f_d$, where f_d is the maximum Doppler frequency. The corresponding normalized discrete-time AutoCorrelation Function (ACF), denoted by $R_{hh}(n)$, is a zero-order Bessel function of the first kind namely $R_{hh}(n) = J_0(2\pi f_d T_b|n|)$, where T_b is the bit duration.
In recent papers [Bad05] [Kom02] [Lin02], the channel has been modeled as a p^{th} order autoregressive process denoted by AR(p). Using low-order AR model for the channel is debatable. On the one hand, some authors (e.g., [Kom02], [Lin02]) motivate this approximation arguing for the model simplicity, especially for AR(1) or AR(2) process, and its usefulness for channel estimation. On the other hand, from a theoretical point of view, according to Kolmogoroff-Szego formula [Pap02], a deterministic model should be used for the channel due to the band-limited nature of its PSD. In between solutions have also been studied. Firstly, a sub-sampled AR Moving Average (ARMA) process followed by a multistage interpolator has been considered for channel simulation [Sch01]. Nevertheless, only a very high down-sampling factor leads to a PSD which is never equal to 0. Secondly, Baddour *et al.* [Bad05] have suggested using high-order AR processes (e.g., $p \geq 50$) for channel simulation[1]. To allow the estimation of the corresponding AR parameters, they "slightly" modify the properties of the channel by considering the sum of the theoretical fading process and a zero-mean white process whose variance ϵ is very small (e.g., $\epsilon = 10^{-7}$ for $f_d T_b = 0.01$). At that stage, the AR parameters are estimated with the Yule-Walker (YW) equations based on the modified ACF namely $R_{hh}^{mod}(n) = J_0(2\pi f_d T_b|n|) + \epsilon\delta(n)$. So, by taking into account the above results, an AR model whose order is high enough will be considered in this thesis to approximate the channel fading process.

The conventional MC-DS-CDMA receiver [Kon96] consists of a correlator along each carrier followed by a Maximal Ratio Combiner (MRC). However, this approach cannot eliminate the MAI and, hence, is not "near-far resistant". In addition, the channel fading processes are assumed to be perfectly known at the receiver, which is not the case in practice. Therefore, our purpose in chapter 2 is to design receivers that are able to suppress

[1]It should be noted that this method was investigated and compared with sum-of-sinusoids based channel simulators presented in [Den93] [Zhe03] by an ERASMUS Spanish student who was co-supervised by Dr. E. Grivel and myself.

the MAI and to counteract the effect of fading. More particularly, we first focus our attention on designing adaptive Minimum Mean Square Error (MMSE) receivers. In the framework of MC-CDMA, Kalofonos *et al.* [Kal03] have proposed to adaptively implement the so-called "MMSE per user" receiver by means of the Least Mean Square (LMS) or Recursive Least Square (RLS) algorithms. In [Mil00b], Miller *et al.* have developed the optimal MMSE receiver for asynchronous MC-DS-CDMA systems. However, as its computational cost is very high, it may be difficult to be implemented in practice. To reduce the computational cost, we propose two adaptive MMSE receiver structures based on the Affine Projection Algorithm (APA) [Jam04]. The so-called "Separate Detection" (SD) scheme consists in using a particular adaptive filter structure for each carrier, whereas the so-called "Joint Detection" (JD) scheme is based on a joint structure defined by the concatenation of the adaptive filter weights dedicated to each carrier. We carry out a comparative study between both structures with various adaptive filters such as the RLS, the Normalized LMS (NLMS) and the APA[2].

However, these adaptive receivers require a training sequence for every active user. To avoid them, we propose two blind adaptive multiuser receiver structures [Jam05a], where only the spreading waveform and the timing of the desired user are required. The first receiver provides a blind adaptive multiuser detector for each carrier followed by a post-detection combiner, while the second receiver consists of a pre-detection combiner followed by a single blind adaptive multiuser detector. To complete the design of these receivers, we have proposed a blind APA-like multiuser detector [Jam05a]. This detector can be seen as a generalization of the blind LMS-based detector [Hon95], on the basis of multiple delayed input signal vectors. A comparative study is then carried out with existing blind adaptive multiuser detectors based on LMS [Hon95] or Kalman filter [Zha02], initially developed for single-carrier DS-CDMA systems.

When the spreading waveforms and the timing of all users are available, we then extend the decorrelating multiuser detector based receiver initially developed for single-carrier DS-CDMA [Wu00] to the multi-carrier case [Jam05b]. The resulting receiver consists of a decorrelating detector and a Kalman filter based channel estimator followed by a MRC [Jam05b]. It has the advantage of completely eliminating the MAI while working in time-varying fading channels.

[2]It should be noted that in [Ruw06], one of the master students at Al-Quds University-Palestine, currently under the supervision of Dr. H. Abdel Nour and myself, has proposed to study the relevance of variable step-size NLMS and APA [Shi04] to implement the SD and JD receiver structures. These algorithms can indeed meet the conflicting requirement of fast convergence and low misadjustment error.

In chapter 3, as receiver design usually requires the explicit estimation of fading channels, we aim at developing channel estimation algorithms for autoregressive time-varying Rayleigh fading channels. More particularly, our purpose is to develop training sequence based methods that make it possible to estimate the channel AR parameters without any *a priori* information about the maximum Doppler frequency f_d. Among the existing methods, Tsatsanis *et al.* [Tsa96] suggest estimating the AR parameters from the channel covariance estimates by means of a YW estimator. However, the method results in biased estimates. Other approaches initially developed in other fields than wireless communications can be considered. Among them, a bias-correction least-square technique has been presented by Zheng [Zhe99], while Davila [Dav98a] has proposed to solve the so-called noise-compensated YW equations by using a subspace based method. Nevertheless, these methods require a long observation window and do not necessarily provide reliable estimates when the signal-to-noise ratio is low. As an alternative, the Expectation-Maximization (EM) algorithm which often implies a Kalman smoothing can be used [Der94]. However, since it operates repeatedly on a batch of data, it results in large storage requirements and high computational cost. In addition, its success depends on the initial conditions. As an alternative, two recursive filters can be cross-coupled to solve the so-called dual estimation issue [And79], i.e. the estimations of both the AR process and its parameters. Each time a new observation is available, the first filter uses the latest estimated AR parameters to estimate the signal, while the second filter uses the estimated signal to update the AR parameters. According to Gannot *et al.* [Gan98], this approach can be viewed as a sequential version of the EM algorithm. Recently, in [Lab06b], a variant based on two interacting Kalman filters has been developed in which the variance of the innovation process in the first filter is used to define the gain of the second filter. Since this solution can be seen as a recursive Instrumental Variable (IV) technique, consistent estimates of the AR parameters are obtained. Then, this technique has been tested in the framework of speech enhancement [Lab04] [Lab06a].
In this thesis, we propose to take advantage of the two-cross-coupled Kalman filter based structure to jointly estimate the fading channel and its AR parameters over each carrier in MC-DS-CDMA systems [Jam05c]. It should be noted that the estimation of MC-DS-CDMA fading channels based on Kalman filtering is also studied in [Has06][3], where the relevance of high-order AR models is investigated. Using Kalman filtering is of interest, but several assumptions must be fulfilled. Thus, Kalman filtering is optimal in

[3]This study was carried out by one of the master students at Al-Quds University-Palestine who was under the supervision of Dr. H. Abdel Nour and myself.

the H_2 sense providing the underlying state-space model is accurate. In addition, the initial state, the driving process and the measurement noise must be independent, white and Gaussian. However, in real cases, these assumptions may no longer be satisfied. For this reason, we propose to investigate the relevance of an alternative approach based on H_∞ filtering, initially developed in the field of control (see, e.g., [Has99]). This filtering aims at minimizing the worst possible effects of the disturbances (e.g., the additive measurement noise) on the estimation error. The approach we propose in this thesis, recently developed in the framework of speech enhancement [Lab07], is based on two-cross-coupled H_∞ filters which makes it possible to jointly estimate the fading process and its AR parameters [Jam07b]. It should be noted that our approach is different from the approach presented in [Cai04] where two H_∞ filters are serially-connected. In the latter, a biased estimation of the AR parameters is expected since the first H_∞ filter estimates the AR parameters directly from the noisy observations.
However, when using the two-cross-coupled Kalman and H_∞ filter based channel estimators, the variance and the power of the measurement noise is assumed to be known, respectively. As an alternative, we propose to view the estimation of the channel AR parameters as an Errors-In-Variables (EIV) issue [Jam06]. In the EIV models [Huf02], initially developed in the fields of statistics and identification, the available data are assumed to be disturbed by additive error or noise terms. The method we present in this thesis, originally developed in the framework of control [Beg90] [Div05b] [Div05a] and derived for speech enhancement in [Bob07], consists in searching the noise variances that enable specific noise compensated autocorrelation matrices of observations to be positive semidefinite [Jam06] [Jam07a]. In addition, the AR parameters can be estimated from the null spaces of these matrices. Once these parameters are estimated, Kalman or H_∞ filtering can be carried out to estimate the fading process.

It should be noted that this PhD thesis is the first one dealing with mobile communication systems in the Signal and Image Group (ESI) at the UMR CNRS 5218 IMS in Bordeaux. It results from the collaboration of both Dr. H. Abdel Nour (Al-Quds University-Palestine) and ESI to exchange more and to address this new topic, through two Integrated Action Projects (IAP) promoting interaction between Palestinian and French Universities. In addition, the various approaches we proposed in chapter 3 were the fruit of collaborations with Prof. R. Guidorzi (Bologna University-Italy), Prof. N. Christov (Lille University-France) and PhD students D. Labarre, W. Bobillet, J. Grolleau at the ESI under the supervision of Dr. E. Grivel and Prof. M. Najim.

Chapter 1

Multi-Carrier DS-CDMA Mobile Wireless Systems

Contents

1.1 Motivation

Over the past decade, the mobile wireless communication industry has experienced rapid growth in the number of mobile subscribers and the amount of traffic. This is due to the increasing demand for high data rate multimedia services. Therefore, the current 3G mobile wireless systems have been designed to provide a wide range of multimedia applications such as voice, image and data transmission with different and variable bit rates up to 2 Mbit/s. The demand for higher data rates is expected to continue for the incoming years since more applications are emerging such as mobile wireless internet and interactive multimedia services. To satisfy these requirements in the Beyond 3G (B3G) and the 4G mobile wireless systems, one of the main challenges is the choice of the multiple access technology that will efficiently share the available scarce bandwidth among a large number of users [Han03] [Jma05].

1.1.1 Multiple access techniques from 1G to 3G mobile systems

Traditionally, mobile wireless communication systems have employed Frequency Division Multiple Access (FDMA) and Time Division Multiple Access (TDMA) techniques to share the available bandwidth among many subscribers [Rap01] [Stu01]. With FDMA technique, the allocated spectrum is divided into several frequency bands where each frequency band is assigned to a single user. Multiple users using separate frequency bands can access the same system at the same time without significant interference from other users concurrently operating in the system. When using TDMA, the time-domain transmission frame is periodically divided into time slots, each assigned to a single user to transmit data information, employing the total allocated bandwidth.

The first Generation (1G) mobile wireless systems, developed in the 1980s, used FDMA as their multiple access scheme. These systems were analog and dedicated only to voice applications. The Advanced Mobile Phone Service (AMPS) in USA and the Total Access Communication System (TACS) in Europe are examples of the 1G mobile wireless systems. In the 1990s, various second Generation (2G) mobile wireless systems were developed such as the Global System for Mobile communications (GSM) in Europe and the Personal Digital Cellular (PDC) system in Japan. Most of these systems employed TDMA as their multiple access scheme. They provide both voice services and low rate data communication services. It should be noted that TDMA is also used in the evolved 2.5G standards from the 2G GSM standard, namely the General Packet Radio Service

(GPRS) and the Enhanced Data rates for GSM Evolution (EDGE) systems. They use packetized data transmission and provide much higher data rates than the 2G systems.

Nevertheless, in both FDMA and TDMA techniques the number of frequency bands or time slots is fixed for a given system, and a single frequency band/time slot is allocated to a single user for the whole period of communications. A fixed frequency band or time slot assignment can guarantee the service quality for real-time and constant-bit-rate voice telephony, which was the main service at that time. However, as the number of services is increasing from simple voice to multimedia traffic (voice, audio, data, images, video) with different needs, fixed frequency band or time slot assignment has shown its lack of efficiency in utilizing the scarce spectrum, especially with the exponential increase in the number of users. To satisfy these requirements, Code Division Multiple Access (CDMA) scheme, based on spread spectrum technology, has emerged [Vit95]. In CDMA systems with Direct Sequence (DS) spectrum spreading (DS-CDMA), the relatively narrow-band users information is spread into a much wider spectrum using a high chip rate spreading code. When using different codes, multiple user information can be transmitted on the same allocated spectrum at the same time and without significant difficulty to detect the desired signal at the receiver. The spreading code of each user is either orthogonal to the codes of all other users or has suitable cross-correlation properties that minimize the MAI caused by other users. As long as the total power of the MAI is less than a threshold, it is possible to detect the desired user signal by using his spreading code which is only known by the intended receiver (e.g., the RAKE receiver [Pro95]). Therefore, CDMA is a dynamic multiple access scheme that has no rigid resource allocation limitation for individual users whereas this is not the case in TDMA and FDMA. In addition, unlike TDMA and FDMA systems, the number of users in a CDMA system is not fixed and a new user can be added to the system at any time. For an insightful comparative study between these multiple access techniques, the reader may refer to [Bai96].

CDMA, originally used for military applications, was first used for civilian mobile communications by Viterbi Qualcomm Inc. This led to the IS-95 2G digital mobile standard [IS-95] in USA. With the exponential increase in the number of users for mobile communications, CDMA, with its proven capacity enhancement over TDMA and FDMA [Bai96], has been chosen as the main multiple access scheme for 3G mobile cellular systems. Examples of such systems are the Universal Mobile Telecommunications System (UMTS) in Europe and the CDMA2000 [CDM01] in USA, both members of the International Mobile Telecommunications-2000 (IMT-2000). They are designed to provide a wide range of broadband multimedia services with variable bit rate up to 2Mbit/s.

Table 1.1: Evolution of mobile wireless systems.

Generation	Services	Multiple access	Standard	Data rate
1G	analog voice	FDMA	AMPS, TACS	1.9 Kbit/s
2G	digital voice, short messages	TDMA, CDMA	GSM, IS-95	14.4 Kbit/s
2.5G	high capacity packetized data	TDMA, CDMA	GPRS, EDGE	384 Kbit/s
3G	broadband data, multimedia	WCDMA, MC/CDMA	UMTS, CDMA2000	2 Mbit/s
B3G/ 4G	interactive multimedia, mobile internet	"to be defined"	"to be defined"	100 Mbit/s

A summary on the evolution of mobile wireless systems is presented in Table 1.1. For more details about the early mobile generations, the reader may refer to the survey paper [Han98] and references therein. For later mobile generations, the reader may read [Tac03]. It should be noted that the data rates indicated in Table 1.1 are for fixed terminals. The status of current wireless systems when taking into account terminal mobility and data rates is depicted in Figure 1.1. As an example, the 3G UMTS wireless system provides 2 Mbit/s for indoor fixed or very slow terminals, 384 Kbit/s for outdoor mobile terminals traveling at speeds less than the vehicular speed (120Km/h), and up to 144 Kbit/s for fast mobile terminals traveling at speeds more than the vehicular speed.

According to Figure 1.1, the current data rates of 3G systems for high speed mobile terminals are insufficient. Therefore, providing high data rates to high speed mobile terminals is a major challenge for the future B3G and 4G mobile wireless systems. These systems, to be defined in the coming few years, are expected to offer up to 100 Mbit/s for stationary terminals and up to 20 Mbit/s for vehicular speed mobile terminals. Such high data rates are necessary to provide services like interactive multimedia, mobile wireless internet, etc.

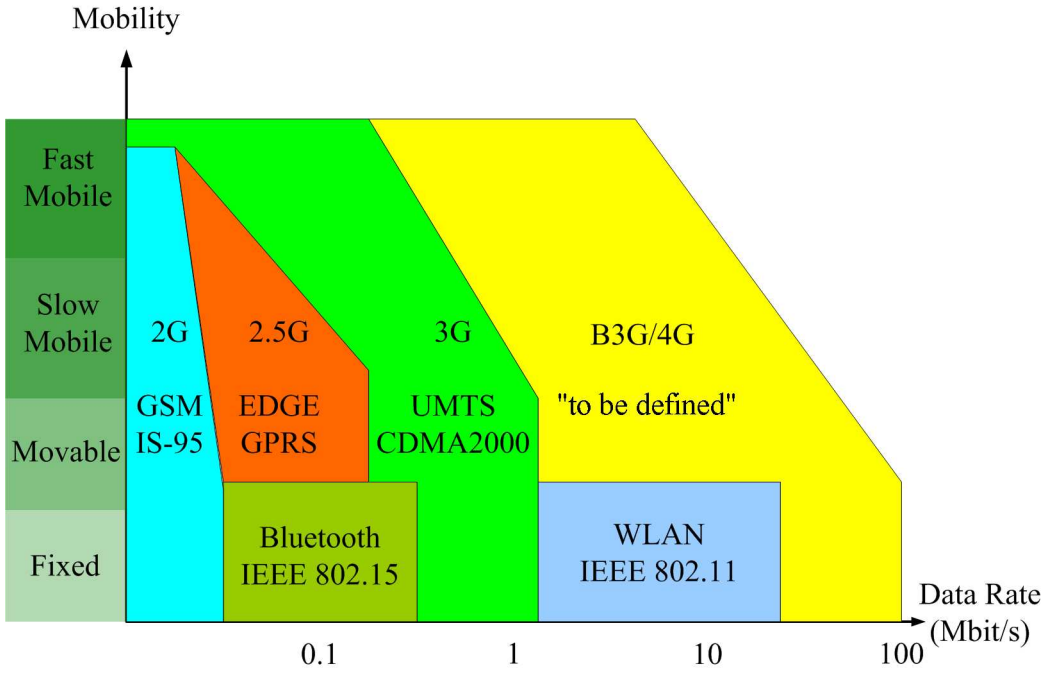

Figure 1.1: Mobility versus data rate for current mobile wireless systems.

1.1.2 Multi-carrier DS-CDMA as a candidate for future mobile systems

To support the requirements of the new emerging high data rate multimedia services, several techniques have been studied for the last years. One of these techniques is the combination of CDMA with Orthogonal Frequency Division Multiplexing (OFDM), referred to as multi-carrier CDMA [Har97] [Wan00]. OFDM [Bin90] is a parallel data transmission scheme in which high data rates can be achieved by the simultaneous transmission over many orthogonal carriers. This multi-carrier transmission scheme makes it possible to convert the severe wide-band frequency-selective fading channel into a large number of frequency non-selective flat fading sub-channels[1].

Thus, the combination of CDMA with OFDM makes it possible to get benefit from the advantages of both schemes [Har97] [Han03]. High system flexibility, high data rate transmission, high spectral efficiency, fading resilience and narrow-band interference suppression capability are some of these adavantages. Various combinations of CDMA with OFDM have been proposed simultaneously and independently by several authors in the year 1993 [Kon93] [Faz93b] [Faz93a] [Yee93] [Cho93] [Das93] [Van93]. In [Har97], the authors have compared these various combinations. They have identified three different

[1]These types of fading will be illustrated in subsection 1.3.1.

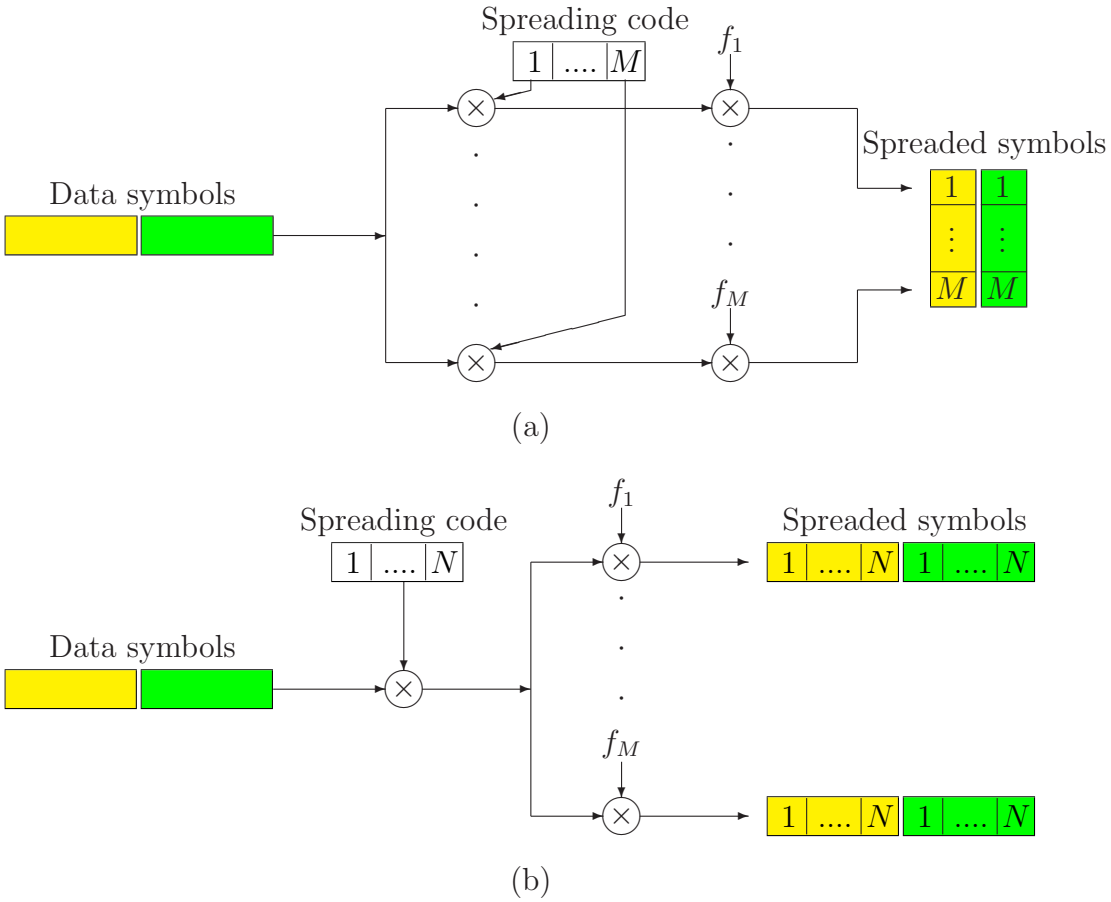

Figure 1.2: (a) MC-CDMA: frequency-domain spreading. (b) MC-DS-CDMA: time-domain spreading. $\{f_m\}_{m=1,\cdots,M}$ denote the carrier frequencies.

structures. Namely, Multi-Carrier CDMA (MC-CDMA) using frequency-domain spreading [Faz93b] [Faz93a] [Yee93] [Cho93], Multi-Carrier Direct-Sequence CDMA (MC-DS-CDMA) using time domain-spreading [Kon93] [Das93] and Multi-Tone CDMA (MT-CDMA) [Van93].

Based on their signal spreading mode, multi-carrier CDMA schemes can now be categorized into three types, as follows:

- **MC-CDMA scheme using frequency-domain spreading**

  This scheme combines OFDM and frequency-domain spreading [Faz03]. A data symbol is first replicated into several parallel copies. Each copy is then multiplied by a chip from a spreading code and modulates one carrier frequency as shown in Figure 1.2(a). The number of carriers M is equal to the code length.

- **MC-DS-CDMA scheme using time-domain spreading**

  In the MC-DS-CDMA system proposed by Kondo *et al.* [Kon93] [Kon96], the data

sequence multiplied by a spreading code of length N modulates several band-limited carriers (see Figure 1.2(b)). The signal transmitted over each carrier is similar to that of the conventional narrow-band single-carrier DS-CDMA scheme. To guarantee independent flat fading on each carrier, the number of carriers and their spacing have to be carefully chosen.

Another MC-DS-CDMA scheme which first performs serial-to-parallel conversion on the input data stream before spreading has been studied in [Das93] [Das94] [Sou96]. In this scheme, the original data stream is first serial-to-parallel converted into several low-rate streams. Then, each of these low-rate streams is spread in the time-domain and modulates several carriers. This scheme is more general than the previous one [Kon96] and can provide higher data rates.

In [Han03], Hanzo *et al.* have carried out a comparative study between single-carrier DS-CDMA, MC-CDMA and MC-DS-CDMA schemes when designing a broadband multiple access systems. According to their study, MC-DS-CDMA provides a trade-off between single-carrier DS-CDMA and MC-CDMA in terms of the system architecture and performance. Thus, MC-DS-CDMA requires lower chip rate spreading codes than single-carrier DS-CDMA since multiple carriers are employed. In addition, as time-domain spreading over each carrier signal is used, it needs a much lower number of carriers than MC-CDMA. Furthermore, MC-DS-CDMA guarantees that each carrier signal undergoes independent fading and, hence, maximizes the frequency diversity gain. This is not the case when using MC-CDMA where the carrier signals might be correlated. Moreover, compared with single-carrier DS-CDMA and MC-CDMA, MC-DS-CDMA has more parameters that can be adjusted such as the chip-duration of the time-domain spreading code, the number of bits involved in the serial-to-parallel conversion and the spacing between two adjacent carriers. Therefore, by adjusting these parameters, the MC-DS-CDMA scheme can support ubiquitous broadband wireless communications [Yan03a].

- **MC-DS-CDMA scheme using Time-domain and Frequency-domain spreading (TF-domain spread MC-DS-CDMA)**

  The TF-domain MC-DS-CDMA system [Yan03a] [Yan03b] [Han03] spreads the input data stream using two signature codes, where one of the signature codes corresponds to the time-domain spreading, while the other is dedicated to frequency-domain spreading. Therefore, this system can be seen as a hybrid of MC-CDMA and MC-DS-CDMA schemes. Hence, it has the advantages of both.

Thus, due to the attractive features of MC-DS-CDMA, it has been adopted as an option for the down-link transmission in the CDMA2000 3G mobile cellular standard [CDM01]. The so-called MC mode in CDMA2000 has been considered to provide an evolution path form existing IS-95 systems, where three carriers (known also as 3X mode), each having the same characteristics as the IS-95 (1X mode) carrier, are involved. It should be noted that MC-DS-CDMA is still one of the promising candidates for the 4G broadband mobile wireless systems [Yan03a]. Therefore, this thesis will focus on MC-DS-CDMA systems and more particularly on the MC-DS-CDMA system presented in [Kon96].

In the following sections, we will study the transmitter model, the channel model and the conventional receiver of this system.

1.2 Transmitter model

In this section, we adopt the transmitter model of the MC-DS-CDMA system presented in [Kon96]. In this model, a binary data sequence multiplied by a spreading sequence modulates M carriers, as shown in Figure 1.3. Assuming that there are K simultaneous users in the system, the transmitted signal of the k^{th} user can be expressed as follows:

$$s_k(t) = \mathrm{Re}\left(\sum_{n=-\infty}^{+\infty} \sum_{m=1}^{M} \sqrt{2P_k} d_k(n) c_k(t - nT_b) e^{j2\pi f_m t} \right) \tag{1.1}$$

where P_k is the transmitted power for each carrier of the k^{th} user signal, $d_k(n) \in \{\pm 1\}$ is the n^{th} Binary Phase Shift Keying (BPSK) modulated data bit of the k^{th} user, T_b is the bit duration and f_m is the m^{th} carrier frequency. In addition, the spreading waveform of the k^{th} user is given by:

$$c_k(t) = \sum_{i=0}^{N-1} c_{ki} \psi(t - iMT_c) \tag{1.2}$$

where $\psi(t)$ is the the chip pulse shape, T_c is the chip duration of a wide-band single-carrier system occupying the same bandwidth as the multi-carrier system, MT_c is the chip duration of the multi-carrier system, $N = T_b/MT_c$ is the processing gain, $c_{ki} \in \{\pm 1/\sqrt{N}\}$ denotes the normalized i^{th} chip of the k^{th} user spreading code $\mathbf{c}_k = [\ c_{k0} \quad c_{k1} \quad \cdots \quad c_{k(N-1)}\ ]^T$. The spreading codes $\{\mathbf{c}_k\}_{k=1,2,\cdots,K}$, known also as Pseudo-Noise (PN) sequences, are characterized by their lengths, autocorrelation and cross-correlation properties [Din98]. They are designed to have very low cross-correlations either between the codes themselves or their shifted versions. This enables the receiver to separate different user signals and to reduce the MAI. The most known spreading codes are the maximal-length or m-sequences,

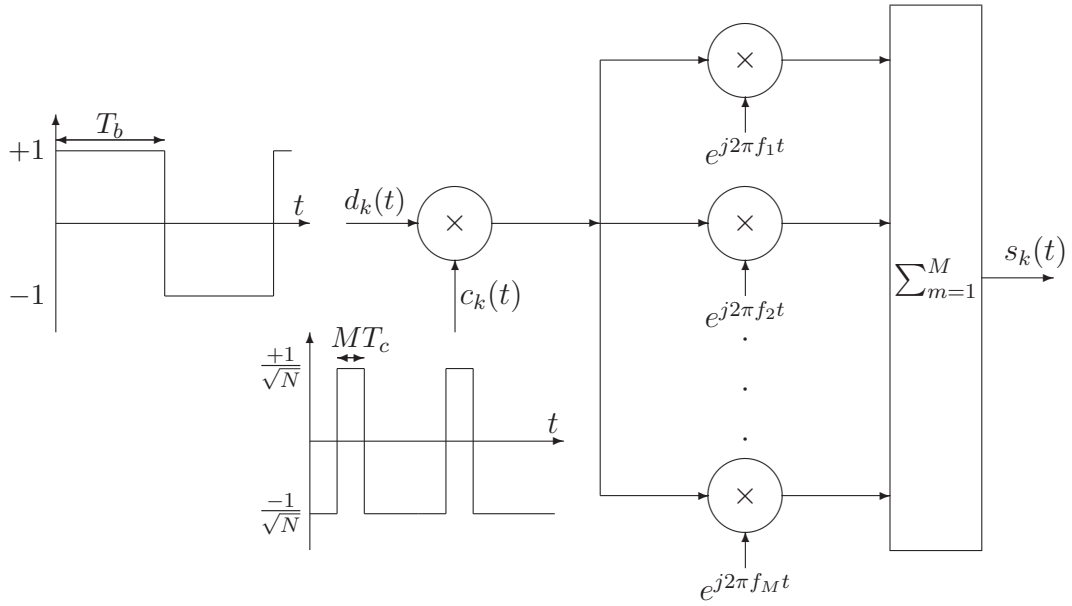

Figure 1.3: The MC-DS-CDMA transmitter of user k.

Gold and Kasami sequences [Din98]. In this thesis, we will use the Gold code sequences as they provide very low cross-correlation between different codes. In addition, they make it possible to generate a larger set of spreading sequences than the m-sequences[2].

In (1.2), the chip pulse shape $\psi(t)$ is normalized to have a unit energy. In addition, it is assumed to be band-limited to $[-W_M/2, W_M/2]$ and satisfies the Nyquist criterion, where W_M is the bandwidth of each carrier signal (see Figure 1.4(a)). This implies that there will be no inter-chip interference at the receiver.

In a multi-carrier system, the carrier frequencies are usually selected to be orthogonal to each other after spreading [Han03], as follows:

$$\int_0^{MT_c} e^{j2\pi f_l t} \cdot e^{j2\pi f_m t} dt = 0, \quad \text{for } l \neq m \tag{1.3}$$

This is done so that the signal in the l^{th} frequency band does not cause interference on the m^{th} frequency band at the receiver. Given (1.3), the minimum frequency spacing between two adjacent carriers satisfies:

$$\Delta f = f_{m+1} - f_m = 1/(MT_c) \tag{1.4}$$

[2]It should be noted that each Gold sequence in a set is generated from two m-sequences by the modulo-2 addition of one m-sequence with another cyclically shifted m-sequence.

Figure 1.4(a) shows the spectrum of an orthogonal multi-carrier narrow-band DS-CDMA signals each with bandwidth W_M given by:

$$W_M = \frac{W_0}{M} = (1+\chi)\frac{1}{MT_c} \tag{1.5}$$

where $0 < \chi \leq 1$ and $W_0 = (1+\chi)(1/T_c)$ is the bandwidth of a wide-band single-carrier DS-CDMA system occupying the same bandwidth as the multi-carrier system.
In a multi-carrier system, the over-all bandwidth W_0 is divided into M equal width frequency bands as shown in Figure 1.4. Hence, by using multi-carrier modulation, a wide-band DS-CDMA signal can be replaced by several narrow-band DS-CDMA signals. Consequently, if the processing gain of a wide-band single-carrier system is $N_0 = T_b/T_c$, the processing gain of each carrier signal is then $N = T_b/MT_c$ and the composite processing gain of this multi-carrier system is $MN = N_0$.

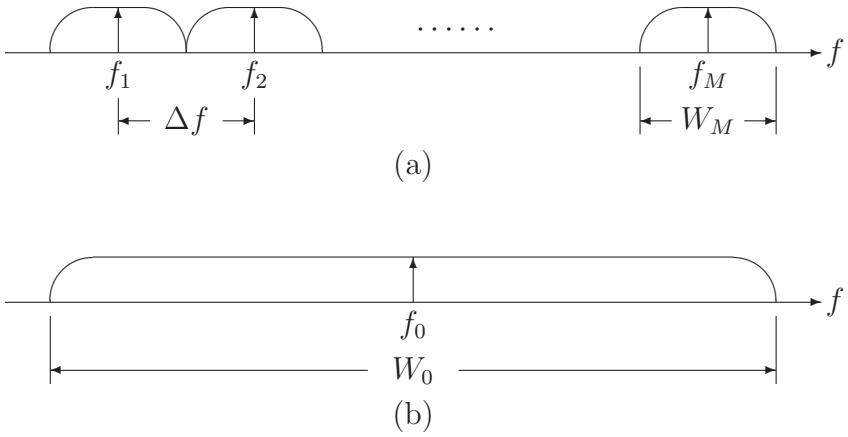

Figure 1.4: (a) PSD of multi-carrier DS-CDMA signal. (b) PSD of wide-band single-carrier DS-CDMA signal.

This multi-carrier system has the following main advantages. Firstly, it has a narrow-band interference suppression capabilities. Secondly, as the entire bandwidth of the system is divided into M equal width frequency bands, lower chip rate is required for each band. Therefore, the multi-carrier system requires a lower speed parallel-type of signal processing, in contrast to a fast serial-type of signal processing in the wide-band single-carrier system. This may be helpful when designing a low-power consumption devices. Thirdly, the multi-carrier system is robust to multi-path fading by providing a frequency diversity gain equal to the number of carriers. This diversity gain is achieved by converting the severe frequency-selective fading encountered in the wide-band single-carrier DS-CDMA system to independent frequency non-selective flat fading over each carrier in the multi-carrier DS-CDMA system. These types of fading will be discussed in the next section.

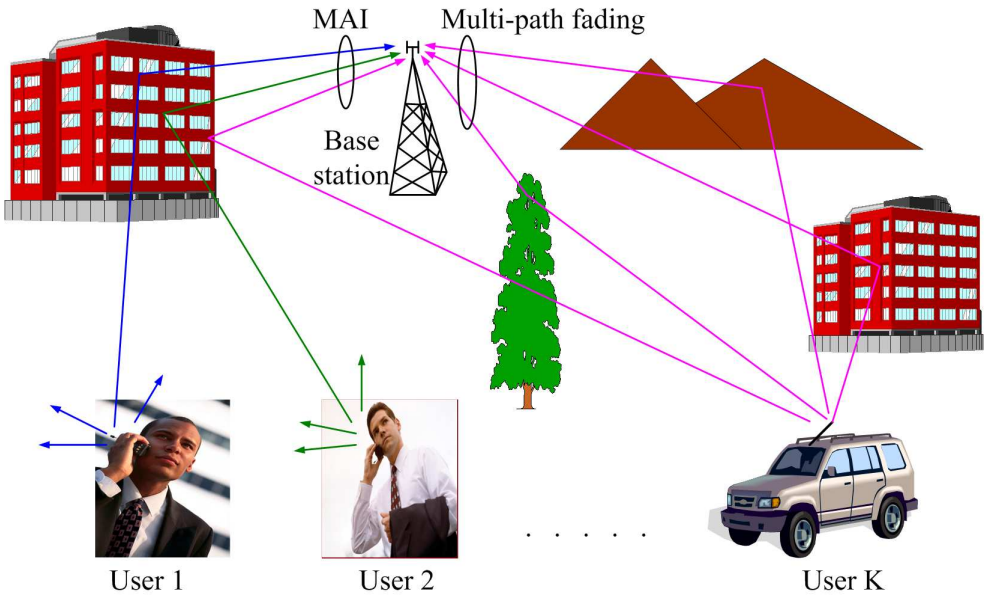

Figure 1.5: Multi-path fading in CDMA systems.

1.3 Channel characteristics and modeling

In mobile communications, the transmitted signal arrives at the receiver from a number of different propagation paths, referred to as multi-paths as shown in Figure 1.5. These paths arise due to reflection, diffraction, and scattering of the transmitted electromagnetic wave from objects such as buildings, hills, trees, etc. that lie in the vicinity of the mobile station and/or base station. Multi-path propagation results in a received signal that is a superposition of several delayed and attenuated copies of the transmitted signal. This gives rise to frequency-selective fading which spreads the transmitted signal in time and, hence, leads to the so-called Inter-Symbol Interference (ISI). When all multi-paths arrive at the receiver within the symbol duration, the resulting fading is called frequency non-selective fading or flat fading. In addition to multi-path fading, due to the relative motion between the transmitter and the receiver and/or the movement of surrounding objects, the received signal is subject to Doppler shifts. This gives rise to time-varying fading. Hence, the transmitted signal through a mobile wireless channel may be generally affected by time-varying frequency-selective fading.

A simple way to model the fading phenomenon was introduced by Bello [Bel63], where he proposed the notion of Wide-Sense Stationary (WSS) uncorrelated scattering. In that model, the transmitted signal propagates through a large number of paths. Each is characterized by its own random amplitude, phase and delay. The signal variations

arriving from these paths with different delays are WSS and uncorrelated. With such a model, Bello [Bel63] was able to define functions that can describe the fading channel in time as well as in frequency. The main functions are the Doppler power spectrum and the delay power spectrum (also known as power delay profile). The Doppler power spectrum gives the average power of the channel output as a function of the Doppler frequency, whereas the delay power spectrum provides the average power of the channel output as a function of the delay. These functions are characterized by some parameters. One of these is the maximum delay spread, denoted by T_m and defined as the range of values over which the delay power spectrum is non-zero. Another important parameter is the maximum Doppler spread or frequency, denoted as f_d and defined as the range of values over which the Doppler power spectrum is non-zero. Moreover, the channel coherence time T_0 is inversely proportional to the maximum Doppler frequency, i.e. $T_0 = 1/f_d$. It is a measure of how rapidly the channel impulse response varies with time. The channel coherence bandwidth B_c is the width of the band of frequencies which are similarly affected by the channel. Thus, this parameter provides a measure of the channel frequency selectivity. It should be noted that the channel coherence bandwidth is inversely proportional to the channel maximum delay spread:

$$B_c \approx 1/T_m \tag{1.6}$$

The types of fading experienced by a signal propagating through a mobile radio channel depend on the nature of the transmitted signal and the characteristics of the channel [Pro95] [Rap01]. While multi-path delay spread leads to time dispersion and frequency-selective fading, Doppler spread leads to frequency dispersion and time-selective (time-varying) fading. Both dispersion mechanisms are independent of one another. These types of fading are investigated in the next subsections.

1.3.1 Frequency-selective versus frequency non-selective fading

The classification of the fading channel as frequency-selective or frequency non-selective depends on the relationship between the transmitted signal bandwidth W and the channel coherence bandwidth B_c. Thus, the fading channel is called frequency-selective when W is much larger than B_c, i.e. $W \gg B_c$. In that case, the different frequency components of the transmitted signal will experience different gains and phase shifts. The impulse response of the frequency-selective channel consists of multiple-taps (i.e., resolvable multi-paths). The multi-path components are resolvable if they are separated in delay by $1/W$. In that case, replicas of the transmitted signal arrive at the receiver over a number of different

resolvable paths resulting in ISI. This is the case when dealing for instance with wide-band single-carrier DS-CDMA signal (see Figure 1.4(b)) whose bandwidth is much greater than the channel coherence bandwidth, i.e. $W_0 \gg B_c$ or equivalently $T_c \ll T_m$. Thus, the complex low-pass equivalent representation of the fading channel impulse response can be written as follows:

$$h(t) = \sum_{l=0}^{L_p-1} |h_l(t)| e^{j\phi_l(t)} \delta(t - lT_c) \tag{1.7}$$

where L_p denotes the number of resolvable multi-path components, which is given by:

$$L_p = \left\lfloor \frac{T_m}{T_c} \right\rfloor + 1 \tag{1.8}$$

In addition, the l^{th} resolvable path is characterized by its time-varying envelope $|h_l(t)|$ and its time-varying phase $\phi_l(t)$.

The frequency-selective fading channel reduces to frequency non-selective flat fading channel when $L_p = 1$ or equivalently when the transmitted signal bandwidth is less than the coherence bandwidth of the channel, i.e. $W \leq B_c$. This is the case for instance when dealing with the M narrow-band DS-CDMA signals (see Figure 1.4(a)), each having a bandwidth $W_M \leq B_c$ or equivalently $MT_c \geq T_m$. Therefore, frequency-selective fading can be converted to frequency non-selective fading by using multi-carrier transmission. For this purpose, according to [Kon96], the number M of carriers is chosen to meet two conditions:

- Each carrier undergoes frequency non-selective flat fading, which means that the normalized delay spread T_m/MT_c satisfies:

$$T_m/MT_c \leq 1 \tag{1.9}$$

- All carriers are subject to independent fading, implying that:

$$W_M \geq B_c \tag{1.10}$$

Given (1.5) and (1.6), the above two conditions are satisfied if:

$$\frac{T_m}{T_c} \leq M \leq (1+\chi)\frac{T_m}{T_c} \tag{1.11}$$

The left inequality of (1.11) is satisfied by choosing $M = L_p$, while the right inequality is satisfied by choosing $\chi \geq T_c/T_m$.

Thus, by carefully selecting the number of carriers M to satisfy (1.11), each carrier will

be affected by independent frequency non-selective flat fading. In that case, the complex low-pass equivalent impulse response of the channel over the m^{th} carrier is given by:

$$h_m(t) = |h_m(t)|e^{j\phi_m(t)}\delta(t) \tag{1.12}$$

where $|h_m(t)|$ and $\phi_m(t)$ respectively denote the time-varying envelop and phase.

1.3.2 Doppler spread and time-varying fading

Channel time-variation are due to the relative motion between the base station and the mobile and/or the motion of the surrounding which in turn results in a Doppler spread. The Doppler spread is a measure of the relative frequency shift between the transmitted signal and the received signal. Consider a mobile moving at a constant speed υ while receiving a signal whose angle of arrival φ, as illustrated in Figure 1.6. The resulting Doppler shift f_D in Hertz is given by:

$$f_D = \frac{\upsilon f_c}{c}\cos(\varphi) \tag{1.13}$$

where f_c is the central carrier frequency and c the light speed. The maximum Doppler frequency f_d is obtained from (1.13) when the angle of arrival is set to zero, as follows:

$$f_d = \frac{\upsilon f_c}{c} \tag{1.14}$$

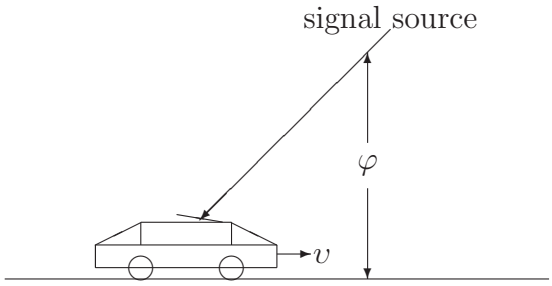

Figure 1.6: Illustration of the Doppler effect.

In a wide-band multi-path fading channel, the transmitted signal arrives at the receiver along L_p resolvable paths (equal to the number of carriers M in the multi-carrier system as in equation (1.11)). However, each resolvable path consists of a superposition of a large number L_s of local uncorrelated scatterers that arrive at the receiver almost simultaneously with a common propagation delay. Each of these scatterers is characterized by its own random amplitude and random phase. Thus, according to [Cla68] [Jak74], the

frequency non-selective fading process over the m^{th} carrier can be modeled as a sum of L_s weighted complex exponentials:

$$h_m(t) = \sum_{l=1}^{L_s} g_{ml} e^{j(2\pi f_d t \cos\varphi_{ml} + \vartheta_{ml})} \tag{1.15}$$

where g_{ml}, φ_{ml} and ϑ_{ml} are, respectively, the random scatterer amplitude, angle of arrival and initial phase associated with the l^{th} scatterer and the m^{th} carrier.

When there are a large number of scatterers, $h_m(t)$ can be approximated as a complex Gaussian process $h_m(t) = |h_m(t)|e^{j\phi_m(t)}$ according to the central limit theorem [Pap02]. In an environment with no direct line-of-sight path between the transmitter and the receiver, the fading process $h_m(t)$ will have zero-mean. In that case, its phase $\phi_m(t)$ is uniformly distributed over $[0, 2\pi)$ and its envelope at any time $\hbar = |h_m(t)|$ has a Rayleigh probability density function defined as follows:

$$f_\hbar(\hbar) = \begin{cases} \frac{\hbar}{\sigma_\hbar^2} e^{-\hbar^2/2\sigma_\hbar^2}, & \hbar \geq 0 \\ 0, & \text{otherwise} \end{cases} \tag{1.16}$$

where $\sigma_\hbar^2 = E[|h_m(t)|^2]$ denotes the average power of the fading process. Note that the carrier subscript is dropped, assuming that the fading processes over all carriers have the same statistics.

A typical Rayleigh fading envelop and phase of a time-varying fading process $h_m(t)$ is shown in Figure 1.7, with $f_d = 50$ Hz, $f_c = 1800$ MHz (GSM carrier), $\upsilon = 30$ Km/h and $T_b = 200\mu s$. Deep fades result from destructive addition of the scatterers while peaks result from their constructive addition.

The time-variation of the fading channel is often characterized by the fading process ACF. This second-order statistic generally depends on the propagation geometry, the velocity of the mobile and the antenna characteristics. A common assumption is that the propagation path consists of a two dimensional isotropic scattering with a vertical monopole antenna at the receiver [Jak74]. Thus, given the fading model described in equation (1.15), the ACF of the m^{th} carrier fading process can be obtained as follows:

$$\begin{aligned} R_{hh}(\tau) &= E[h_m(t+\tau)h_m^*(t)] \\ &= \sum_{l=1}^{L_s}\sum_{i=1}^{L_s} E\left[g_{ml} e^{j(2\pi f_d(t+\tau)\cos\varphi_{ml} + \vartheta_{ml})} g_{mi} e^{-j(2\pi f_d t \cos\varphi_{mi} + \vartheta_{mi})}\right] \end{aligned} \tag{1.17}$$

Under the wide-sense stationary uncorrelated scattering assumption suggested by Bello [Bel63], the different scattering rays are uncorrelated, such that $E[g_{ml}g_{mi}] = E[g_{ml}^2]\delta(l-i)$.

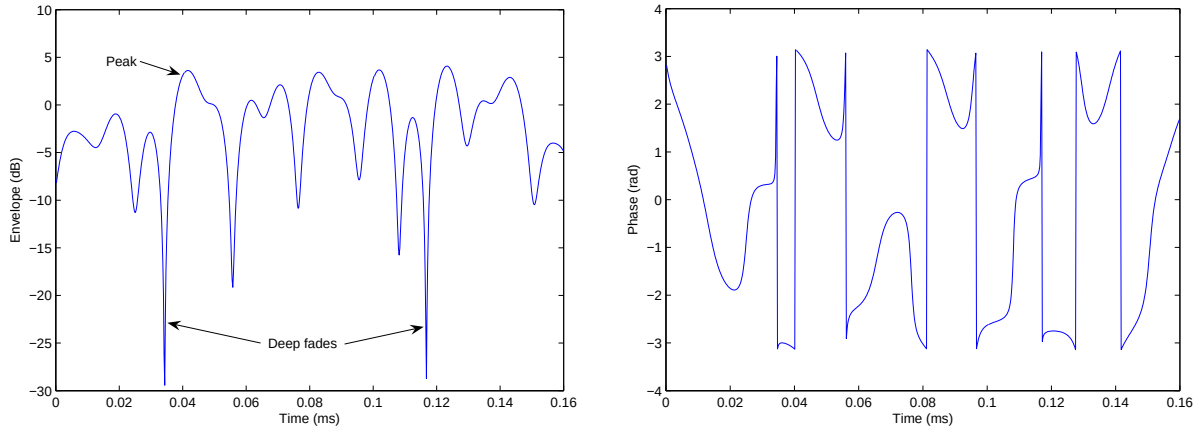

(a) Rayleigh envelop of the fading process.

(b) Phase of the fading process.

Figure 1.7: The envelope and phase of Rayleigh fading channel.

Hence, the ACF can be written in the following manner:

$$R_{hh}(\tau) = \sum_{l=1}^{L_s} E[g_{ml}^2] E[e^{j2\pi f_d \tau \cos\varphi_{ml}}] \tag{1.18}$$

Then, assuming that the scattered signals arrive from any direction with equal probability, the ACF is given by:

$$\begin{aligned} R_{hh}(\tau) &= \frac{\sigma_h^2}{2\pi} \int_0^{2\pi} e^{j2\pi f_d \tau \cos\varphi_{ml}} d\varphi_{ml} \\ &= \sigma_h^2 J_0(2\pi f_d \tau) \end{aligned} \tag{1.19}$$

where $J_0(.)$ is the zero-order Bessel function of the first kind and $\sigma_h^2 = \sum_{l=1}^{L_s} E[g_{ml}^2]$.
It should be noted that the real and imaginary portions of $h_m(t)$, denoted respectively as $h_m^{(r)}(t)$ and $h_m^{(i)}(t)$, are uncorrelated and have the same autocorrelation function [Stu01]:

$$R_{h_m^{(r)} h_m^{(r)}}(\tau) = R_{h_m^{(i)} h_m^{(i)}}(\tau) = \frac{\sigma_h^2}{2} J_0(2\pi f_d \tau) \tag{1.20}$$

$$R_{h_m^{(i)} h_m^{(r)}}(\tau) = R_{h_m^{(r)} h_m^{(i)}}(\tau) = 0 \tag{1.21}$$

The Doppler power spectrum can therefore be obtained by taking the Fourier transform of the ACF. The resulting Doppler power spectrum of $h_m(t)$ is band-limited and U-shaped. Moreover, it exhibits twin peaks at $\pm f_d$, as follows [Jak74]:

$$\Psi(f) = \begin{cases} \frac{\sigma_h^2}{\pi f_d \sqrt{1-(f/f_d)^2}}, & |f| \leq f_d \\ 0, & \text{else-where} \end{cases} \tag{1.22}$$

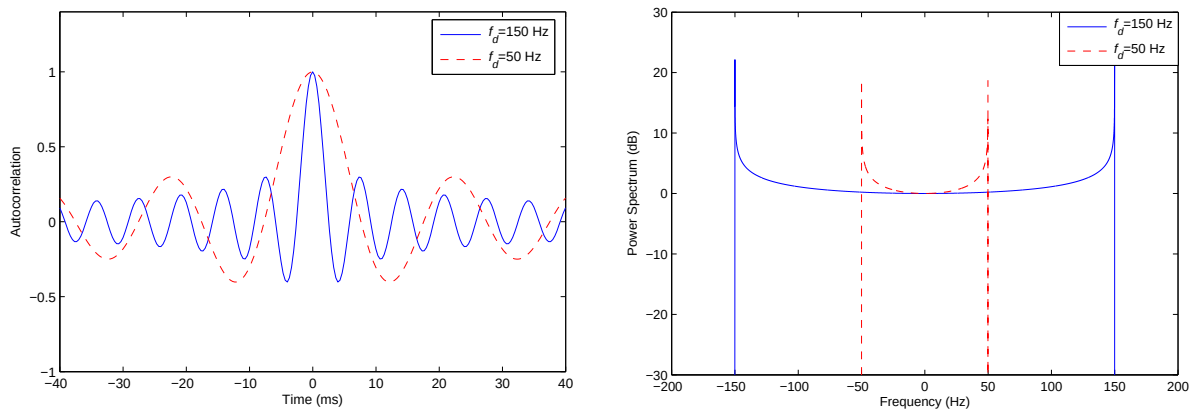

(a) Channel autocorrelation function.

(b) Channel Doppler power spectrum.

Figure 1.8: Channel ACF and Doppler power spectrum. $f_d = 50$ Hz and $f_d = 150$ Hz.

The channel ACF and Doppler power spectrum are shown in Figure 1.8 for maximum Doppler frequencies $f_d = 50$ Hz and $f_d = 150$ Hz. Thus, with $f_c = 1800$ MHz, we notice that increasing the mobile speed from 30 Km/h to 90 Km/h results in a wider Doppler spectrum bandwidth. Therefore, the higher the mobile speed the higher the fading rate, and accordingly the faster the time-variation of the channel. In addition, as the channel ACF is real valued, the corresponding PSD is symmetric around $f = 0$.
By sampling the continuous-time channel model (1.15) and ACF (1.19) at symbol rate $1/T_b$, a discrete-time model and ACF can be respectively obtained as follows :

$$h_m(n) = \sum_{l=1}^{L_s} g_{ml} e^{j(2\pi f_d T_b n \cos\varphi_{ml} + \vartheta_l)} \tag{1.23}$$

and

$$R_{hh}(n) = \sigma_h^2 J_0(2\pi f_d T_b |n|) \tag{1.24}$$

where $f_d T_b$ denotes the Doppler rate.

In the following subsection, we will see how the theoretical channel model can be simulated by using sum-of-sinusoids models.

1.3.3 Sum-of-sinusoids simulation models

Based on the theoretical model of the channel (1.15), and by selecting the following values for the scatterer amplitude g_{ml}, angle of arrival φ_{ml} and initial phase ϑ_{ml} associated with the l^{th} scatterer and the m^{th} carrier:

$$g_{ml} = \frac{1}{\sqrt{L_s}} \tag{1.25}$$

$$\varphi_{ml} = \frac{2\pi l}{L_s}, \quad l = 1, 2, \cdots, L_s \tag{1.26}$$

$$\vartheta_{mn} = 0 \tag{1.27}$$

Jakes derived the well-known sum-of-sinusoids simulation model for Rayleigh fading channels [Jak74]. However, the simplifying relationships forced in (1.25), (1.26) and (1.27) make this model deterministic and wide-sense non-stationary [Pop01]. Therefore, various modifications of the Jakes' simulator have been proposed in the literature. Thus, Pop *et al.* [Pop01] have proposed an improved simulator by introducing random phase shifts in the sinusoids to address the stationarity issue. In [Den93], a modified model has been proposed to generate multiple independent fading processes by using orthogonal Walsh-Hadamard codewords[3]. In the latter model, to provide quadrantal symmetry for all Doppler shifts leading to equal power oscillators, the arrival angles φ_{ml} are modified as follows:

$$\varphi_{ml} = \frac{2\pi(l - 0.5)}{L_s}, \quad l = 1, 2, \cdots, L_s \tag{1.28}$$

Thus, the fading process along the m^{th} carrier can be generated as follows:

$$h_m(n) = \sqrt{\frac{2}{L_o}} \sum_{l=1}^{L_o} \mathbf{q}_m(l)[\cos(\pi l/L_o) + j\sin(\pi l/L_o)] \cos(2\pi f_d T_b n \cos\varphi_{ml} + \vartheta_{ml}) \tag{1.29}$$

where $L_o = L_s/4$ is the number of oscillators, $\sqrt{2/L_o}$ a normalization factor, $\mathbf{q}_m(l) \in \{\pm 1\}$, $l = 1, \cdots, L_o$ the m^{th} Walsh-Hadamard codeword. Randomizing ϑ_{ml} provides different waveform realizations.

However, in the above simulators, the autocorrelations and cross-correlations of the real and imaginary parts do not match the desired correlation properties given by equations (1.20) and (1.21), even if the number of sinusoids tends to infinity. For this reason, Zheng *et al.* [Zhe03] have proposed a simulation model whose second order statistics correspond to the desired ones even if a few sinusoids are used. This is achieved by properly introducing randomness to g_{ml}, φ_{ml} and ϑ_{ml} as required by the theoretical model rather than using deterministic values as in equations (1.25)-(1.28).

Nevertheless, these sum-of-sinusoids models are dedicated to channel simulation and cannot be used in practice to design channel estimation algorithms due to the following reasons.

- Firstly, these models are non-linear.

[3]The m^{th} Walsh-Hadamard vector $\mathbf{q}_m(l) \in \{\pm 1\}$, $l = 1, \cdots, L_o$ in a set of M vectors gives zero inner product value with the others, i.e. $\mathbf{q}_m^T \mathbf{q}_n = 0, \ \forall m \neq n$.

- Secondly, in addition to f_d, the sum-of-sinusoids models usually involve three parameters (i.e., g_{ml}, φ_{ml} and ϑ_{ml}) to be defined for each scatterer. Thus, for a typical scenario of $L_s = 400$ scatterer, there will be a huge number of parameters.
- Thirdly, the estimation of these parameters will not be an easy task.

In [Gia98], to reduce the number of parameters to be estimated when designing a channel estimator, the channel is modeled as a superposition of few time-varying complex exponential basis functions with time-invariant coefficients. However, this so-called basis expansion model is deterministic while the theoretical model of the channel is stochastic. As an alternative to the sum-of-sinusoids models, we will investigate the relevance of AR models in the next subsection.

1.3.4 Autoregressive channel modeling

The AR model is widely used in many digital signal processing applications to approximate discrete-time random signals of interest [Kay88]. Such application areas include speech coding [Che92], speech enhancement [Gri02] [Lab06a], sea clutter modeling in radar application [Nog98], digital communications [Bad05] and biomedical applications, to just name a few. Indeed, this model is simple, linear and contains few parameters that can be easily estimated.

In recent papers [Kom02] [Lin02] [Bad05], the fading process $h_m(n)$ has been approximated by a p^{th} order AR process, denoted by AR(p) and defined as follows:

$$h_m(n) = -\sum_{i=1}^{p} a_i h_m(n-i) + u_m(n) \tag{1.30}$$

where $\{a_i\}_{i=1,\dots,p}$ are the AR model parameters and $u_m(n)$ denotes the zero-mean complex white Gaussian driving process with variance σ_u^2.

The corresponding PSD of the AR(p) process has the rational following form [Kay88]:

$$\Psi_{AR}(f_n) = \frac{\sigma_u^2}{|1 + \sum_{i=1}^{p} a_i \exp\left(-j2\pi f_n i\right)|^2} \tag{1.31}$$

where f_n is the normalized frequency.

The AR model can be used to either simulate fading channels as in [Bad05], or to design an estimation algorithm as in [Tsa96] [Lin02] [Kom02]. However, in both cases, two issues have to be investigated. Firstly, the selection of the AR model order p that best approximates the fading channel. Secondly, the estimation of both the AR parameters $\{a_i\}_{i=1,\dots,p}$ and the driving process variance σ_u^2.

In [The92], several criteria (e.g., Akaike information criterion) to select the AR model order are discussed. However, these criteria work well only for true AR processes, which is not the case when dealing with band-limited Doppler fading processes.
In the following, the selection of the AR model order and the determination of the AR parameters are investigated.

1.3.4.1 Determination of the AR parameters

The relationship between the AR parameters and the fading process ACF is given by the well-known YW equations [Kay88]:

$$\mathbf{R}_{hh}\boldsymbol{\theta} = -\mathbf{r}_h \tag{1.32}$$

where $\mathbf{R}_{hh}$ is the fading channel autocorrelation matrix of size $p \times p$, defined as follows:

$$\mathbf{R}_{hh} = \begin{bmatrix} R_{hh}(0) & R_{hh}(-1) & \cdots & R_{hh}(-p+1) \\ R_{hh}(1) & R_{hh}(0) & \cdots & R_{hh}(-p+2) \\ \vdots & \vdots & \ddots & \vdots \\ R_{hh}(p-1) & R_{hh}(p-2) & \cdots & R_{hh}(0) \end{bmatrix} \tag{1.33}$$

and $\boldsymbol{\theta}$ is a $p \times 1$ vector storing the AR parameters:

$$\boldsymbol{\theta} = \begin{bmatrix} a_1 & a_2 & \cdots & a_p \end{bmatrix}^T \tag{1.34}$$

In addition, $\mathbf{r}_h = \begin{bmatrix} R_{hh}(1) & R_{hh}(2) & \cdots & R_{hh}(p) \end{bmatrix}^T$ is the $p \times 1$ channel autocorrelation vector. Moreover, by using (1.30), the variance of the driving process can be expressed in the following manner:

$$\sigma_u^2 = R_{hh}(0) + \sum_{i=1}^{p} a_i R_{hh}(-i) \tag{1.35}$$

Providing that the Doppler frequency f_d is known, $R_{hh}(n)$ defined in (1.24) is known and hence the AR parameters could be computed by solving the YW equations (1.32). It should be noted that, to avoid the inversion of $\mathbf{R}_{hh}$, the YW equations can be efficiently solved by using the Levinson-Durbin recursion[4] with complexity $O(p^2)$ instead of $O(p^3)$. Once the AR(p) parameters of the fading process are estimated, the autocorrelation function of the resulting AR(p) process has the following form [Kay88]:

$$\hat{R}_{hh}(n) = \begin{cases} R_{hh}(n), & 0 \leq n \leq p \\ -\sum_{i=1}^{p} a_i \hat{R}_{hh}(n-i), & n > p \end{cases} \tag{1.36}$$

In the following, we will study the relevance of low and high-order AR models.

[4]See the MATLAB function *levinson* for a possible implementation.

1.3.4.2 Poor approximation of low-order AR models

For the special case of AR(1) model, the YW solution for the AR(1) parameter and the driving process variance are given by:

$$\begin{cases} a_1 = -J_0(2\pi f_d T_b) \\ \sigma_u^2 = (1 - a_1^2)\sigma_h^2 \end{cases} \tag{1.37}$$

Although AR(1) model is very simple, it results in a poor approximation of the Jakes model as its PSD can provide only one peak at $f_d = 0$ Hz, which is only the case for static terminals.

In [Lin95] [Wu00] [Lin02], the authors have modeled the fading channel by an AR(2) model with poles[5] located close to the unit circle in the z-plane, at an angle $\frac{2\pi f_d T_b}{\sqrt{2}}$. The AR(2) parameters are then given by:

$$\begin{cases} a_1 = -2r_d \cos\left(\frac{2\pi f_d T_b}{\sqrt{2}}\right) \\ a_2 = r_d^2 \end{cases} \tag{1.38}$$

where $r_d \in [0.9, 0.999]$ is the pole radius that corresponds to the steepness of the peak of the power spectrum.

The above choice of the AR(2) parameters is motivated by the quasi-periodic behavior of the Rayleigh fading process (see figure 1.7(a)). Indeed, for small time-lags n, the Bessel autocorrelation function of the channel $J_0(2\pi f_d T_b|n|)$ is similar to that of a sinusoid with unit-amplitude, frequency f_o and a uniformly distributed phase on $[0, 2\pi)$, given by $\cos(2\pi f_o T_b|n|)$. To illustrate it, let us consider the Taylor series expansion of both $J_0(2\pi f_d T_b|n|)$ and $\cos(2\pi f_o T_b|n|)$, as follows:

$$\begin{cases} J_0(2\pi f_d T_b|n|) = 1 - \frac{(2\pi f_d T_b|n|)^2}{2^2} + \frac{(2\pi f_d T_b|n|)^4}{2^2 4^2} - \frac{(2\pi f_d T_b|n|)^6}{2^2 4^2 6^2} + \cdots \\ \cos(2\pi f_o T_b|n|) = 1 - \frac{(2\pi f_o T_b|n|)^2}{2!} + \frac{(2\pi f_o T_b|n|)^4}{4!} - \frac{(2\pi f_o T_b|n|)^6}{6!} + \cdots \end{cases} \tag{1.39}$$

If we consider the first two expansion terms in equation (1.39), the two autocorrelation functions are equal for $f_o = \frac{f_d}{\sqrt{2}}$. Thus, the peak frequency of an AR(2) model fitting the fading process is at $\frac{f_d}{\sqrt{2}}$ instead of f_d.

Figure 1.9 shows the PSD and the pole locations inside the unit circle in the z-plane of an AR(2) process that should fit the Jakes model with $f_c = 1800$ MHz, $T_b = 400\mu s$ and different maximum Doppler frequencies (i.e., $f_d = 100$ Hz, $f_d = 250$ Hz and $f_d = 500$ Hz). The corresponding AR(2) parameters are obtained by solving the YW equations and are

[5] $H(z) = \frac{1}{1+\sum_i a_i z^{-i}} = \frac{1}{\Pi_i (1 - p_i z^{-1})}$, where p_i is the so-called pole.

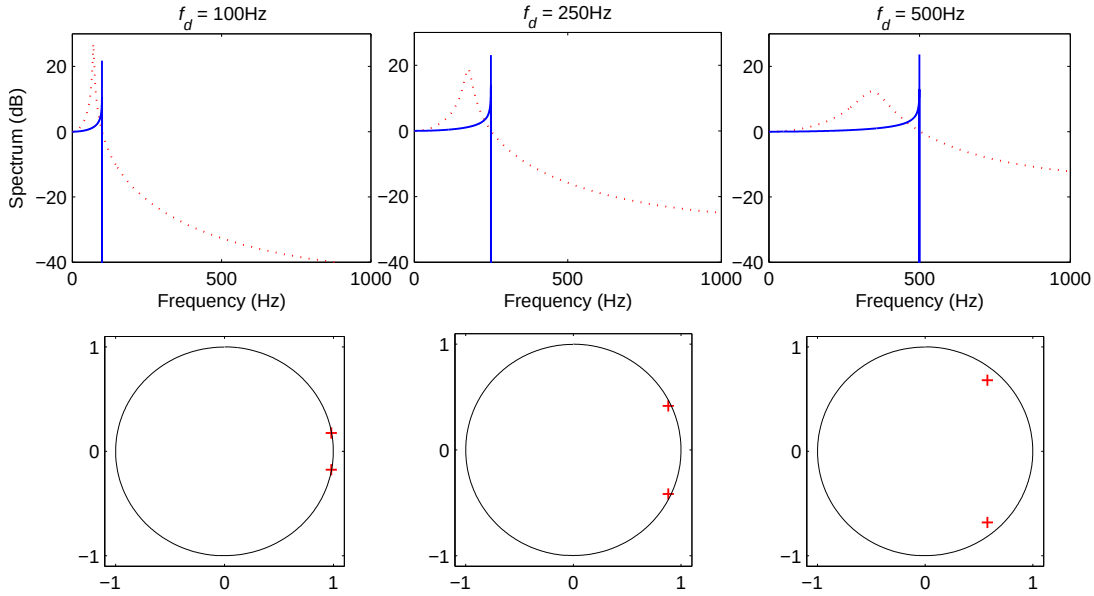

Figure 1.9: PSD and poles of an AR(2) process fitting the Jakes Doppler spectrum with $f_d = 100$ Hz, $f_d = 250$ Hz and $f_d = 500$ Hz. The poles are respectively equal to $0.9960e^{\pm j0.0565\pi}$, $0.9748e^{\pm j0.1406\pi}$ and $0.8926e^{\pm j0.2762\pi}$.

Table 1.2: The AR(2) parameters for a mobile wireless system with $f_c = 1800$ MHz, $T_b = 400\mu s$ and different maximum Doppler frequencies.

mobile speed v (Km/h)	Doppler frequency f_d (Hz)	Doppler rate $f_d T_b$	a_1	a_2	σ_u^2
60	100	0.04	-1.9608	0.9921	0.0005
150	250	0.1	-1.7625	0.9503	0.0178
300	500	0.2	-1.1544	0.7967	0.2145

summarized in Table 1.2. It is evident that an AR(2) process results in a spectral peak at $\frac{f_d}{\sqrt{2}}$. In addition, decreasing the maximum Doppler frequency results in adjacent poles that are very close to the unit circle in the z-plane.

From the above discussion, it is clear that low-order AR models (e.g., AR(1), AR(2)) yield poor approximation of the fading channel statistics. This motivates us to study the relevance of high-order AR models to better approximate the Jakes model.

1.3.4.3 Relevance of high-order AR models

Although several authors (see, e.g., [Tsa96], [Wu00], [Che01], [Lin02], [Kom02]) suggest using AR(1) and/or AR(2) processes to model the fading channel arguing for model simplicity, these processes are not well suited to approximate a band-limited spectrum.

Increasing the AR model order will provide a better approximation of the theoretical model. Nevertheless, when solving the YW equations in that case, one has to pay attention to the condition number of the autocorrelation matrix $\mathbf{R}_{hh}$ as it will determine the accuracy of the solution. In that case, the value of the driving processes variance σ_u^2 plays a key role. Indeed, σ_u^2 can be seen as the MMSE of the one-step predictor of order p for the fading process $h(n)$. This prediction error is given by the Kolmogoroff-Szego formula (see [Pap02] pp. 600):

$$\sigma_u^2 = \exp\left(\frac{1}{2\pi}\int_{-\pi}^{\pi} \ln \Psi_{AR}(\omega) d\omega\right) \tag{1.40}$$

where $\omega = 2\pi f_n$ is the normalized angular frequency. It is known that the prediction error σ_u^2 is a non-increasing function of the model order p (see [Pap02] pp. 600). From (1.40), if the asymptotic PSD of the AR process is zero over some frequency interval, the asymptotic prediction error is zero (i.e., $\sigma_u^2 \to 0$ as $p \to \infty$).

To investigate how fast σ_u^2 converges to its asymptotic value, we present in Figure 1.10 the behavior of σ_u^2 as a function of the AR model order for various values of Doppler rate $f_d T_b$. From Figure 1.10, the rate of decay of σ_u^2 is very fast and is inversely proportional to the Doppler rate. In addition, σ_u^2 goes to zero at small AR model orders for Doppler rates $f_d T_b \leq 0.1$.

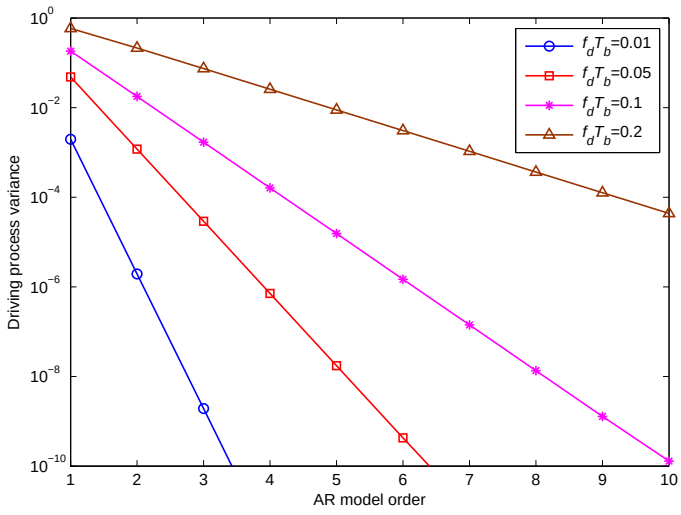

Figure 1.10: Driving process variance versus AR model order for various Doppler rates.

A measure of singularity of the channel autocorrelation matrix $\mathbf{R}_{hh}$ can be provided by the driving process variance as follows [Bad05]:

$$\det[\mathbf{R}_{hh}] = \prod_{i=0}^{p-1} \sigma_i^2 \tag{1.41}$$

where σ_i^2 is the driving process variance corresponding to an AR(i) model of the fading process. Thus, $\mathbf{R}_{hh}$ becomes singular when $\prod_{i=0}^{p-1} \sigma_i^2 = 0$. In addition, it is observed that the eigenvalue spread of $\mathbf{R}_{hh}$ is very large, which results in an ill-conditioning problem. In that cases, errors in the calculated AR parameters are expected when solving the YW equations (1.32) for all but very small AR model orders.

To overcome the band-limitation of the fading process and the resulting deterministic model, two solutions have recently been proposed [Sch01] [Bad05], in the framework of channel simulation.

On the one hand, in [Sch01], a sub-sampled ARMA process followed by a multistage interpolator has been considered. Indeed, when down-sampling, the normalized maximum Doppler frequency moves towards 1/2 such as the PSD is never equal to 0. Nevertheless, this requires a very high down-sampling factor.

On the other hand, Baddour *et al.* [Bad05] have suggested to "slightly" modify the properties of the channel by considering the sum of the theoretical fading process and an additive zero-mean white process whose variance ϵ is very small. In that case, the PSD of the resulting process is no longer band-limited and the corresponding ACF becomes:

$$R_{hh}^{mod}(n) = \sigma_h^2 J_0(2\pi f_d T_b |n|) + \epsilon\delta(n) \tag{1.42}$$

Adding the spectral bias ϵ reduces the condition number of $\mathbf{R}_{hh}$ and, hence, overcome the ill-conditioning problem when solving the YW equations. In addition, the resulting AR(p) process is a nondeterministic regular process whose driving process variance σ_u^2 no longer decays to zero when increasing the order p. Indeed, σ_u^2 can now be expressed as:

$$\sigma_u^2 = \exp\left(\frac{1}{2\pi}\int_{-\pi}^{\pi} \ln(\Psi_{AR}(\omega) + \epsilon) d\omega\right) \tag{1.43}$$

Therefore, for the asymptotic case of AR(∞), the driving process variance σ_u^2 will be lower bounded by ϵ. It was observed in [Bad05] that the value of the added bias ϵ which results in the most accurate AR parameters computation depends mainly on the Doppler rate $f_d T_b$. Typical values of ϵ, which represent a tradeoff between the improved condition number of $\mathbf{R}_{hh}$ and the bias introduced in the model, are given in Table 1.3. These values were empirically obtained in [Bad05].

As the band-limitation issue can be solved by the above method, using high-order AR models to approximate the fading channel becomes possible. Thus, increasing the AR model order leads to a better fit between the statistics of the resulting AR process and the realistic Jakes channel. This is illustrated in Figure 1.11 where we present the ACF

Table 1.3: Typical values of the added bias ϵ for different Doppler rates.

Doppler Rate f_dT_b	added bias ϵ
0.001	10^{-5}
0.005	10^{-6}
0.01	10^{-7}
0.05	10^{-8}
0.1	10^{-9}

and PSD of the Jakes model and that of the fitted AR process whose order is 1, 2, 5 and 20. According to this figure, the AR(20) model provides much better approximation to the theoretical Jakes model than low-order AR models. In [Bad05], Baddour *et al.* have used a very high-order AR models (e.g., $p \geq 50$) to accurately model and simulate fading channels. However, in the framework of channel estimation based on Kalman or H_∞ filtering, such a model order results in an estimation algorithms with very high computational cost. Therefore, a compromise between the modeling approximation and the computational cost has to be found in that case.

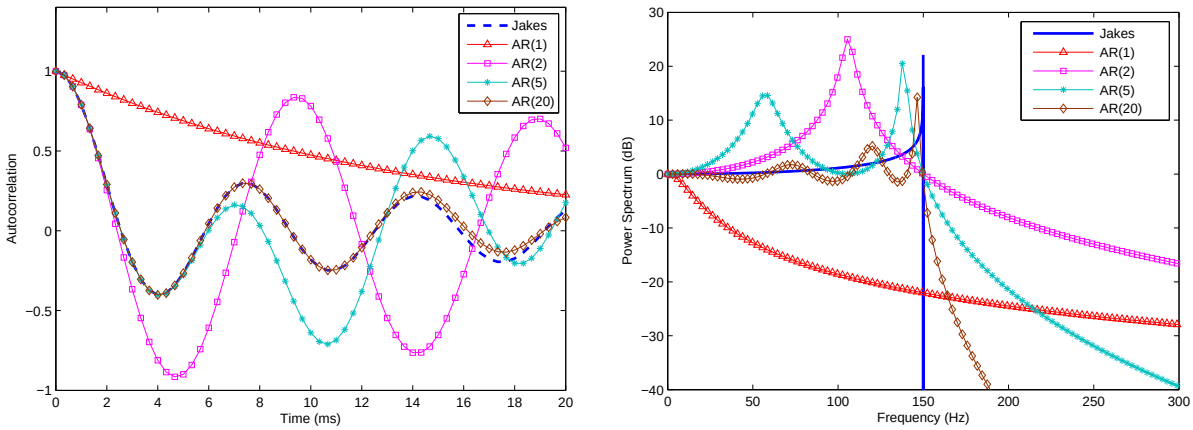

(a) ACF of Jakes model and that of AR processes. (b) PSD of Jakes model and that of AR processes.

Figure 1.11: ACF and PSD of the Jakes fading channel and that of the fitted AR processes whose order is 1, 2, 5 and 20. $f_dT_b = 0.05$.

Following the above discussion, an AR model whose order is high enough will be considered in this thesis to approximate the channel fading process either in the field of channel simulation or estimation.

1.4 Conventional receiver

The transmitted multi-carrier signal of the k^{th} user (1.1) propagates through a frequency-selective Rayleigh fading channel. Providing that the number M of carriers, the carrier spacing and the bandwidth of the chip pulse shape $\psi(t)$ are suitably chosen [Kon96], each carrier can be assumed to undergo independent flat fading (see subsection 1.3.1). In addition to the fading, the transmitted signal at the m^{th} carrier is also disturbed by an Additive White Gaussian Noise (AWGN) process $\eta_m(t)$. The noise processes $\{\eta_m(t)\}_{m=1,2,...,M}$ are assumed to be mutually independent and identically distributed, with equal variance σ_η^2. Hence, the continuous time received signal on the systems uplink (i.e., the asynchronous case) at the m^{th} carrier in its complex analytic form is given by:

$$r_m(t) = \sum_{n=-\infty}^{+\infty} \sum_{k=1}^{K} \sqrt{2P_k} d_k(n) c_k(t - nT_b - \tau_k) h_{mk}(n) e^{j2\pi f_m t} + \eta_m(t) \tag{1.44}$$

where $\tau_k \in (0, T_b)$ is the delay of the k^{th} user signal. The fading processes $\{h_{mk}(n) = |h_{mk}(n)|e^{j\phi_{mk}(n)}\}_{m=1,2,\cdots,M;k=1,2,\cdots,K}$ are mutually independent and identically distributed complex Gaussian random processes. Indeed, as mentioned in subsection 1.3.2, $h_{mk}(n)$ is zero-mean with a uniformly distributed phase $\phi_{mk}(n)$ on $[0, 2\pi)$ and a Rayleigh distributed envelop $|h_{mk}(n)|$. The variances of $\{h_{mk}(n)\}_{m=1,2,\cdots,M;k=1,2,\cdots,K}$ are all assumed equal to σ_h^2. Here, the fading is assumed to be time-varying whereas it is assumed to be time-invariant in [Kon96].

To retrieve the desired symbol sequence of the first user $d_1(n)$, from the received signals $\{r_m(t)\}_{m=1,2,...,M}$, let us consider the conventional correlator (matched-filter) based MC-DS-CDMA receiver proposed by Kondo *et al.* in [Kon96]. This receiver is illustrated in Figure 1.12 and operates as follows. Firstly, the received multi-carrier signal is demodulated over M carriers. It should be noted that the multi-carrier modulation and demodulation steps depicted in Figures 1.3 and 1.12 can be efficiently implemented by using the Inverse FFT (IFFT) and FFT techniques, respectively [Bin90]. The demodulated signal over the m^{th} carrier is then processed with a chip-matched filter, which consists of an integrator with duration MT_c. The samples from a chip-rate $1/MT_c$ sampler are then stored during a one-bit interval, resulting in the following $N \times 1$ vector:

$$\mathbf{x}_m(n) = \sum_{k=1}^{K} \sqrt{P_k} h_{mk}(n) [d_k(n)\mathbf{f}_k + d_k(n-1)\mathbf{g}_k] + \boldsymbol{\eta}_m(n) \tag{1.45}$$

where $\mathbf{f}_k$ and $\mathbf{g}_k$ depend on the left and right cyclic shifts of the spreading code $\mathbf{c}_k$ of the k^{th} user. In addition, $\boldsymbol{\eta}_m(n)$ is an $N \times 1$ vector of AWGN samples with zero-mean and covariance matrix $\sigma_\eta^2 \mathbf{I}_N$.

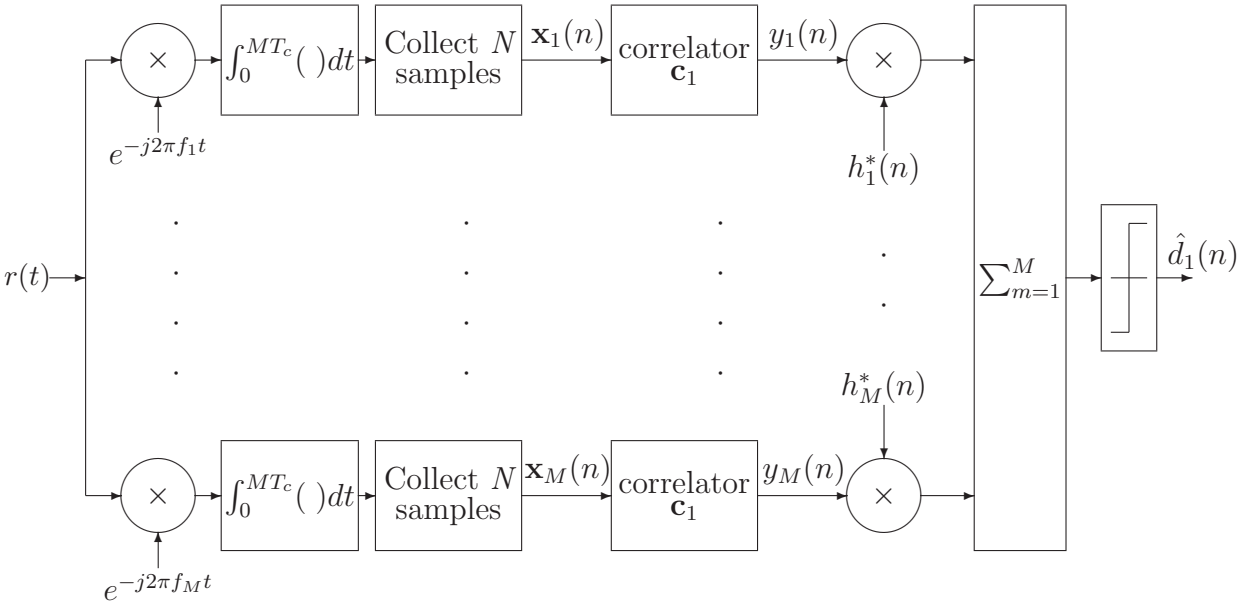

Figure 1.12: Conventional MC-DS-CDMA receiver structure for user 1.

For the systems down-link (i.e., the synchronous case), all users are synchronized, i.e. $\{\tau_k = 0\}_{k=0,1\cdots,K}$. In addition, all user signals over the m^{th} carrier are affected by the same fading process $h_m(n) = |h_m(n)|e^{j\phi_m(n)}$. Therefore, in that case, the received $N \times 1$ vector is given by:

$$\mathbf{x}_m(n) = \sum_{k=1}^{K} \sqrt{P_k} d_k(n) h_m(n) \mathbf{c}_k + \boldsymbol{\eta}_m(n) \tag{1.46}$$

The received vector at the m^{th} carrier $\mathbf{x}_m(n)$ is then correlated with the spreading code of the first user $\mathbf{c}_1$, resulting in de-spreading the information of the first user as follows:

$$y_m(n) = \mathbf{c}_1^T \mathbf{x}_m(n) = \sqrt{P_1} d_1(n) h_m(n) + \sum_{k=2}^{K} \sqrt{P_k} d_k(n) h_m(n) \mathbf{c}_1^T \mathbf{c}_k + \mathbf{c}_1^T \boldsymbol{\eta}_m(n) \tag{1.47}$$

where the output of the first user correlator consists of three parts:

- the first part $\sqrt{P_1} d_1(n) h_m(n)$ is due to the information of the desired user,
- the second part $\sum_{k=2}^{K} \sqrt{P_k} d_k(n) h_m(n) \mathbf{c}_1^T \mathbf{c}_k$ is due to the MAI caused by other users,
- the third part $\mathbf{c}_1^T \boldsymbol{\eta}_m(n)$ with variance σ_η^2 is due to the AWGN.

The MAI part in the right hand side of (1.47) is imposed by the cross-correlation of the spreading codes of different users. The spreading codes cross-correlations, defined as $\rho_{ij} = \mathbf{c}_i^T \mathbf{c}_j$ with $i \neq j$, are usually designed to be very small compared to their autocorrelations $\rho_{ii} = \mathbf{c}_i^T \mathbf{c}_i = 1$. However, as the number of users K or their powers P_k increases, the MAI becomes substantial.

It should be noted that the correlator detector in (1.47) follows a single-user detection strategy in which each user is detected separately without regard for other users. In addition, the MAI term is assumed to be approximated as a Gaussian noise which can be then added to the additive noise. This approximation is justified [Pap02] from the central limit theorem when the number of active users is very high.
To counteract the effect of fading, the frequency diversity inherent in the MC-DS-CDMA system can be exploited by using a diversity combining technique such as the MRC [Pro95]. Therefore, the conventional receiver uses the MRC to compensate for the fading by coherently add the contribution of all carriers, as follows:

$$y_{MRC}(n) = \sum_{m=1}^{M} h_m^*(n) y_m(n) \tag{1.48}$$

Thus, by multiplying with $h_m^*(n) = |h_m(n)|e^{-j\phi_m(n)}$, the output of the correlator over each carrier is co-phased and weighted by a factor that is proportional to the signal amplitude. Thus, carriers with strong signal are further amplified, while carriers with weak signal are attenuated. In that sense, the MRC is an optimal diversity combining technique that maximizes the SNR.
Finally, a decision about the desired user data symbol can thus be obtained as follows:

$$\hat{d}_1(n) = \text{sgn}\left(\text{Re}\left(\sum_{m=1}^{M} h_m^*(n) y_m(n)\right)\right) \tag{1.49}$$

where the fading processes $\{h_m(n)\}_{m=1,2,\cdots,M}$ are assumed to be available at the receiver.
However, the conventional MC-DS-CDMA receiver [Kon96] has two drawbacks.

- Firstly, the fading processes over all carriers are assumed to be available at the receiver, which is not the case in practice.

- Secondly, as this receiver uses the spreading code of the desired user in the form of a correlator to de-spread his information, it cannot eliminate the MAI caused by other users.

Indeed, when the number of users is increased, the amount of the MAI will also increased and, hence, the BER performance of the receiver will deteriorate. In addition, this receiver cannot work well in a near-far scenario, where far users from the base station receive lower power than users who are near the base station. This is because the near-far problem will result in more severe MAI.

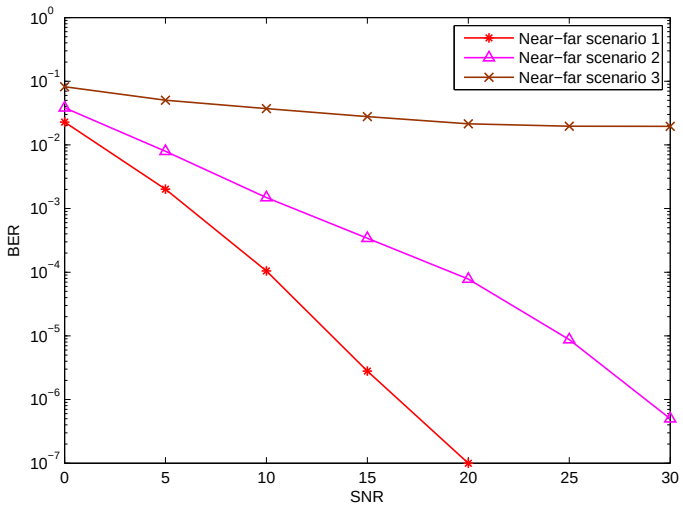

Figure 1.13: Effect of the MAI and the near-far problem on the BER performance of the conventional correlator based MC-DS-CDMA receiver.

The effects of the MAI and the near-far problem on the BER performance of the conventional receiver can be illustrated by the following simulation example. Let us consider a MC-DS-CDMA system with BPSK modulation, three carriers $M = 3$ and $K = 10$ active users. In the simulation, three near-far scenarios are investigated:

- Near-far scenario # 1: the desired user (i.e., $k = 1$) signal has the same power as all other interfering user signals (i.e., $P_1 = P_2 = \cdots = P_K$, perfect power control case). Let us define the Interference-to-Signal Ratio (ISR) as follows:

$$\text{ISR} = 10 \log_{10} \left(\frac{P_k}{P_1} \right), \qquad 2 \leq k \leq K \tag{1.50}$$

  Thus, in the perfect power control case ISR=0 dB.

- Near-far scenario # 2: the interfering users (i.e., $k \neq 1$) have 10 dB power advantage over the desired user (i.e., ISR=10 dB).

- Near-far scenario # 3: the interfering users have 15 dB power advantage over the desired user (i.e., ISR=15 dB).

Figure 1.13 confirms that the BER performance of the correlator based receiver is limited by the MAI and the near-far problem.

1.5 Conclusions

MC-DS-CDMA is a promising multiple access technique that combines the advantages of both multi-carrier modulation and DS-CDMA. It can support the requirements of the new emerging high data rate interactive multimedia services in the B3G and 4G mobile wireless systems.

In this chapter, we have presented the transmitter model, the channel model and the conventional receiver of MC-DS-CDMA based mobile wireless system. This system is designed to provide high data rate transmission to high mobility users. High data rate transmission leads to severe frequency-selective fading. Thus, when the number of carriers and their spacing are suitably chosen, each carrier is assumed to undergo independent frequency-flat fading. In addition, due to user mobility, each carrier is subject to Doppler shifts resulting in time-varying fading. Therefore, the channel over each carrier is characterized as frequency-flat and time-varying. We study the relevance of AR modeling for these channels where low-order and high-order models are evaluated. As low-order AR models yield poor approximation of the fading channel, we propose to consider an AR model whose order is high enough to approximate the fading channel.

When considering the conventional MC-DS-CDMA receiver, the fading process over each carrier is assumed to be available, which is not the case in practice and should be estimated. In addition, this receiver is severely limited by the MAI and the near-far problem. Therefore, in the next chapter, we propose several receiver structures that can partially or completely remove the MAI while working in Rayleigh fading channels. Moreover, in chapter 3, we introduce several channel estimation schemes that can effectively estimate and track AR fading channels.

Chapter 2

Receiver Design

Contents

2.1 State of the art

Despite the various advantages of CDMA systems, the MAI and the near-far effect are two problems to be addressed. Therefore, in the last two decades, significant efforts have been made to develop multiuser detection receivers to suppress the MAI and to mitigate the near-far problem. See [Ver98] and references therein. Most of these receivers were developed for single-carrier DS-CDMA systems in AWGN channels. In these cases, one or more of the following items are assumed to be known at the receiver:

1. the spreading waveform (code) of the desired user,
2. the spreading waveforms (codes) of the interfering users,
3. the timing (propagation delay) of the desired user,
4. the timing (propagation delay) of each of the interfering users,
5. the received amplitudes of all users,
6. the training data sequence of every active user.

The RAKE receiver, as implemented in the IS-95 standard [IS-95], requires the spreading waveform and the timing of the desired user. However, this receiver cannot eliminate the MAI and is "limited" by the near-far problem. To avoid the near-far effect, the IS-95 system is based on stringent closed loop power control which, however, decreases the system capacity. The optimal multiuser receiver proposed by Verdú in [Ver86] consists of a bank of matched filters, one for each user, followed by a Viterbi algorithm to carry-out Maximum Likelihood (ML) sequence estimation. It can completely eliminate the MAI and can solve the near-far problem. However, its computational complexity increases exponentially with the number of users. In addition, it requires the knowledge of the spreading waveforms, the timing and the amplitudes of all users. To reduce the computational cost of the optimal receiver, several linear multiuser receivers have been proposed [Ver98]. They can result in similar performance[1] as the optimal receiver while having a linear complexity in the number of users. Thus, the decorrelating receiver [Lup89] [Lup90] requires the spreading waveforms and the timing of all users to achieve optimal near-far resistance and to completely eliminate the MAI. As an alternative, the MMSE receiver (see, e.g., [Mad94], [Hon00]) has been proven to be as near-far resistant as

[1] In terms of MAI suppression, near-far resistance and BER.

the decorrelating receiver while more suitable for adaptive implementation. The adaptive MMSE receivers (see, e.g., [Mil95], [Woo98], [Hon00], [Mil00a]) are usually implemented with adaptive filters such as the LMS or the RLS [Hay02]. Besides, the NLMS and the APA algorithms have been tested to design MMSE receivers for WCDMA systems [Tri03]. These adaptive receivers make it possible to suppress the MAI and can implicitly compensate for the effect of the fading channel. In addition, they offer an attractive trade-off between performance, complexity and the need for side information (i.e., spreading codes, timing for all users, etc.). The only overhead of these receivers is that they need a training sequence for every active user. To avoid the use of training sequences, a blind[2] LMS-based multiuser receiver was proposed by Honig *et al.* [Hon95]. This type of receiver is based on the minimization of the Mean Output Energy (MOE) of the receiver subject to a certain code-aided constraint[3] to guarantee no cancelation of the desired signal. It requires only the knowledge of the spreading sequence and the timing of the desired user. Blind adaptive multiuser detectors based on the RLS [Poo97] and the Kalman filter [Zha02] algorithms have also been developed. Indeed, they make it possible to improve the convergence features and tracking capabilities when compared with the LMS-based detector. In [Muc04], the authors have proposed a derived version of the blind LMS-based detector [Hon95], which makes it possible to operate in a time-varying multi-path fading channels. It should be noted that blind adaptive receivers can also be implemented by using subspace approaches [Wan98] and high-order statistics based methods. The reader may refer to [Mad98] for a tutorial survey about these techniques. Other multiuser detection techniques include the non-linear multistage and decision-feedback receivers [Mos96].

In this chapter, our purpose is to design receivers for MC-DS-CDMA mobile wireless systems in Rayleigh fading channels. The conventional correlator based MC-DS-CDMA receiver [Kon96] presented in the previous chapter cannot eliminate the MAI caused by other users and, hence, is not near-far resistant. In addition, the fading processes over all carriers are assumed to be available at the receiver, which is not the case in practice. Therefore, several approaches have recently been developed to suppress the MAI and/or to estimate and counteract the effect of fading.

The first approach consists in designing a MMSE receiver. Two structures are proposed in [Mil00b]: the first one consists in carrying out a Wiener filter along each

[2]The adjective "blind" in this context means that the receiver does not require training sequences for MAI suppression and multiuser detection.

[3]The spreading code of the desired user, always available at the receiver, is orthogonal to the adaptive part of the detector responsible about MAI suppression (see equations (2.26)-(2.28)).

carrier, whereas the second one is defined by the joint optimization of the filter weights of all carriers. In both structures, the Wiener filtering is performed using the least-square estimated fading processes. However, as these receivers require the estimation and the inversion of the received signal autocorrelation matrix, their computational cost is high. Hence, they may be difficult to implement in practice. In [Gro06], Grolleau *et al.* have proposed a reduced-rank MMSE receiver based on a matrix polynomial expansion of the inverse of the received signal autocorrelation matrix. This receiver makes it possible to get a compromise between the computational cost and the performance in terms of BER. Its asymptotic version (i.e., when the spreading code length and the number of active users goes to infinity with their ratio being constant) is also derived by using the so-called random matrix theory. In the framework of MC-CDMA, Kalofonos *et al.* [Kal03] have studied two types of MMSE detectors in Rayleigh fading channels. Firstly, to carry out the so-called "MMSE per carrier" detector, the fading processes are estimated by means of the LMS or the RLS algorithm. The authors also examine the relevance of Kalman filtering for channel estimation. Secondly, the so-called "MMSE per user" detector is adaptively implemented by using LMS or RLS algorithms and no explicit channel estimation is required.

Blind MMSE receivers have also been studied. Thus, in [Lok99], Lok *et al.* have proposed a blind adaptive receiver for MC-DS-CDMA systems in Rayleigh fading channels. Instead of using the MRC after despreading, a blind stochastic gradient algorithm similar to the LMS is carried out, maximizing the signal to noise-plus-MAI ratio. Their method can be viewed as a form of MMSE multiuser detection in the frequency-domain. Nevertheless, the authors did not use the existing "time-domain" blind multiuser detection techniques (e.g., [Hon95] [Poo97], [Zha02]) to effectively suppress the MAI. In [Nam00], a subspace-based MMSE receiver for a MC-DS-CDMA system was proposed. The orthogonality between the noise subspace and the desired signal vector is exploited to blindly estimate the channel required for the construction of the linear MMSE detector.

Other approaches have also been considered. Thus, in [Liu01], the authors have proposed a class of spreading codes that allows the correlator-based receiver [Kon96] to yield BER performance close to that of the optimal MMSE receiver for slowly fading channels. In [Xu01], the receiver provides a RAKE for each carrier to mitigate the effect of frequency-selective fading. The outputs of the RAKEs are then combined by using a MRC. However, in this receiver, the fading processes are assumed to be available. In addition, it cannot suppress the MAI. In [Wan04], the authors have proposed an adaptive Parallel Interference Cancellation (PIC) multiuser detection scheme that operates in slowly fading

channels. This scheme provides an adaptive MAI estimation algorithm before the PIC stage to improve the accuracy of the MAI cancelation.

In the following, we present five new MC-DS-CDMA receiver structures. Thus, in section 2.2, to reduce the computational cost of the optimal MMSE receiver presented in [Mil00b], we propose two adaptive MMSE receiver structures based on the APA [Jam04]. A comparative study is then carried out with other adaptive algorithms such as the NLMS and the RLS. In section 2.3, to avoid the use of a training sequence for every active user, we propose two blind adaptive multiuser detection receiver structures based on a blind APA-like multiuser detector [Jam05a]. In that case, only the spreading waveform and the timing of the desired user are required. A comparative study is then carried out with existing blind adaptive multiuser detectors based on LMS [Hon95] or Kalman filter [Zha02], initially derived for single-carrier DS-CDMA systems. In section 2.4, when the spreading waveforms and timing of all users are available, we propose to extend the decorrelating multiuser detector based receiver originally developed for single-carrier DS-CDMA in [Wu00] to the multi-carrier case [Jam05b].

2.2 Adaptive MMSE receivers

In this section, we propose two adaptive MMSE receiver structures based on the APA [Jam04]. The so-called "Separate Detection" (SD) structure consists in using a particular adaptive filter structure for each carrier, whereas the so-called "Joint Detection" (JD) structure is based on a joint structure defined by the concatenation of the adaptive filter weights dedicated to each carrier. We carry out a comparative study between both structures with various adaptive filters such as RLS, NLMS and APA.

2.2.1 Receiver structure with separate detection

The proposed adaptive MMSE receiver for asynchronous MC-DS-CDMA systems with the separate detection of the received signals over M carriers is shown in Figure 2.1. Thus, to retrieve the symbol sequence of the desired user $d_1(n)$ from the received signals $\{r_m(t)\}_{m=1,2,\cdots,M}$ given in (1.44), let us first recall the $N \times 1$ discrete-time received vector over the m^{th} carrier given in (1.45), as follows:

$$\mathbf{x}_m(n) = \sum_{k=1}^{K} \sqrt{P_k} h_{mk} [d_k(n)\mathbf{f}_k + d_k(n-1)\mathbf{g}_k] + \boldsymbol{\eta}_m(n) \tag{2.1}$$

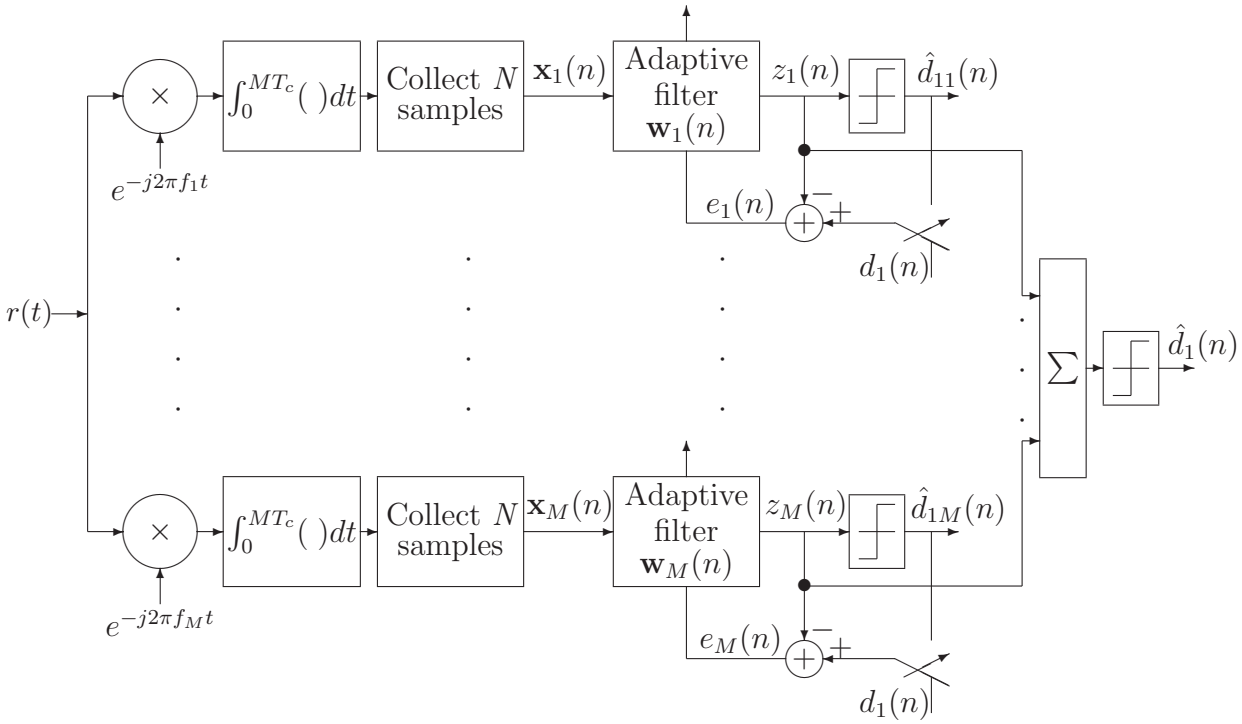

Figure 2.1: Adaptive MMSE receiver structure with separate detection.

Here, the fading coefficients $\{h_{mk} = |h_{mk}|e^{j\phi_{mk}}\}_{m=1,2,\cdots,M;k=1,2,\cdots,K}$ are assumed to be time-invariant in a given transmission frame[4], but might be time-varying from one frame to another. In addition, the receiver is assumed to be synchronized[5] with the desired user, i.e. $\mathbf{f}_1 = \mathbf{c}_1$ and $\mathbf{g}_1 = \mathbf{0}$. Thus, equation (2.1) can be re-written in the following manner:

$$\mathbf{x}_m(n) = \sqrt{P_1}h_{m1}d_1(n)\mathbf{c}_1 + \sum_{k=2}^{K}\sqrt{P_k}h_{mk}[d_k(n)\mathbf{f}_k + d_k(n-1)\mathbf{g}_k] + \boldsymbol{\eta}_m(n) \tag{2.2}$$

where the first part of (2.2) is due to the information of the desired user, the second part is due to the MAI caused by other asynchronous interfering users and the third part is the additive noise.

At that stage, the MMSE receiver consists in defining the impulse response of the filter:

$$\mathbf{w}_m(n) = \begin{bmatrix} w_m(1) & w_m(2) & \cdots & w_m(N) \end{bmatrix}^T \tag{2.3}$$

that minimizes the following Mean Square Error (MSE) criterion:

$$J_{MSE}[\mathbf{w}_m(n)] = E\left[|e_m(n)|^2\right] = E\left[\left|d_1(n) - \mathbf{w}_m^H(n)\mathbf{x}_m(n)\right|^2\right] \tag{2.4}$$

[4]A frame is a data structure that consists of fields predetermined by a protocol for the transmission of user information symbols and pilot/training symbols.

[5]It should be noted that receiver synchronization is not an easy task (see, e.g., [Str96] [Cai02]). However, this topic is outside the scope of this thesis.

This leads to the well known Wiener-Hopf solution [Hay02]:

$$\mathbf{w}_m(n) = \mathbf{R}_m^{-1}(n)\mathbf{p}_m(n) \tag{2.5}$$

where, $\mathbf{R}_m(n) = E[\mathbf{x}_m(n)\mathbf{x}_m^H(n)]$ denotes the autocorrelation matrix of the m^{th} carrier-output vector and $\mathbf{p}_m(n) = E[d_1^*(n)\mathbf{x}_m(n)]$ the cross-correlation vector between desired symbol of the first user and the m^{th} carrier-output vector.
Nevertheless, instead of solving the Wiener-Hopf equation given in (2.5) which requires the estimation and the inversion of $\mathbf{R}_m(n)$, an adaptive approach can be considered and has the advantage of reducing the computational cost $O(N^3)$. In addition, the spreading waveform and the fading coefficients are not required at the receiver. Once the training period is over, the filter weights can either be locked for a stationary environment or track channel variations in a decision directed manner. At that stage, the training sequence is replaced by the estimated data symbol of the desired user along each carrier, obtained as follows:

$$\hat{d}_{1m}(n) = \mathrm{sgn}\left(\mathrm{Re}\left(\mathbf{w}_m^H(n)\mathbf{x}_m(n)\right)\right) \tag{2.6}$$

The final symbol decision of the desired user is achieved by combining the contributions from the adaptive filter outputs as follows:

$$\hat{d}_1(n) = \mathrm{sgn}\left(\mathrm{Re}\left(\sum_{m=1}^{M}\mathbf{w}_m^H(n)\mathbf{x}_m(n)\right)\right) \tag{2.7}$$

As an alternative to the separate detection based receiver, a joint detection based one is considered in the next subsection.

2.2.2 Receiver structure with joint detection

One can derive the adaptive MMSE receiver with the joint detection of the received signals over M carriers (see Figure 2.2), by replacing in the above separate detection approach:

- the vector $\mathbf{x}_m(n)$ by a $MN \times 1$ vector $\mathbf{x}_{con}(n)$ concatenating the M discrete-time outputs:

$$\mathbf{x}_{con}(n) = \left[\begin{array}{cccc} \mathbf{x}_1^T(n) & \mathbf{x}_2^T(n) & \cdots & \mathbf{x}_M^T(n) \end{array}\right]^T \tag{2.8}$$

- the vector $\mathbf{w}_m(n)$ by a $MN \times 1$ vector $\mathbf{w}_{con}(n)$ concatenating the M filter weights:

$$\mathbf{w}_{con}(n) = \left[\begin{array}{cccc} \mathbf{w}_1^T(n) & \mathbf{w}_2^T(n) & \cdots & \mathbf{w}_M^T(n) \end{array}\right]^T \tag{2.9}$$

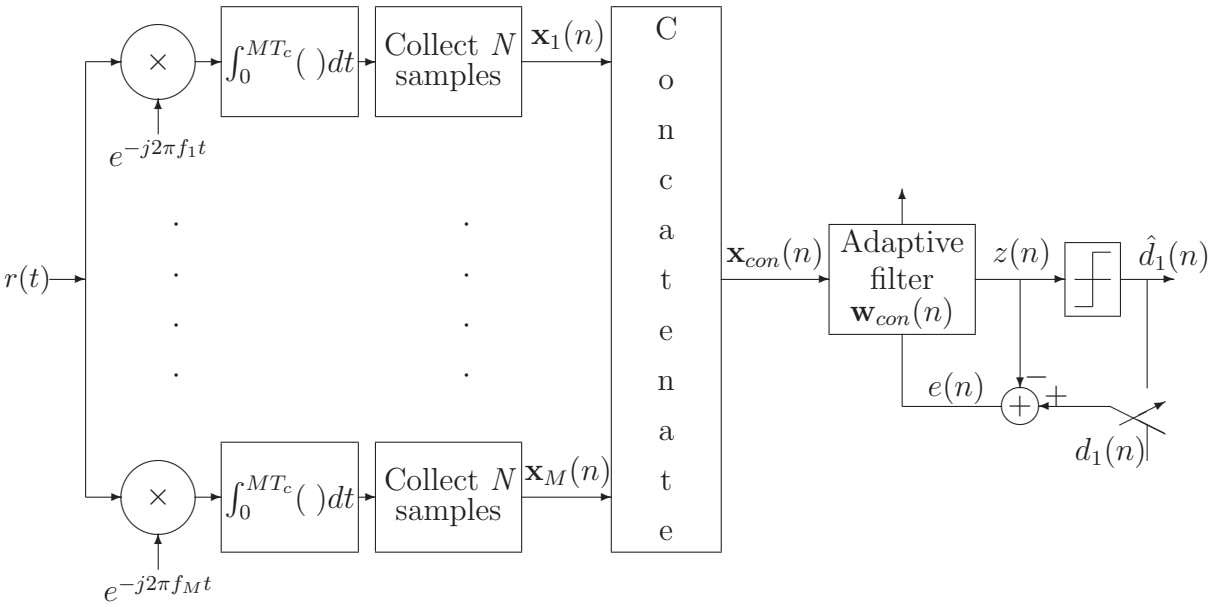

Figure 2.2: Adaptive MMSE receiver structure with joint detection.

In that case, we aim at minimizing the following MSE criterion:

$$J_{MSE}[\mathbf{w}_{con}(n)] = E\left[\left|d_1(n) - \mathbf{w}_{con}^H(n)\mathbf{x}_{con}(n)\right|^2\right] = E\left[|d_1(n) - z(n)|^2\right] \tag{2.10}$$

The final symbol decision of the desired user is then given by:

$$\hat{d}_1(n) = \text{sgn}\left(\text{Re}\left(\mathbf{w}_{con}^H(n)\mathbf{x}_{con}(n)\right)\right) \tag{2.11}$$

It should be noted that equation (2.11) reduces to that in (2.6) when $M = 1$.

2.2.3 Adaptive implementation

To simplify matters, we introduce $\mathbf{x}(n)$ and $\mathbf{w}(n)$ to respectively denote:

- the input vector $\mathbf{x}_m(n)$ and the filter weights $\mathbf{w}_m(n)$ when using the separate detection scheme,
- the concatenated input vector $\mathbf{x}_{con}(n)$ and the concatenated vector weights $\mathbf{w}_{con}(n)$ when considering the joint detection scheme.

2.2.3.1 The NLMS algorithm

When considering the LMS [Hay02], the weights $\mathbf{w}(n)$ are updated with a correction proportional to the input vector $\mathbf{x}(n)$, which may however lead to gradient noise ampli-

fication problem. For this reason, we consider the regularized normalized version of this algorithm. The weight update equation of the NLMS is given by [Hay02]:

$$\mathbf{w}(n+1) = \mathbf{w}(n) + \frac{\mu_{\text{N}}}{\delta + \|\mathbf{x}(n)\|^2}\mathbf{x}(n)\left(\tilde{d}_1(n) - \mathbf{w}^H(n)\mathbf{x}(n)\right)^* \tag{2.12}$$

where

$$\tilde{d}_1(n) = \begin{cases} d_1(n), & \text{in the training mode} \\ \hat{d}_1(n), & \text{in the decision directed mode} \end{cases} \tag{2.13}$$

In addition, the normalized step-size $\mu_{\text{N}} \in (0, 2)$ controls the adaptation speed and δ is introduced to increase stability when $\|\mathbf{x}(n)\|^2$ is too small.

It should be noted that the NLMS suffers from slow convergence when the input data are correlated. This is the case for instance when dealing with CDMA systems where correlations between users codes result in severe MAI. To improve the convergence speed in that case, the affine projection algorithm can be used.

2.2.3.2 The APA algorithm

The APA has been extensively exploited in applications involving speech and acoustics, especially for acoustic echo cancelation of voice [Gay95] [Hay03]. Nevertheless, its applications in mobile wireless communications are still limited.
The APA can be formulated as the minimization of the squared Euclidean norm of the change in the weight vector [Hay02]:

$$\min\|\Delta\mathbf{w}(n+1)\|^2 = \min\|\mathbf{w}(n+1) - \mathbf{w}(n)\|^2 \tag{2.14}$$

subject to L constraints:

$$\begin{aligned} \mathbf{x}^H(n)\mathbf{w}(n+1) &= \tilde{d}_1(n) \\ \mathbf{x}^H(n-1)\mathbf{w}(n+1) &= \tilde{d}_1(n-1) \\ &\vdots \\ \mathbf{x}^H(n-L+1)\mathbf{w}(n+1) &= \tilde{d}_1(n-L+1) \end{aligned} \tag{2.15}$$

If we define:

$$\mathbf{X}(n) = \begin{bmatrix} \mathbf{x}(n) & \mathbf{x}(n-1) & \cdots & \mathbf{x}(n-L+1) \end{bmatrix} \tag{2.16}$$

$$\mathbf{d}(n) = \begin{bmatrix} \tilde{d}_1(n) & \tilde{d}_1(n-1) & \cdots & \tilde{d}_1(n-L+1) \end{bmatrix}^T \tag{2.17}$$

$$\mathbf{e}(n) = \mathbf{d}(n) - \mathbf{X}^H(n)\mathbf{w}(n) \tag{2.18}$$

then, the solution of the above optimization problem (2.14)-(2.15) using the method of Lagrange multipliers leads to the APA weight update equation [Hay02]:

$$\mathbf{w}(n+1) = \mathbf{w}(n) + \mu_{\text{N}}\mathbf{X}(n)\left[\delta\mathbf{I}_L + \mathbf{X}^H(n)\mathbf{X}(n)\right]^{-1}\mathbf{e}^*(n) \tag{2.19}$$

where $\mu_{\text{N}} \in (0,2)$ is the step-size and δ is a small positive constant used for regularization. It should be noted that when $L = 1$, the weight update equation of the APA (2.19) reduces to that of the NLMS algorithm (2.12). Indeed, whereas the NLMS updates the weights $\mathbf{w}(n)$ by using the current input vector $\mathbf{x}(n)$, the APA updates the weights by using the current and the $L-1$ delayed input vectors. Therefore, the APA can be viewed as a generalization of the NLMS [Mor96].
In both APA and NLMS algorithms, the step-size μ_{N} that governs the convergence rate and the steady state excess mean square error must be carefully adjusted. To meet the conflicting requirement of fast convergence and low steady state excess mean square error, Ruweished *et al.* [Ruw06] have proposed to study the relevance of variable step-size NLMS and APA algorithms recently developed in [Shi04]. They showed that the variable step-size algorithms can provide better convergence features and can yield lower BER results than the fixed step-size algorithms.

2.2.3.3 The RLS algorithm

The RLS algorithm aims at minimizing the weighted least square error [Hay02] [Naj06]:

$$J_{RLS} = \sum_{i=0}^{n}\lambda^{n-i}|e(i,n)|^2 = \sum_{i=0}^{n}\lambda^{n-i}\left|\tilde{d}_1(i) - \mathbf{w}^H(n)\mathbf{x}(i)\right|^2 \tag{2.20}$$

where $0 < \lambda < 1$ is the exponential forgetting factor.
The RLS algorithm operates in three steps at each recursion:

$$\mathbf{k}(n+1) = \frac{\mathbf{P}(n)\mathbf{x}(n+1)}{\lambda + \mathbf{x}^H(n+1)\mathbf{P}(n)\mathbf{x}(n+1)} \tag{2.21}$$

$$\mathbf{w}(n+1) = \mathbf{w}(n) + \mathbf{k}(n+1)\left(\tilde{d}_1(n+1) - \mathbf{w}^H(n)\mathbf{x}(n+1)\right)^* \tag{2.22}$$

$$\mathbf{P}(n+1) = \frac{1}{\lambda}\left(\mathbf{P}(n) - \mathbf{k}(n+1)\mathbf{x}^H(n+1)\mathbf{P}(n)\right) \tag{2.23}$$

with $\mathbf{P}(0) = \delta^{-1}\mathbf{I}_N$, where δ is a small positive constant.

Table 2.1: Computational cost of the various adaptive filters when considering two design structures for the receiver. Usually, $L \ll N$.

Adaptive filter	Separate Detection (SD)	Joint Detection (JD)
NLMS	$O(MN)$	$O(MN)$
APA	$O(MNL^2)$	$O(MNL^2)$
RLS	$O(MN^2)$	$O(M^2N^2)$

2.2.3.4 Computational cost of the various implementations

Table 2.1 summarizes the computational complexity of the SD and JD receiver structures when implemented with the various adaptive filters (NLMS, APA and RLS). While the NLMS algorithm has the lowest complexity, the APA algorithm has a scalable complexity by changing the scalable parameter L. Thus, the complexity of the APA reduces to that of the NLMS when $L = 1$ and approaches that of the RLS when L is high. The parameter L is usually selected to be much less than the filter order (i.e., $L \ll N$).
In addition, the order of complexity of the SD and JD receiver structures are the same when considering either the NLMS or the APA, but this is not the case when using the RLS algorithm where the JD structure has higher complexity than the SD structure. Therefore, using the APA in a JD receiver structure is *a priori* preferable.

2.2.4 Simulation results

In this subsection, we carry out a comparative study between NLMS, APA and RLS when they are used to implement the SD or JD receiver structure. In addition, the BER performance of these receivers is compared with that of the correlator based receiver proposed in [Kon96].

An asynchronous uplink transmission scenario is considered with $K = 6$ active users and M carriers. The spreading sequences of all users are gold codes of length $N = 31$. The desired user is the first one (i.e., $k = 1$), and all other users are interferers on the desired user with ISR defined by equation (1.50). The delays are chosen to satisfy $\tau_k = 2(k-1)MT_c,\ \ 1 \leq k \leq K$. As a Rayleigh fading is considered, the channels $\{h_{mk}\}_{m=1,2,\cdots,M;k=1,2,\cdots,K}$ are generated according to the complex Gaussian distribution with zero-mean and unit-variance. In all of the simulations, a training period of 500 symbols is used for the various adaptive algorithms. This long training period is usually available at the start of the transmission [Tsa96].

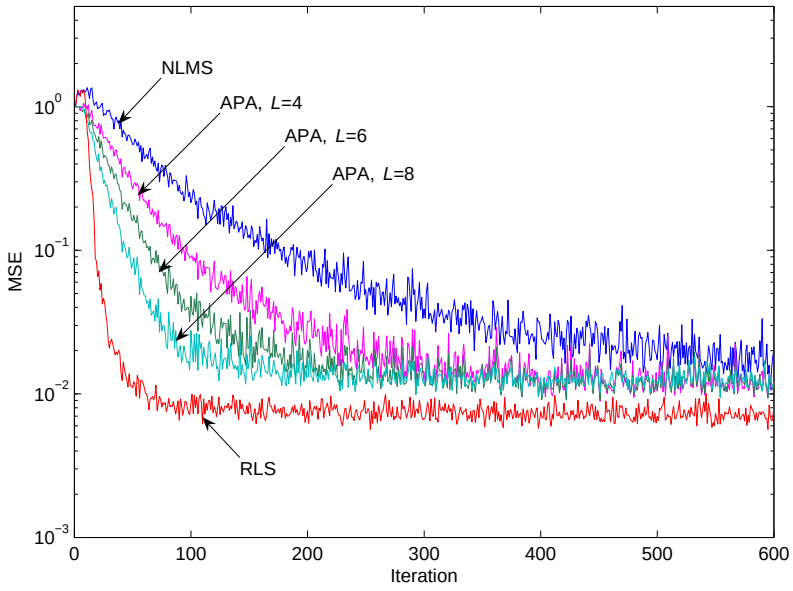

Figure 2.3: Convergence characteristics of NLMS, APA and RLS for the JD receiver structure. The SNR of the desired user is assigned to 20 dB. ISR=10 dB and $M = 3$.

Our simulations confirm that the higher L, the higher the convergence speed of the APA algorithm. In Figure 2.3, APA converges faster than the NLMS. Satisfactory MSE convergence is also observed in around 200 iterations, compared to about 550 for the NLMS. Nevertheless, the RLS algorithm converges more quickly. From Figure 2.4 and Figure 2.5, the JD receiver outperforms the SD one with the three adaptive algorithms, when considering the BER. In addition, both receivers outperform the correlator based receiver which is saturated when the ISR=10 dB. Furthermore, increasing L in the APA yields much better BER performance than that of the NLMS and comparable performance with that of the RLS. Besides, APA makes it possible to reduce the computational cost when compared with the RLS, especially with the JD receiver structure (see Table 2.1). For the various reasons mentioned above, APA in the JD receiver structure corresponds to a trade-off between BER performance and complexity.

Figure 2.6 shows the effects of the number of carriers on the BER performance of the various receivers. We can notice that a significant frequency diversity gain is obtained when increasing the number of carriers from $M = 1$ to $M = 3$. In addition, the SD and JD receivers provide the same performance when $M = 1$. Figure 2.7 shows the effects of the ISR on the BER performance of the various receivers. When increasing the ISR, the performance of the correlator based receiver degrade greatly, whereas the SD and JD receivers are near-far resistant and yield much better BER than the correlator based one.

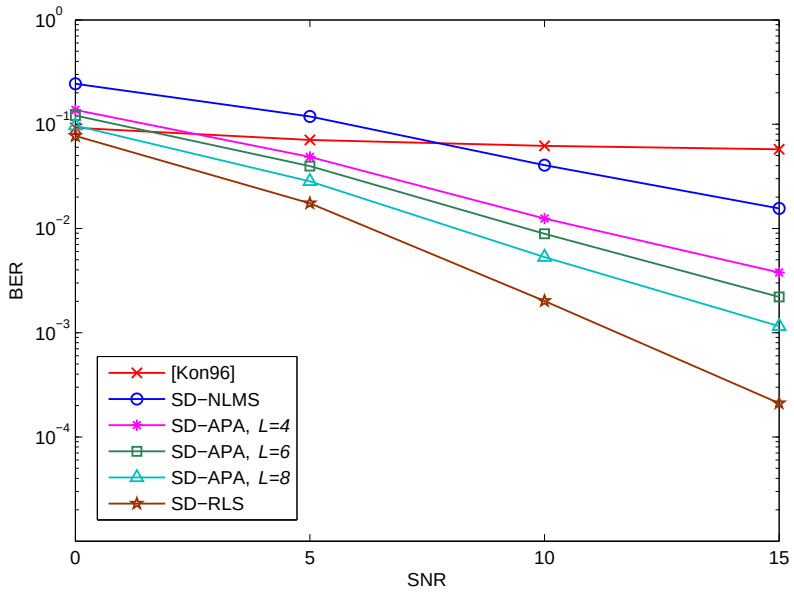

Figure 2.4: BER performance of the SD receiver structure with the various adaptive filters compared with that of the correlator based receiver [Kon96]. ISR=10 dB and $M = 3$.

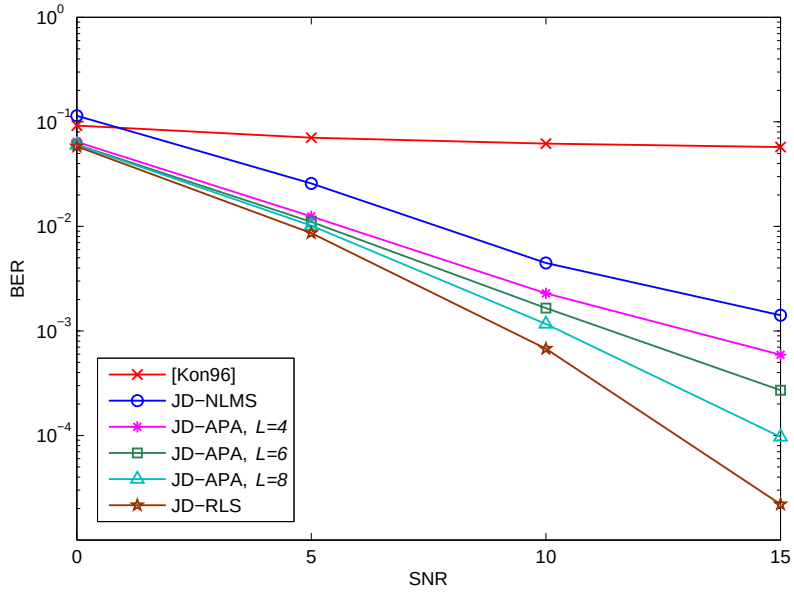

Figure 2.5: BER performance of the JD receiver structure with the various adaptive filters compared with that of the correlator based receiver [Kon96]. ISR=10 dB and $M = 3$.

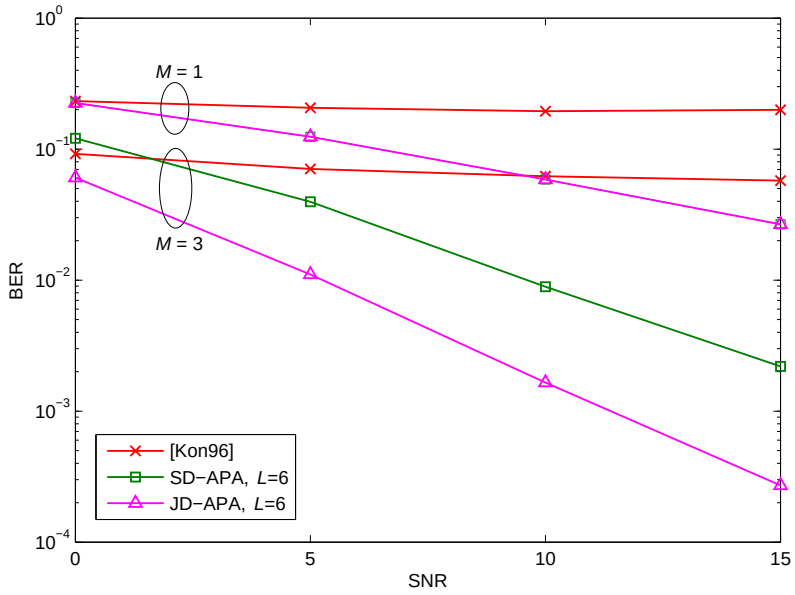

Figure 2.6: BER performance of the various receivers for number of carriers equal to $M = 1$ and $M = 3$. ISR=10 dB.

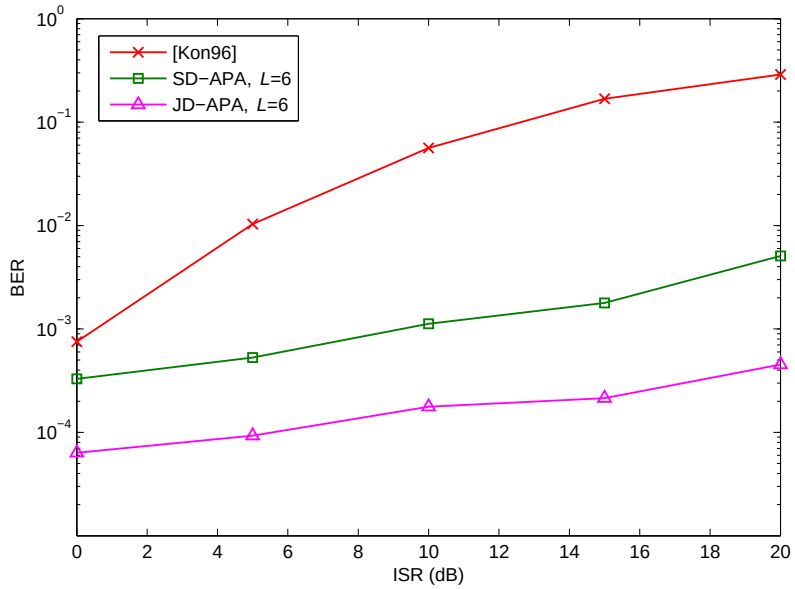

Figure 2.7: Effects of the interference to signal ratio (ISR) on the BER performance of the various receivers. $M = 3$ and SNR=15dB.

Although the adaptive MMSE receivers provide significant results, they require a training data sequence for every active user. As an alternative, we propose to investigate blind adaptive multiuser detection receivers in the next section.

2.3 Blind adaptive multiuser detection receivers

Unlike the adaptive MMSE receivers, blind adaptive interference suppression receivers do not require training sequences. It has been shown in the original work by Honig *et al.* [Hon95] that, by knowing only the spreading code and the timing of the desired user, the MMSE multiuser receiver can be implemented blindly. They have developed the first blind LMS-based multiuser detection receiver in the absence of multi-path fading. It is based on the minimization of a MOE criterion by using a stochastic gradient approach. However, this method is not convenient in a time-varying environment. For this reason, other approaches have been proposed.

- On the one hand, blind detectors based on RLS [Poo97] and Kalman filter [Zha02] algorithms make it possible to improve the convergence features and tracking capabilities in a dynamic environment, such as in the case of birth or death of interferers.

- On the other hand, Mucchi *et al.* [Muc04] have proposed a derived version of the pioneering blind LMS-based detector [Hon95], which makes it possible to operate in a time-varying frequency-selective multi-path fading channels. For this purpose, they first complete channel compensation and time alignment on the signal replicas along each independent path and then combine the resulting signals before or after multiuser detection, resulting in two receiver schemes. The first scheme is called the RAKE blind adaptive multiuser detection receiver where combining is performed after multiuser detection. The second scheme is called pre-detection combining blind adaptive multiuser detection receiver where combining is performed before multiuser detection. The pre-detection combining based receiver has the advantage of using only one detector for the combined replicas instead of one detector for each signal replica. In addition, according to [Muc04], this yields a remarkable complexity reduction, more reliable decision variable and more robust convergence procedure.

However, the above blind adaptive multiuser detection techniques were only developed for single-carrier DS-CDMA systems. In this section, our purpose is to design blind adaptive multiuser detection receivers for synchronous MC-DS-CDMA systems in Rayleigh fading

channels. For this purpose, we first reformulate the ideas presented in [Muc04] to design two blind adaptive receivers for MC-DS-CDMA systems. Namely:

- the first receiver provides a blind adaptive multiuser detector for each carrier followed by a post-detection combiner,

- the second receiver consists of a pre-detection combiner followed by a single blind adaptive multiuser detector.

To implement them, we have proposed a blind APA-like multiuser detector [Jam05a]. The proposed detector can be seen as a generalization of the blind LMS-based detector [Hon95], on the basis of multiple delayed input signal vectors. A comparative study is then carried out with existing blind LMS [Hon95] and Kalman filter [Zha02] based multiuser detectors initially developed for single-carrier DS-CDMA systems.

2.3.1 Receiver structure with post-detection combining

In this subsection, we propose a blind adaptive multiuser receiver with post-detection combining for synchronous MC-DS-CDMA systems in time-varying fading channels (see Figure 2.8). Thus, to retrieve the symbol sequence of the first user $d_1(n)$, we first recall the $N \times 1$ discrete-time received vector over the m^{th} carrier given in (1.46), as follows:

$$\mathbf{x}_m(n) = \sqrt{P_1} d_1(n) h_m(n) \mathbf{c}_1 + \sum_{k=2}^{K} \sqrt{P_k} d_k(n) h_m(n) \mathbf{c}_k + \boldsymbol{\eta}_m(n) \tag{2.24}$$

Here, as our goal is to suppress the MAI, we assume that the fading processes $\{h_m(n)\}_{m=1,2,\cdots,M}$ are available at the receiver[6]. Thus, channel compensation over the m^{th} carrier can be performed in the following manner:

$$\begin{aligned} \underline{\mathbf{x}}_m(n) &= \mathrm{Re}\left(h_m^*(n)\mathbf{x}_m(n)\right) \\ &= \sqrt{P_1} d_1(n) |h_m(n)|^2 \mathbf{c}_1 + \sum_{k=2}^{K} \sqrt{P_k} d_k(n) |h_m(n)|^2 \mathbf{c}_k + \mathrm{Re}\left(h_m^*(n)\boldsymbol{\eta}_m(n)\right) \end{aligned} \tag{2.25}$$

where the multiplication with $h_m^*(n) = |h_m(n)| e^{-j\phi_m(n)}$ compensates for the phase and weights the signal amplitude by a positive time-varying factor $|h_m(n)|^2$.

[6]The estimation of the channel fading processes will be investigated in the next chapter.

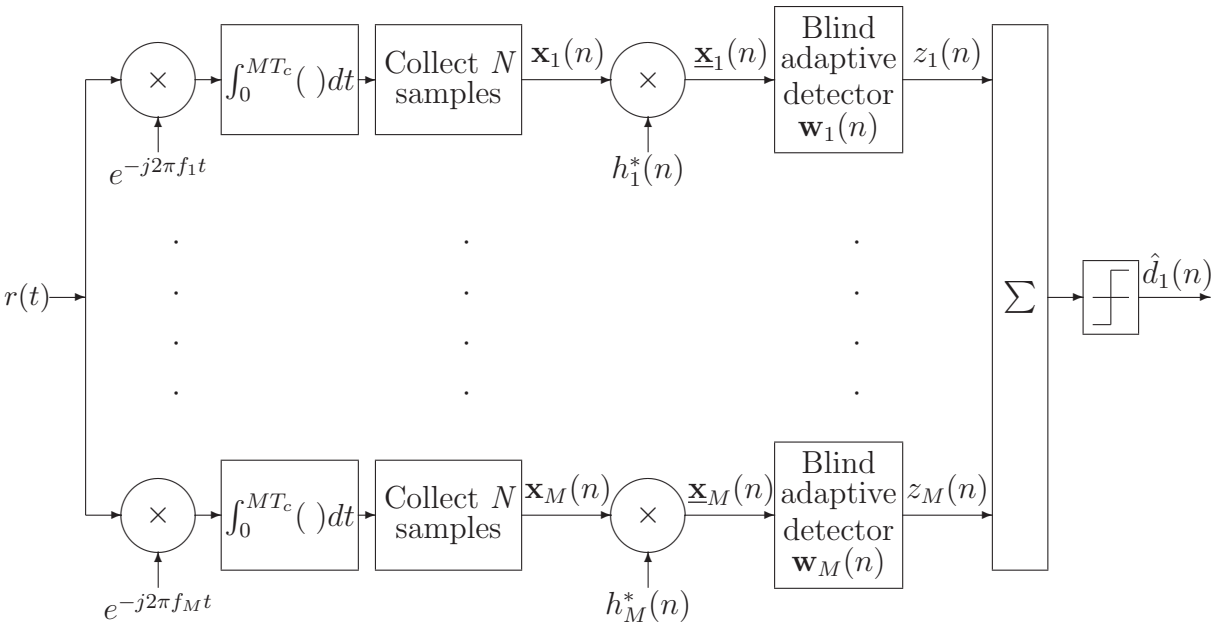

Figure 2.8: Blind adaptive receiver structure with post-detection combining.

After channel compensation, the resulting vector $\underline{\mathbf{x}}_m(n)$ over the m^{th} carrier defines the input to a blind adaptive multiuser detector whose canonical linear representation for user 1 was firstly established in [Hon95], as follows:

$$\mathbf{w}_m(n) = \mathbf{c}_1 + \mathbf{a}_m(n) \tag{2.26}$$

subject to the constraint:

$$\mathbf{c}_1^T \mathbf{a}_m(n) = 0 \tag{2.27}$$

or equivalently, since $\mathbf{c}_1^T \mathbf{c}_1 = 1$:

$$\mathbf{c}_1^T \mathbf{w}_m(n) = 1 \tag{2.28}$$

where $\mathbf{c}_1$ is the normalized spreading vector of the first user and $\mathbf{a}_m(n)$ is the adaptive part of the detector. Thus, the practical implementation of this detector is achieved by means of two orthogonal filters (see Figure 2.9): the spreading code of the desired user $\mathbf{c}_1$ and the adaptive part $\mathbf{a}_m(n)$ that is used to eliminate the MAI.
The detector $\mathbf{w}_m(n)$ is designed to minimize the MOE cost function:

$$J_{MOE}[\mathbf{w}_m(n)] = E\left[|\mathbf{w}_m^T(n)\underline{\mathbf{x}}_m(n)|^2\right] \tag{2.29}$$

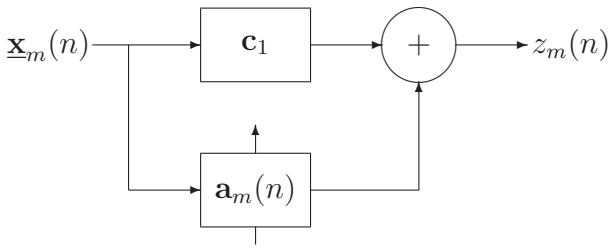

Figure 2.9: Blind adaptive multiuser detector $\mathbf{w}_m(n) = \mathbf{c}_1 + \mathbf{a}_m(n)$.

It should be noted that the MOE criterion given by (2.29) is related to a "scaled" version of the MSE criterion given by (2.4) as follows:

$$\begin{aligned} J_{MSE}[\mathbf{w}_m(n)] &= E\left[\left|\sqrt{P_1}d_1(n) - \mathbf{w}_m^T(n)\underline{\mathbf{x}}_m(n)\right|^2\right] \\ &= J_{MOE}[\mathbf{w}_m(n)] - P_1 \end{aligned} \tag{2.30}$$

where it is assumed that $E[|h_m(n)|^2] = \sigma_h^2 = 1$. As P_1 is a constant, minimizing the MOE criterion will also minimize the MSE criterion. Hence, the MOE multiuser detector is equivalent to the MSE based one [Hon95]. Since the MOE criterion does not depend on the data symbol $d_1(n)$, there will be no need for training sequences. Therefore, this leads to the blind adaptive implementations that will be presented in subsection 2.3.3.
The outputs of the blind adaptive detectors over all carriers are finally combined by a post-detection combiner resulting in the following decision about the desired user data symbol:

$$\hat{d}_1(n) = \text{sgn}\left(\sum_{m=1}^{M} \mathbf{w}_m^T(n)\underline{\mathbf{x}}_m(n)\right) \tag{2.31}$$

In the next subsection, as the post-detection based receiver structure requires M blind adaptive multiuser detectors, we propose a blind adaptive receiver based on pre-detection combining which requires only one multiuser detector.

2.3.2 Receiver structure with pre-detection combining

The proposed blind adaptive MOE receiver with pre-detection MRC is shown in Figure 2.10. Thus, after channel compensation and time alignment, the resulting vectors $\{\underline{\mathbf{x}}_m(n)\}_{m=1,2,\cdots,M}$ given by (2.25) are combined before detection as follows:

$$\underline{\mathbf{x}}_{tot}(n) = \sum_{m=1}^{M} \underline{\mathbf{x}}_m(n) \tag{2.32}$$

The combined vector $\underline{\mathbf{x}}_{tot}(n)$ is then processed with a single blind adaptive multiuser detector $\mathbf{w}(n) = \mathbf{c}_1 + \mathbf{a}(n)$ as in (2.26), in order to minimize the following MOE criterion:

$$J_{MOE}[\mathbf{w}(n)] = E\left[|\mathbf{w}^T(n)\underline{\mathbf{x}}_{tot}(n)|^2\right] \tag{2.33}$$

where $\mathbf{a}(n)$ is the adaptive part of the detector which satisfies $\mathbf{c}_1^T\mathbf{a}(n) = 0$.
Finally, the symbol decision of the desired user can be obtained as follows:

$$\hat{d}_1(n) = \text{sgn}\left(\mathbf{w}^T(n)\underline{\mathbf{x}}_{tot}(n)\right) \tag{2.34}$$

where the detector $\mathbf{w}(n)$ will be implemented adaptively in the next subsection.
It should be noted that the pre-detection combining receiver structure has the advantage of reducing greatly the computational cost by using only one detector for the combined vector instead of a detector for each carrier.

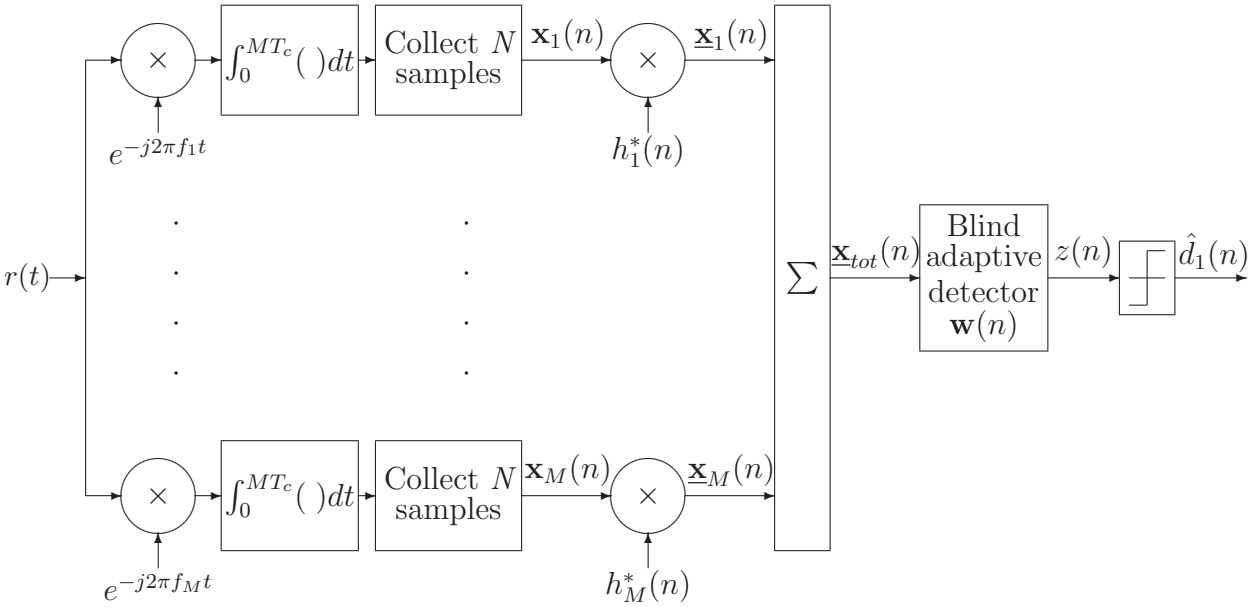

Figure 2.10: Blind adaptive receiver structure with pre-detection combining.

To implement the post-detection and pre-detection based blind adaptive receivers, various blind adaptive algorithms are considered in the next subsection.

2.3.3 Blind adaptive implementation

To use unique notations, let $\underline{\mathbf{x}}(n)$ and $\mathbf{w}(n)$ respectively denote :

- the received vector $\underline{\mathbf{x}}_m(n)$ and the filter weights $\mathbf{w}_m(n)$ when considering the post-detection receiver structure,
- the combined received vector $\underline{\mathbf{x}}_{tot}(n)$ and the filter weights $\mathbf{w}(n)$ when using the pre-detection receiver structure.

2.3.3.1 Normalized blind LMS based multiuser detector

By using a stochastic gradient approach, Honig *et al.* [Hon95] have proposed to derive an adaptive implementation for the detector (2.26) that minimizes the MOE criterion (2.29). Thus, they first evaluated the unconstraint gradient of the MOE cost function (2.29) as follows:

$$\nabla J_{MOE}[\mathbf{w}(n)] = \nabla E\left[|\mathbf{w}^T(n)\underline{\mathbf{x}}(n)|^2\right] = 2\left[\mathbf{w}^T(n)\underline{\mathbf{x}}(n)\right]\underline{\mathbf{x}}(n) \tag{2.35}$$

The projected gradient, orthogonal to $\mathbf{c}_1$ is then obtained:

$$\nabla J_{MOE}[\mathbf{w}(n)]_{\mathbf{c}_1} = 2\left[\mathbf{w}^T(n)\underline{\mathbf{x}}(n)\right]\left[\underline{\mathbf{x}}(n) - \left(\mathbf{c}_1^T\underline{\mathbf{x}}(n)\right)\mathbf{c}_1\right] \tag{2.36}$$

Therefore, a stochastic gradient blind algorithm to update the adaptive part of the detector can be written as follows [Hon95] :

$$\begin{aligned}\mathbf{a}(n) &= \mathbf{a}(n-1) - \mu\nabla J_{MOE}[\mathbf{w}(n-1)]_{\mathbf{c}_1} \\ &= \mathbf{a}(n-1) - \mu z(n)\left[\underline{\mathbf{x}}(n) - z_{\text{MF}}(n)\mathbf{c}_1\right]\end{aligned} \tag{2.37}$$

where $z(n) = \mathbf{w}^T(n-1)\underline{\mathbf{x}}(n)$ is the output of the detector, $z_{\text{MF}}(n) = \mathbf{c}_1^T\underline{\mathbf{x}}(n)$ is the output of the conventional matched-filter, and μ is the step-size that controls the adaptation speed.
To avoid the gradient noise amplification problem, a normalized version of this algorithm (as the NLMS algorithm) can be written as follows [Wen01]:

$$\mathbf{a}(n) = \mathbf{a}(n-1) - \frac{\mu_{\text{N}}}{\delta + \|\underline{\mathbf{x}}(n)\|^2} z(n)\left[\underline{\mathbf{x}}(n) - z_{\text{MF}}(n)\mathbf{c}_1\right] \tag{2.38}$$

where $\mu_{\text{N}} \in (0, 2)$ is the normalized step-size and δ is a small positive regularization constant that insures stability when $\|\underline{\mathbf{x}}(n)\|^2$ is too small.

2.3.3.2 Blind APA-like multiuser detector

To improve the convergence features in high MAI environments and time-varying fading scenarios, we propose to generalize the algorithm in (2.38) by using L delayed input signal vectors [Jam05a]. Toward this end, we first define the following received and code matrices of L column each:

$$\mathbf{X}(n) = \left[\begin{array}{cccc} \underline{\mathbf{x}}(n) & \underline{\mathbf{x}}(n-1) & \cdots & \underline{\mathbf{x}}(n-L+1) \end{array} \right] \tag{2.39}$$

$$\mathbf{C}_1 = \left[\begin{array}{cccc} \mathbf{c}_1 & \mathbf{c}_1 & \cdots & \mathbf{c}_1 \end{array} \right] \tag{2.40}$$

In addition, the MOE cost function in (2.29) is modified to account for L delayed input signal vectors:

$$J_{MOE}[\mathbf{w}(n)] = E\left[\|\mathbf{X}^T(n)\mathbf{w}(n)\|^2\right] \tag{2.41}$$

Taking the unconstraint gradient of the MOE cost function:

$$\nabla J_{MOE}[\mathbf{w}(n)] = \nabla E\left[\|\mathbf{X}^T(n)\mathbf{w}(n)\|^2\right] = 2\mathbf{X}(n)\left[\mathbf{X}^T(n)\mathbf{w}(n)\right] \tag{2.42}$$

The projected gradient, orthogonal to $\mathbf{C}_1$ satisfies:

$$\nabla J_{MOE}[\mathbf{w}(n)]_{\mathbf{C}_1} = 2\left[\mathbf{X}(n) - \mathbf{C}_1\left(\mathbf{C}_1^T\mathbf{X}(n)\right)\right]\left[\mathbf{X}^T(n)\mathbf{w}(n)\right] \tag{2.43}$$

Then, a stochastic gradient algorithm that updates the adaptive part of the detector (2.26) can be written as follows:

$$\mathbf{a}(n) = \mathbf{a}(n-1) - \mu\nabla J_{MOE}[\mathbf{w}(n-1)]_{\mathbf{C}_1} \tag{2.44}$$

where μ is the step-size.

Substituting (2.43) in (2.44) and introducing a factor $[\delta\mathbf{I}_L + \mathbf{X}^T(n)\mathbf{X}(n)]^{-1}$ similar to that in the APA, a new blind algorithm (APA-like) to update $\mathbf{a}(n)$ can be expressed by [Jam05a]:

$$\mathbf{a}(n) = \mathbf{a}(n-1) - \mu_{\text{N}}\left[\mathbf{X}(n) - \mathbf{C}_1\mathbf{Z}_{\text{MF}}(n)\right]\left[\delta\mathbf{I}_L + \mathbf{X}^T(n)\mathbf{X}(n)\right]^{-1}\mathbf{z}(n) \tag{2.45}$$

where $\mathbf{z}(n) = \mathbf{X}^T(n)\mathbf{w}(n-1)$, $\mathbf{Z}_{\text{MF}}(n) = \mathbf{C}_1^T\mathbf{X}(n)$, $\mu_{\text{N}} \in (0,2)$ and δ is the regularization constant.

To insure that the orthogonally condition $\mathbf{c}_1^T\mathbf{a}(n) = 0$ is satisfied at each iteration, we replace $\mathbf{a}(n)$ by its orthogonal projection onto $\mathbf{c}_1$:

$$\mathbf{a}(n) = \mathbf{a}(n) - \left(\mathbf{c}_1^T\mathbf{a}(n)\right)\mathbf{c}_1 \tag{2.46}$$

It should be noted that when $L = 1$, the blind APA-like multiuser detector (2.45) reduces to the normalized blind LMS multiuser detector (2.38).

2.3.3.3 Blind multiuser detection based on Kalman filtering

In [Zha02], Zhang *et al.* have proposed to use an alternative standard representation for the blind adaptive multiuser detector:

$$\mathbf{w}(n) = \mathbf{c}_1 - \mathbf{A}_1\mathbf{a}(n) \tag{2.47}$$

where the columns of the $N \times N-1$ matrix $\mathbf{A}_1$ span the null space of $\mathbf{c}_1$, i.e.:

$$\mathbf{c}_1^T\mathbf{A}_1 = \mathbf{0} \tag{2.48}$$

It should be noted that $\mathbf{A}_1$ can be pre-computed off-line via one of many orthogonalization procedures such as the Gram-Schmidt orthogonalization. Unlike (2.26), the adaptive part $\mathbf{a}(n)$ in (2.47) is now of size $(N-1) \times 1$ and has the advantage of being unconstraint.
Let us define the output of the detector as follows:

$$z(n) = \mathbf{w}^T(n)\underline{\mathbf{x}}(n) \tag{2.49}$$

then $z(n)$ has zero-mean and its variance is given by (due to equations (2.29) and (2.30)):

$$E[|z(n)|^2] = J_{MOE}[\mathbf{w}(n)] = J_{MSE}[\mathbf{w}(n)] + P_1 \tag{2.50}$$

Thus, when the detector is optimal (i.e., $J_{MSE}[\mathbf{w}(n)]$ attains its MMSE value), the variance of $z(n)$ corresponds to the minimum MOE and is dominated by the power of the desired user P_1.
Substituting (2.47) in (2.49) results in the following measurement equation:

$$z_{\text{MF}}(n) = \underline{\mathbf{d}}^T(n)\mathbf{a}(n) + z(n) \tag{2.51}$$

where $z_{\text{MF}}(n) = \mathbf{c}_1^T\underline{\mathbf{x}}(n)$ and $\underline{\mathbf{d}}^T(n) = \underline{\mathbf{x}}^T(n)\mathbf{A}_1$.
If the detector is assumed to be time-invariant, one can write:

$$\mathbf{a}(n) = \mathbf{a}(n-1) \tag{2.52}$$

As (2.51) and (2.52) define a state-space representation of the adaptive part of the detector, Kalman filtering makes it possible to recursively update $\mathbf{a}(n)$ [Zha02].

2.3.3.4 Computational cost of the various algorithms

Here, we provide the computational cost of the various blind adaptive multiuser detectors when used to implement the post-detection and pre-detection combining receiver structures. According to Table 2.2, the pre-detection combining receiver structure with the

Table 2.2: Computational complexity of the various blind adaptive multiuser detectors when considering the post-detection and pre-detection combining receiver structures.

Blind adaptive detector	Post-detection combining	Pre-detection combining
LMS based detector [Hon95]	$O(MN)$	$O(N)$
APA-like detector	$O(MNL^2)$	$O(NL^2)$
Kalman based detector [Zha02]	$O(MN^2)$	$O(N^2)$

various blind adaptive detectors has the advantage of greatly reducing the computational cost when compared with the post-detection combining based one. In addition, the proposed blind APA-like detector has the advantage of providing a scalable complexity by adjusting the parameter L which is usually much less than the filter length (i.e., $L \ll N$). The scalable complexity of the APA-like detector can be traded with the performance as we will see in the simulation results presented in the next subsection. Therefore, the APA-like detector with the pre-detection combining scheme is *a priori* preferable to design the receiver.

2.3.4 Simulation results

In this subsection, we first carry out a comparative study between the following blind adaptive multiuser detectors:

- the normalized version of the standard blind LMS multiuser detector [Hon95],
- the proposed blind APA-like multiuser detector,
- the blind Kalman filter based multiuser detector [Zha02],

when they are used to implement the pre-detection and post-detection combining receiver structures.
In addition, we compare the performances of the proposed blind APA-like detector with the training based APA filter presented in subsection 2.2.3.

A synchronous MC-DS-CDMA system with K active users and $M = 4$ carriers is considered. The spreading sequences used are gold codes of length $N = 31$. The fading processes $\{h_m(n)\}_{m=1,2,\cdots,M}$ are generated according to the complex Gaussian distribution with zero-mean and unit-variance. User 1 is assumed to be the desired user with SNR per transmitted carrier kept constant at 10 dB.

In the first example, a high MAI scenario is assumed with 14 multiple-access interfering users (i.e., $K = 15$), among which five users have ISR (see equation 1.50) of 10 dB each, five users have ISR of 20 dB each, two users have ISR of 30 dB each and two other users have ISR of 40 dB each. According to Figure 2.11, the pre-detection combining receiver slightly outperforms the post-detection receiver with the various blind adaptive detectors, when considering the BER performence. In addition, the proposed blind APA-like detector provides much better BER performance and convergence features than the normalized blind LMS detector. Nevertheless, the blind Kalman detector yields the best BER performance and convergence features, but at the price of increased computational cost (see Table 2.2). Figure 2.12 demonstrates the average Signal to Interference-plus-Noise Ratio (SINR) performance of the various blind detectors in the pre-detection combining receiver. The average SINR is defined as follows:

$$\mathrm{SINR}(n) = \frac{\sum_{l=1}^{loop} |\mathbf{w}^T(n)(\sqrt{P_1}d_1(n)\mathbf{c}_{1,tot})|^2}{\sum_{l=1}^{loop} |\mathbf{w}^T(n)[\underline{\mathbf{x}}(n) - \sqrt{P_1}d_1(n)\mathbf{c}_{1,tot}]|^2} \tag{2.53}$$

where

$$\mathbf{c}_{1,tot} = \sum_{m=1}^{M} |h_m(n)|^2 \mathbf{c}_1 \tag{2.54}$$

and the average is performed over $loop = 300$. The SINR improvement of the proposed APA-like detector is better than that obtained with the normalized blind LMS detector and approaches that of the blind Kalman detector, when L is getting higher.
Therefore, for the various reasons mentioned above, we recommend to use the blind APA-like detector with the pre-detection combining scheme to design the receiver.

To illustrate the advantages of the blind adaptive MOE detectors over the training based adaptive MMSE filters presented in the previous section, we consider a high MAI scenario with 8 interfering users for which the ISR=20 dB (this hence corresponds to a severe near-far scenario). Figure 2.13 shows the SINR performance improvement of the proposed APA-like detector and the training based APA filter in the pre-detection combining receiver. According to this figure, the blind detector yields better SINR performance improvement than the training based filter which suffers from slow convergence in this severe near-far scenario. This is due to the fact that the blind detector uses the code sequence of the desired user in addition to an adaptive part, whereas the training based filter starts adaptation from a zero initial weight vector. Thus, in a high MAI environment, it is recommended to use a blind adaptive detector to efficiently suppress the MAI and to mitigate the near-far problem.

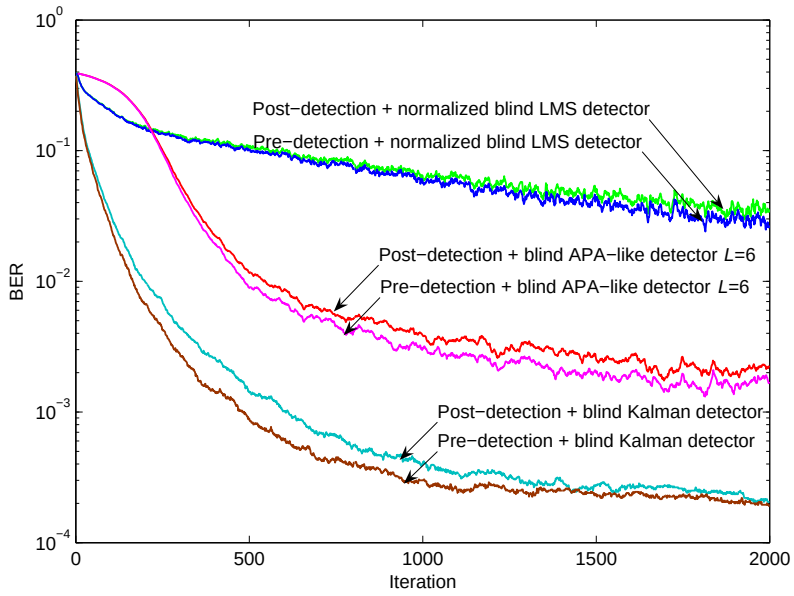

Figure 2.11: BER performance of the pre-detection and post-detection receivers with the various blind adaptive multiuser detectors.

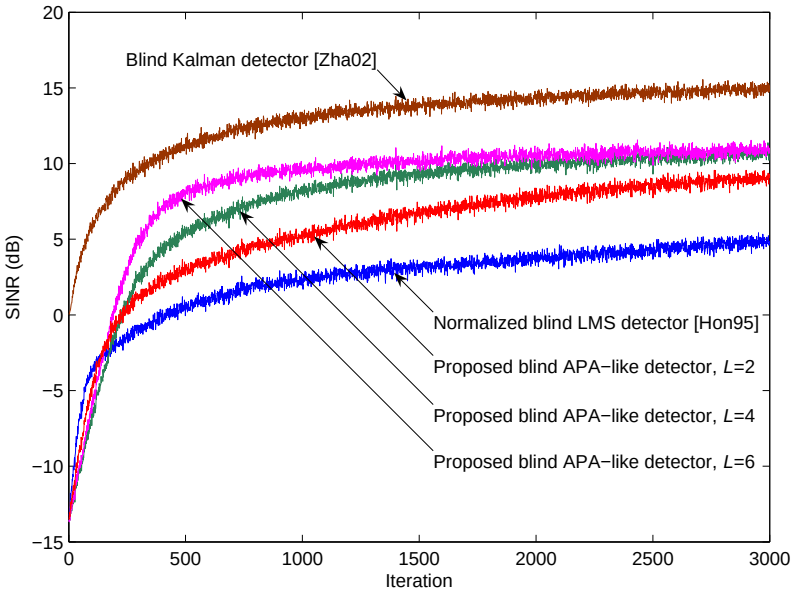

Figure 2.12: SINR improvement of the various blind adaptive detectors in the pre-detection combining receiver.

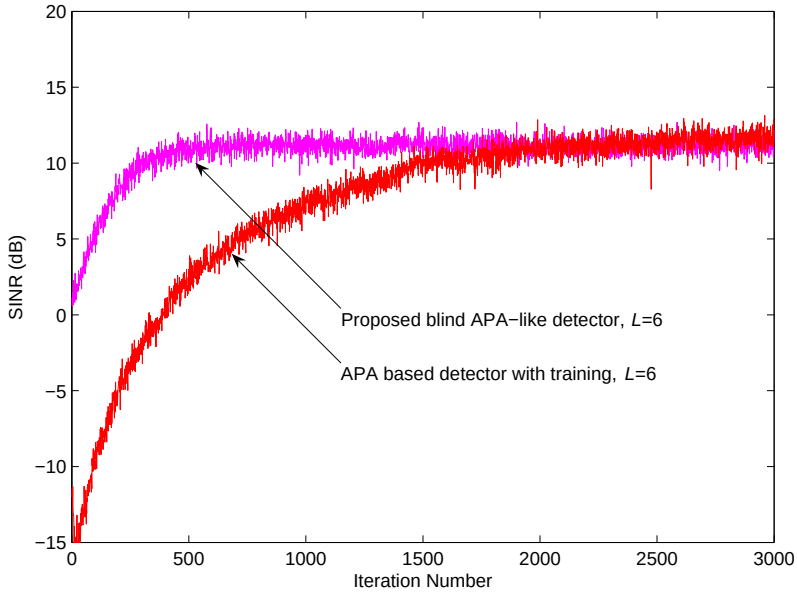

Figure 2.13: SINR improvement of the proposed blind APA-like detector and the training based APA filter in the pre-detection combining receiver.

2.4 Receiver design based on decorrelation detection

As an alternative to the MMSE multiuser receivers, the decorrelating multiuser detector based receivers are designed to completely eliminate the MAI caused by other users, using the spreading sequences of all users [Ver98]. In this section, we first present the state of the art on single-carrier DS-CDMA receiver design based on the decorrelating detector. Then, we propose a MC-DS-CDMA receiver structure consisting of a decorrelating detector, a Kalman filter based channel estimator and a MRC [Jam05b].

2.4.1 Decorrelation detection for single-carrier DS-CDMA

Given the spreading codes of all active users $\{\mathbf{c}_k\}_{k=1,\cdots,K}$, the decorrelating multiuser detector for user 1 can be written in the following form [Ver98]:

$$\mathbf{w}_1 = \sum_{k=1}^{K} [\mathbf{R}^{-1}]_{1k} \mathbf{c}_k \tag{2.55}$$

where $\mathbf{R} = [\ \mathbf{c}_1 \quad \mathbf{c}_2 \quad \cdots \quad \mathbf{c}_K\ ]^T [\ \mathbf{c}_1 \quad \mathbf{c}_2 \quad \cdots \quad \mathbf{c}_K\ ]$ is the normalized cross-correlation matrix of the spreading vectors and $[\mathbf{R}^{-1}]_{ij}$ denotes the $(i,j)^{th}$ element of the inverse of the matrix $\mathbf{R}$.

Such decorrelating multiuser detector satisfies:

$$\mathbf{w}_1^T \mathbf{c}_1 = 1 \tag{2.56}$$

and

$$\mathbf{w}_1^T \mathbf{c}_k = 0, \quad k = 2, \cdots, K \tag{2.57}$$

Equations (2.56) and (2.57) can be verified as follows :

$$\begin{aligned} \mathbf{w}_1^T \mathbf{c}_k &= \sum_{i=1}^{K} [\mathbf{R}^{-1}]_{1i} \mathbf{c}_i^T \mathbf{c}_k \\ &= \sum_{i=1}^{K} [\mathbf{R}^{-1}]_{1i} [\mathbf{R}]_{ik} \\ &= [\mathbf{R}^{-1}\mathbf{R}]_{1k} \\ &= [\mathbf{I}]_{1k} \\ &= \begin{cases} 1, & k = 1 \\ 0, & k = 2, \cdots, K \end{cases} \end{aligned} \tag{2.58}$$

It is obvious from (2.57) that the decorrelating detector is orthogonal to the subspace spanned by the spreading sequences of all interfering users. Therefore, the decorrelating detector can completely eliminate the MAI and can achieve optimal near-far resistance what ever the ISR of the interfering users. It should be emphasized that the decorrelating detector does not require the knowledge of the power of all users.

The decorrelating detector based receiver for synchronous DS-CDMA systems is first proposed by Lupas and Verdú [Lup89]. The generalization to asynchronous DS-CDMA systems is then reported in [Lup90]. However, only AWGN channels are considered. Since then, the extension of these receivers to operate in fading channels has been extensively studied by several authors. Thus, Zvonar *et al.* [Zvo94] have analyzed the performance of the decorrelating detector in slowly time-varying flat-fading channels. Nevertheless, the fading processes are assumed to be available at the receiver. In [Kaw95], Kawahara *et al.* have proposed to combine decorrelation multiuser detection with channel estimation for asynchronous DS-CDMA systems in multi-path slowly fading channels. The fading processes are estimated by using a training based RLS algorithm. In [Sto99], a decorrelating detector based receiver structure is considered for application in rapidly time-varying Rayleigh fading channels where the fading processes are estimated adaptively using the LMS or the RLS algorithm. Recently, in [Wu00], Wu *et al.* have compared the performances of a Kalman filter based channel estimator combined with various multiuser

detectors, such as the decorrelating detector, the decision-feedback detector, the parallel and successive interference cancelation. According to their study, the decorrelating detector is the most robust detector against the MAI and the near-far problem.

2.4.2 MC-DS-CDMA receiver based on decorrelation detection

Although decorrelation multiuser detection have been extensively used for single-carrier DS-CDMA systems, few approaches are developed for MC-DS-CDMA systems. Thus, Yang *et al.* [Yan06] have proposed several decorrelation multiuser detection schemes for TF-domain spreading MC-DS-CDMA systems in AWGN channels. However, they did not investigate these schemes in fading channels. In [Rhe03], the authors have developed a multichannel joint detection scheme for MC-DS-CDMA systems in time-invariant frequency-selective fading channels. The scheme consists of a decorrelating detector followed by a RAKE multi-path combiner for each carrier. Nevertheless, perfect channel knowledge is assumed at the receiver.

Here, we propose to extend, to the multi-carrier case, the combination of decorrelation multiuser detection and Kalman channel estimation scheme presented in [Wu00]. In particular, our scheme [Jam05b] operates in three steps (see Figure 2.14):

1. the decorrelating multiuser detector is carried out along each carrier to completely eliminate the MAI,

2. the fading channel responses, modeled by AR processes, are estimated by using Kalman filtering,

3. the fading processes estimates are fed into a frequency diversity MRC rule to obtain the data symbol estimate.

Thus, to retrieve the desired symbol sequence of the first user $d_1(n)$ from the received signal, let us recall the $N \times 1$ discrete time received vector over the m^{th} carrier given in (1.46), as follows:

$$\mathbf{x}_m(n) = \sqrt{P_1} d_1(n) h_m(n) \mathbf{c}_1 + \sum_{k=2}^{K} \sqrt{P_k} d_k(n) h_m(n) \mathbf{c}_k + \boldsymbol{\eta}_m(n) \tag{2.59}$$

where the fading processes $\{h_m(n)\}_{m=1,2,\cdots,M}$ are assumed to be rapidly time-varying.
At that stage, the received vector at the m^{th} carrier $\mathbf{x}_m(n)$ is processed by the decorrelating

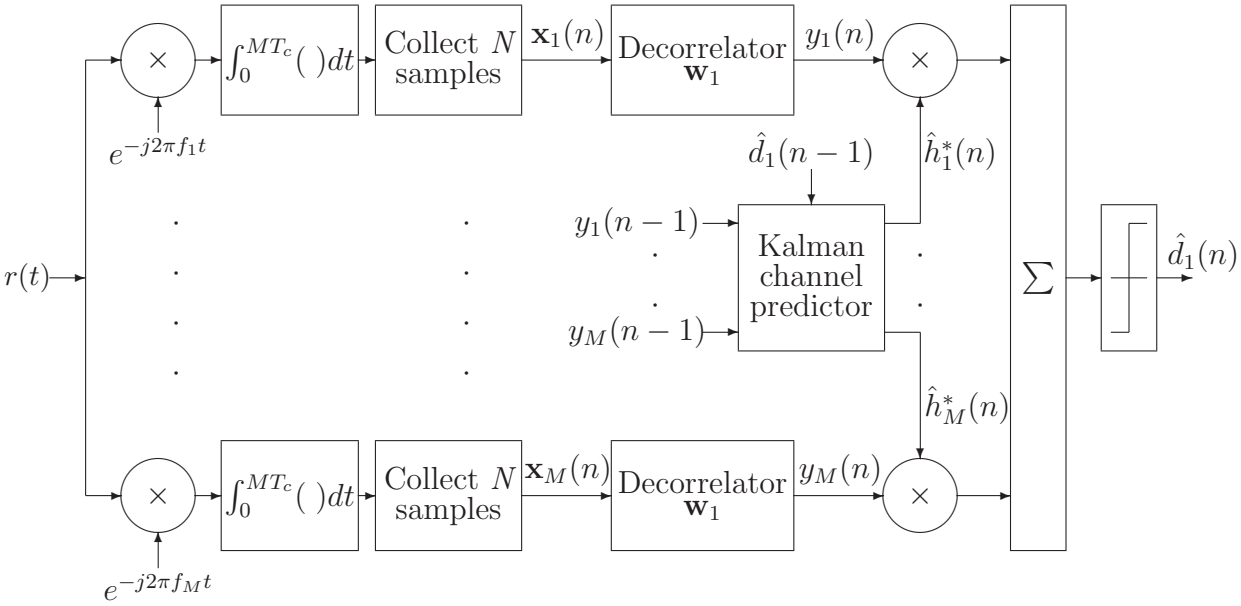

Figure 2.14: MC-DS-CDMA receiver structure with decorrelation detection for user 1.

detector $\mathbf{w}_1$ given by (2.55). By taking into account (2.56) and (2.57), the decorrelating detector yields the following observation:

$$y_m(n) = \mathbf{w}_1^T \mathbf{x}_m(n) = \sqrt{P_1} d_1(n) h_m(n) + v_m(n) \tag{2.60}$$

where $v_m(n) = \mathbf{w}_1^T \boldsymbol{\eta}_m(n)$ is a zero-mean Gaussian noise with variance $\sigma_v^2 = \sigma_\eta^2 [\mathbf{R}^{-1}]_{11}$. From equation (2.60), the decorrelating detector is able to completely eliminate the MAI caused by other users, but at the expense of slightly enhancing the additive noise.
Based on the observations $\{y_m(n)\}_{m=1,\cdots,M}$ and by using an AR model for the fading processes, Kalman filtering can be carried out to provide an estimation of the fading processes $\{\hat{h}_m(n)\}_{m=1,2,\ldots,M}$ [Jam05b] [Jam05c]. The estimation of AR fading channels based on Kalman filtering will be investigated in chapter 3. This also includes the development of several channel estimation techniques that can be directly applied to the proposed receiver in Figure 2.14.
Finally, MRC makes it possible to provide the estimate of the desired user data symbol as follows:

$$\hat{d}_1(n) = \text{sgn}\left(\text{Re}\left(\sum_{m=1}^{M} h_m^*(n) y_m(n)\right)\right) \tag{2.61}$$

2.4.3 Simulation results

In this subsection, we first carry out a comparative simulation study between the proposed decorrelating detector based receiver and the correlator based one presented in [Kon96].

A synchronous MC-DS-CDMA system is considered with M carriers and K active users, each using a gold code of length $N = 31$ to spread his information. The fading processes $\{h_m(n)\}_{m=1,2,...,M}$ are generated according to the modified Jakes model [Den93] given by equation (1.29), with $L_o = 16$ oscillators and Doppler rate $f_d T_b = 0.05$. Here, to focus our attention on the effect of the MAI on both receivers, the fading processes are assumed to be available at the receiver. The performance of the decorrelating detector based receiver when the fading processes are estimated by various approaches will be presented in the next chapter.

Figure 2.15 shows the effects of the ISR on the BER performance of both receivers for number of carriers equal to $M = 1$ and $M = 3$. On the one hand, the BER of the decorrelating detector based receiver does not depend on the ISR and, hence, it is near-far resistant. On the other hand, the BER of the correlator detector based receiver is highly dependent on the ISR, where degradation of the BER can be noticed starting at low ISR. In addition, for the decorrelating detector based receiver, a high frequency diversity gain is obtained when increasing the number of carrier from $M = 1$ to $M = 3$. This is not the case for the correlator based receiver when the ISR is high.

According to Figure 2.16, increasing the number of users greatly increases the BER of the correlator based receiver. On the other hand, the decorrelating detector based receiver is insensitive to the number of users. This is due to the fact that, contrary to the correlator based receiver, the decorrelating detector based receiver can completely eliminate the MAI caused by other users.

Here, we also present a simulation example that illustrates the performance of the proposed decorrelating detector based receiver compared with that of the adaptive receivers proposed in the previous sections. Namely, the training based SD receiver with APA and the post-detection combining receiver with blind APA-like detector. To focus on the MAI suppression capabilities of these receivers, we consider only AWGN channels (without the effect of fading) with $K = 10$, $M = 3$, SNR=5 dB and ISR=15 dB. According to Figure 2.17, the decorrelating detector based receiver provides the lowest BER results without the need for any training period. This is due to the fact that it uses the spreading codes of all users and, hence, can completely eliminate the MAI. The blind APA based receiver has faster convergence than the training APA based one, but it results in higher steady state BER. To take the advantages of both adaptive receivers, their combination can also be considered. Thus, the blind APA-like detector is first carried out up to iteration number 500. As the blind APA-like detector uses the spreading code of the desired user, this will ensure the fast suppression of high amount of MAI.

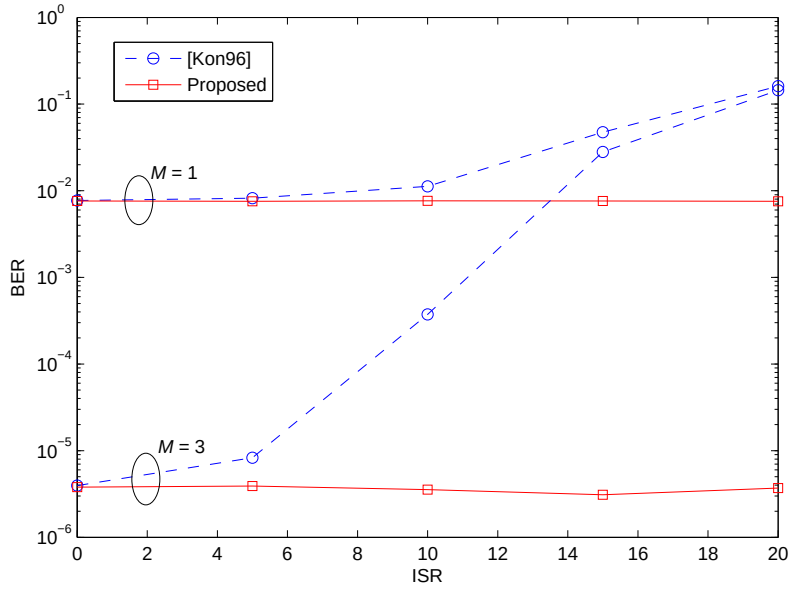

Figure 2.15: BER performance versus ISR for the proposed receiver and the correlator based one [Kon96]. Number of carriers considered are $M = 1$ and $M = 3$. $K = 10$ and SNR=15 dB.

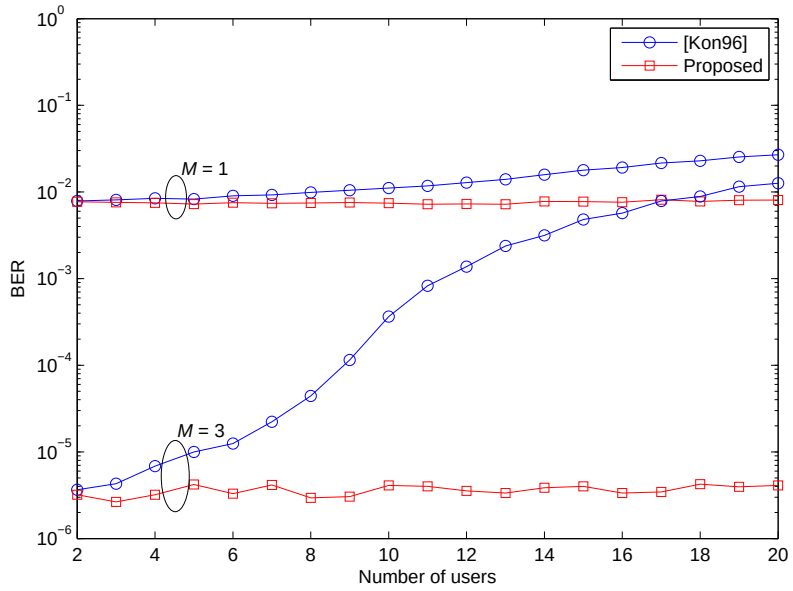

Figure 2.16: BER performance versus number of active users K for the proposed receiver and the one in [Kon96]. Number of carriers considered are $M = 1$ and $M = 3$. ISR=10 dB and SNR=15 dB.

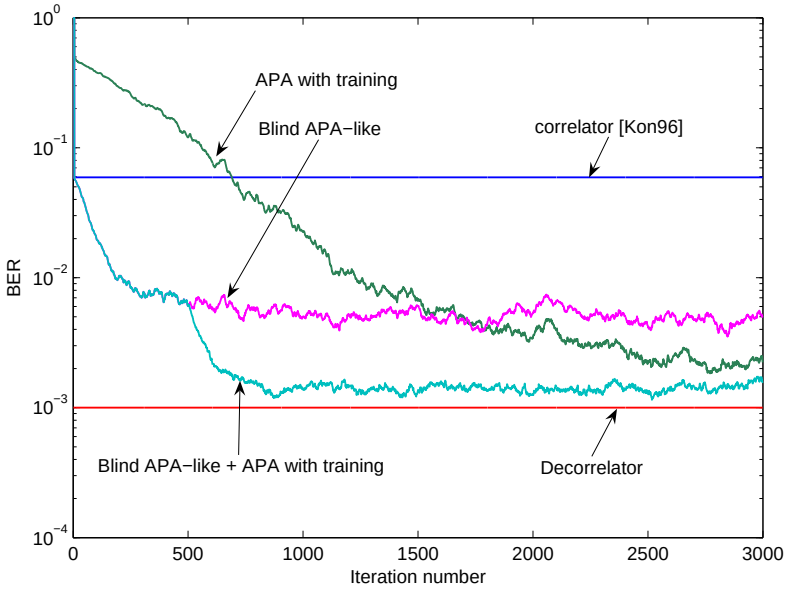

Figure 2.17: BER performance versus iteration number for the various receivers. $M = 3$, $K = 10$, ISR=15 dB and SNR=5 dB.

At that stage, starting from the final filter weight values provided by the blind APA-like detector (at iteration 500), a training based APA can then be used to continue eliminating the residual MAI and can provide a BER performance close to that of the decorrelating detector based receiver.

2.5 Conclusions

In this chapter, we have proposed five MAI suppression receivers for MC-DS-CDMA systems in Rayleigh fading channels [Jam04] [Jam05a] [Jam05b].

We first presented two adaptive MMSE receiver structures based on adaptive filters such as NLMS, APA and RLS [Jam04]. The so-called SD structure consists in considering a particular adaptive filter for each carrier, whereas the so-called JD structure is defined by the concatenation of the adaptive filter weights dedicated to each carrier. Simulation results show that the JD structure provides lower BER than the SD structure. In addition, the order of complexity of both structures are the same when considering the APA, but this is not the case for the RLS filter where the JD structure has higher computational cost than the SD one. Therefore, APA in the JD structure corresponds to a trade-off between performance and computational cost.

However, as adaptive receivers require training sequences, we have proposed two

blind adaptive MOE receivers based on an APA-like multiuser detector [Jam05a], where only the spreading sequence and the timing of the desired user are required. The so-called post-detection combining based receiver structure provides a blind adaptive detector for each carrier where combining is performed after detection. The so-called pre-detection combining based receiver structure uses a single blind adaptive detector after combining the signals of all carriers. Therefore, the computational cost of the pre-detection combining based receiver is much less than that of the post-detection combining based one. Simulation results show that the pre-detection combining based receiver provides slightly lower BER results than the post-detection combining based one. In addition, the comparative study we carried out with existing blind LMS and Kalman filter based detectors shows that the proposed APA-like detector can provide a trade-off between performance and computational cost. Furthermore, the proposed blind APA-like detector is shown to outperform the training based APA in severe near-far scenarios, when considering the BER and SINR improvement.

When the spreading codes of all active users are available, we propose a receiver structure based on the decorrelating detector which includes also a Kalman channel estimator and a MRC [Jam05b]. The comparative simulation study we have carried out shows that, while the correlator based receiver is highly sensitive to the MAI and the near-far problem, the proposed receiver can completely eliminate the MAI and is insensitive to the near-far problem. In addition, the proposed receiver can provide approximately the same BER performance as the adaptive receivers without the need of any training sequences for MAI suppression.

Nevertheless, the design of receivers usually requires the explicit estimation of the fading process over each carrier to achieve optimal diversity combining and coherent symbol detection. For this reason, we will focus our attention on channel estimation in the next chapter.

Chapter 3

Estimation of Autoregressive Fading Channels

Contents

3.1 Introduction

Current mobile wireless systems are designed to provide high data rates at high terminal speeds. High data rate transmission usually leads to severe frequency-selective fading, which can be transformed to frequency-flat fading by using multi-carrier modulation such as in MC-DS-CDMA or OFDM systems. In addition, due to terminal mobility, the received signal is subject to Doppler shifts resulting in time-varying fading. Thus, estimating the time-varying frequency-flat fading channels is essential to achieve optimal diversity combining and coherent symbol detection at the receiver.

Channel estimation techniques can be roughly classified into three basic categories: training sequence/pilot aided techniques, blind techniques and semi-blind techniques. A survey about these estimation techniques can be found in [Tug00], where the Maximum-Likelihood (ML) channel estimator is also derived for each technique.

Training sequence/pilot aided channel estimation techniques make it possible to estimate the channel from the received noisy signal given known training symbols that are multiplexed with the transmitted data symbols. The number of training symbols, the power allocated for each training symbol and the locations of these symbols in the data stream affect the system performance. For a review paper about pilot-assisted wireless transmission, the reader can refer to [Ton04] and references therein. Although the transmission of training symbols/pilots is bandwidth and power consuming, most of mobile standards use training sequence/pilot schemes to estimate the channel.

When dealing with the blind techniques, the channel is estimated from the received signal without embedding training symbols into data transmission (see, e.g., [Mou95] [AM97] [Gia98] [Lou00]). Their major advantage over training based techniques is the improved bandwidth exploitation. However, as they require longer observation window than training based methods, they are more suited for slowly time-varying channels.

Semi-blind techniques [Las03] are obtained by combining training-based and blind techniques. These methods aim at estimating the channel by using not only the known training symbols and the corresponding noisy observations, but also the observations corresponding to the transmitted information symbols. The use of semi-blind estimation techniques is motivated from the fact that, in current standards, there are always some known training symbols. Nevertheless, the computational cost of these semi-blind methods is higher than those of training or blind techniques.

In this thesis, we will focus our attention on training based channel estimation techniques. They may be designed with or without *a priori* modeling of the fading channel.

On the one hand, the fading channel can be estimated based on the linear Least Squares (LS) criterion without any *a priori* modeling of the channel. Thus, in [Mil00b], the MC-DS-CDMA fading channels are estimated by a LS estimator. To reduce the computational cost of the LS estimator, various adaptive implementations can be considered [Hay02]. Therefore, in [Ewe94], the authors have carried out a comparative study between the LMS, RLS and sign algorithms to track time-varying channels. In [Kal03], Kalofonos *et al.* have proposed to estimate the fading process over each carrier in a MC-CDMA system based on the LMS or RLS algorithms. Note that these adaptive estimators do not exploit the channel statistics given by its ACF (1.19) and PSD (1.22).

On the other hand, the stochastic properties of the channel can be exploited by using a suitable model for the fading channel. For this purpose, a p^{th} order AR model has been used in many recent works (see, e.g., [Lin95], [Tsa96], [Wu00], [Kom02], [Bad05], [Sad06]). Thus, in [Tsa96] [Wu00] [Kom02], the authors employ first and/or second order AR models to design channel estimation algorithms based on Kalman filtering. To reduce the computational cost $O(p^3)$ of the estimation algorithm, Lindbom *et al.* [Lin02] have proposed the so-called Wiener LMS algorithm. It exploits low-order AR models (up to AR(3)) with known parameters to track time-varying fading channels. Nevertheless, as low-order AR models result in poor approximation of narrow-band fading processes, Baddour *et al.* [Bad05] have proposed to use very high-order AR models (e.g., $p \geq 50$) to better approximate fading channels. Although their approach is dedicated to channel simulation, it can also be used as a basis for the design of channel estimation algorithms. Therefore, in this chapter, by taking into account the work of Baddour *et al.* [Bad05] and the discussion about AR channel modeling in subsection 1.3.4, we propose to use AR models whose order is high enough (e.g., $p \geq 5$) to simulate and estimate fading channels.

In section 3.2, we present the Kalman filtering based channel estimator and compare it with the LMS and RLS channel estimators. To avoid the restrictive Gaussian assumptions required by Kalman filtering, we then study the relevance of H_∞ filtering [Has99] in section 3.3. In that case, the estimation criterion is to minimize the worst possible effects of the noise disturbances on the estimation error. As both Kalman and H_∞ filtering require the estimation of the AR parameters, a state of the art on AR parameter estimation from noisy observations is provided in section 3.4. This includes the LS estimator used for instance in [Tsa96] and the two-serially-connected Kalman or H_∞ filter based estimators [Cai04]. However, as these estimators yield biased estimates, the noise-compensated LS techniques (e.g., [Wu97], [Dav98a], [Zhe99], [Zhe05]) and methods based on the EM algorithm (e.g., [Der94], [Gan98], [Gan03]) are also reviewed. As an alternative, in

section 3.5, we propose to take advantage of the two-cross-coupled Kalman filter based structure [Lab06b] to design a new channel estimation algorithm [Jam05c]. One Kalman filter is used to estimate the fading AR process while the second one makes it possible to estimate the corresponding AR parameters from the estimated fading process. In section 3.6, a two-cross-coupled H_∞ filter based structure, recently developed in the framework of speech enhancement [Lab06b] [Lab07], is reformulated to estimate time-varying fading channels and their corresponding AR parameters [Jam07b]. Then, in section 3.7, we propose to take advantage of the EIV models, initially developed in the framework of control [Beg90] [Div05b] [Div05a] and derived for AR parameter estimation in [Bob07], to estimate the fading channel AR parameters [Jam06] [Jam07a]. The proposed method consists in searching the noise variances that enable specific noise compensated autocorrelation matrices of observations to be positive semidefinite. In addition, the AR parameters can be estimated from the null space of these matrices. In section 3.8, a comparative study on the estimation of MC-DS-CDMA fading channels is carried out between the various channel estimators.

3.2 On-line least squares channel estimation

Let us consider a BPSK[1] signal propagating through a time-varying frequency-flat Rayleigh fading channel. After demodulation, the signal is passed through the matched-filter and sampled at symbol rate $1/T_b$. The resulting discrete-time received signal can be represented as follows:

$$r(n) = h(n)d(n) + v(n) \tag{3.1}$$

where $d(n) \in \{-1, 1\}$ is the n^{th} transmitted data bit, $h(n)$ is the fading process and $v(n)$ is assumed to be a complex AWGN process with zero-mean and variance σ_v^2.
It should be noted that the received signal in (3.1) is similar to the signal in (2.60) with $P_1 = 1$, which is the output of the decorrelating detector over the m^{th} carrier in a MC-DS-CDMA system. Thus, although we focus our attention on the BPSK transmission over time-varying frequency-flat Rayleigh fading channels, the approaches we develop in the following could be directly applied to the estimation of MC-DS-CDMA fading channels using the receiver structure given in Figure 2.14.

[1] Although we deal only with BPSK (i.e., $d(n) \in \{-1, 1\}$) for the sake of simplicity, the methods we introduce in the following can also work with any linearly modulated signal.

3.2.1 Review about LMS and RLS based channel estimators

Given the noisy received signal (3.1), we aim at estimating the fading process $h(n)$. For this purpose, the LMS channel estimator provides the estimate $\hat{h}(n)$ of the fading process $h(n)$ by minimizing the following mean square error:

$$\text{MSE} = E\left[|r(n) - h(n)d(n)|^2\right] \tag{3.2}$$

Thus, the new channel estimate at time $n+1$ using information available up to time n is given by [Kal03]:

$$\hat{h}(n+1) = \hat{h}(n) + \mu(r(n) - \hat{h}(n)d(n))d(n) \tag{3.3}$$

where μ is the LMS step-size and $\hat{h}(0) = 0$.

To improve the convergence features and the tracking capabilities, a RLS estimator with a forgetting factor λ can be used. The RLS channel estimator [Kal03] calculates the estimate of the channel by minimizing the weighted LS criterion:

$$J_{LS} = \sum_{i=0}^{n} \lambda^{n-i} \left|r(i) - h(i)d(i)\right|^2 \tag{3.4}$$

where $0 < \lambda < 1$ is the exponential forgetting factor.

It should be noted that the data symbols $d(n)$ involved in the LMS and RLS channel estimators are assumed to be available in the so-called training mode. In that mode, the data symbols $d(n)$ are called training symbols or training sequence which are available both at the transmitter and the receiver. Once the training period is over, the receiver can track channel variations in a decision directed manner. In the decision directed mode, the training symbols are replaced with the decisions $\hat{d}(n)$ (e.g., from (2.61) for instance). Such a decision directed approach has been used in [Kal03], where the authors assume that the decisions of the previous data symbols are all correct, i.e. $\hat{d}(n) = d(n)$. In our work hereafter, we will follow the same decision directed approach.

3.2.2 Kalman filtering based channel estimator

Since our purpose is to estimate the fading sequence $h(n)$, modeled by a p^{th} order AR(p) process as in (1.30), the $p \times 1$ state vector is defined as follows:

$$\mathbf{h}(n) = \begin{bmatrix} h(n) & h(n-1) & \cdots & h(n-p+1) \end{bmatrix}^T \tag{3.5}$$

Thus, the resulting state-space representation of the fading channel system (3.1) and (1.30) is given by:

$$\begin{cases} \mathbf{h}(n) = \mathbf{\Phi}\mathbf{h}(n-1) + \mathbf{g}u(n) \\ r(n) = \mathbf{d}^T(n)\mathbf{h}(n) + v(n) \end{cases} \tag{3.6}$$

where $\mathbf{\Phi} = \begin{bmatrix} -a_1 & -a_2 & \cdots & -a_p \\ 1 & 0 & \cdots & 0 \\ & \ddots & & \vdots \\ 0 & \cdots & 1 & 0 \end{bmatrix}$ is the transition matrix, $\mathbf{g} = [\ 1 \quad 0 \quad \cdots \quad 0\ ]^T$ is the input vector and $\mathbf{d}(n) = [\ d(n) \quad 0 \quad \cdots \quad 0\ ]^T$ is the observation vector. In addition, the variances of $v(n)$ and $u(n)$ are respectively denoted by σ_v^2 and σ_u^2. Furthermore, $v(n)$ and $u(n)$ are assumed to be uncorrelated with each others and with the elements of the initial state vector $\mathbf{h}(0)$.

Based on the state-space representation (3.6) of the fading channel system, Kalman filtering can provide the optimal linear least mean squares estimate of the state vector $\mathbf{h}(n)$. More specifically, let $\hat{\mathbf{h}}(n/n-1)$ denote the *a priori* estimate of $\mathbf{h}(n)$ given $n-1$ observations $\{r(1), r(2), \cdots, r(n-1)\}$ while $\hat{\mathbf{h}}(n/n)$ denotes the *a posteriori* estimate of $\mathbf{h}(n)$ given n observations $\{r(1), r(2), \cdots, r(n)\}$. Then, the corresponding *a priori* and *a posteriori* error covariance matrices are $\mathbf{P}(n/n-1) = E[(\mathbf{h}(n)-\hat{\mathbf{h}}(n/n-1))(\mathbf{h}(n)-\hat{\mathbf{h}}(n/n-1))^H]$ and $\mathbf{P}(n/n) = E[(\mathbf{h}(n) - \hat{\mathbf{h}}(n/n))(\mathbf{h}(n) - \hat{\mathbf{h}}(n/n))^H]$, respectively.

Thus, Kalman filtering is designed to minimize the trace of $\mathbf{P}(n/n)$. The Kalman filtering algorithm can be summarized as follows [And79] [Naj06]:

$$\hat{\mathbf{h}}(n/n-1) = \mathbf{\Phi}\hat{\mathbf{h}}(n-1/n-1) \tag{3.7a}$$

$$\mathbf{P}(n/n-1) = \mathbf{\Phi}\mathbf{P}(n-1/n-1)\mathbf{\Phi}^H + \mathbf{g}\sigma_u^2\mathbf{g}^T \tag{3.7b}$$

$$\nu(n) = r(n) - \mathbf{d}^T(n)\hat{\mathbf{h}}(n/n-1) \tag{3.7c}$$

$$\mathbf{K}(n) = \mathbf{P}(n/n-1)\mathbf{d}(n)(\mathbf{d}^T(n)\mathbf{P}(n/n-1)\mathbf{d}(n) + \sigma_v^2)^{-1} \tag{3.7d}$$

$$\hat{\mathbf{h}}(n/n) = \hat{\mathbf{h}}(n/n-1) + \mathbf{K}(n)\nu(n) \tag{3.7e}$$

$$\hat{h}(n) = \hat{h}(n/n) = \mathbf{g}^T\hat{\mathbf{h}}(n/n) \tag{3.7f}$$

$$\mathbf{P}(n/n) = \mathbf{P}(n/n-1) - \mathbf{K}(n)\mathbf{d}^T(n)\mathbf{P}(n/n-1) \tag{3.7g}$$

where $\mathbf{K}(n)$ is the Kalman gain and $\nu(n)$ the innovation process.

When Kalman filtering is optimal, the innovation process $\nu(n)$ is a zero-mean white noise with variance:

$$C(n) = E[\nu(n)\nu^*(n)] = \mathbf{d}^T(n)\mathbf{P}(n/n-1)\mathbf{d}(n) + \sigma_v^2 \tag{3.8}$$

It should be noted that when there is no *a priori* knowledge about the initial state vector and the initial error covariance matrix, they can be assigned to zero vector and identity matrix respectively, i.e. $\hat{\mathbf{h}}(0/0) = \mathbf{0}$ and $\mathbf{P}(0/0) = \varsigma \mathbf{I}_p$ where ς is a positive constant. Large values of ς reflect lack of knowledge whereas small values reflect confidence.
Thus, in the training mode, as the data symbol $d(n)$ involved in the observation vector $\mathbf{d}(n)$ is available, the Kalman filtering algorithm can be carried out to provide the estimate $\hat{h}(n/n)$ of the fading process $h(n)$. Once the training period is over, the joint estimation problem of both the fading process $h(n)$ and the data symbol $d(n)$ should be addressed. This joint estimation problem can be decomposed into the estimation of the data symbol at time n and then the prediction of the fading process at time $n+1$. For this purpose, a predicted version $\hat{h}(n+1/n)$ of the fading process $h(n+1)$ can be obtained from (3.7a) and (3.7e)-(3.7f), as follows:

$$\hat{\mathbf{h}}(n+1/n) = \mathbf{\Phi}\hat{\mathbf{h}}(n/n) = \mathbf{\Phi}\hat{\mathbf{h}}(n/n-1) + \mathbf{\Phi}\mathbf{K}(n)\nu(n) \tag{3.9a}$$

$$\hat{h}(n+1) = \hat{h}(n+1/n) = \mathbf{g}^T\hat{\mathbf{h}}(n+1/n) \tag{3.9b}$$

where $\hat{\mathbf{h}}(0/-1) = \mathbf{0}$ and $\mathbf{P}(0/-1) = \varsigma \mathbf{I}_p$.
More particularly, as a decision of the data symbol $\hat{d}(n)$ has been made at time n, it can then be used to predict the fading process at time $n+1$ as in (3.9). The predicted fading process $\hat{h}(n+1)$ is then employed to obtain a decision about the data symbol at time $n+1$.

Using Kalman filtering is of interest, but several assumptions must be fulfilled. Indeed, Kalman filtering is optimal in the MMSE sense providing the underlying state-space model is accurate. Moreover, the driving process and the additive measurement noise must be independent, white and Gaussian. However, these assumptions do not always hold in practice due to the two following reasons:

1. The AR model does not fit exactly the fading process especially for low-order AR models (see subsection 1.3.4). This results in model uncertainty that we have to take into account.

2. The noise variances and the AR parameters are usually unknown and must be estimated. This also results in model parameter uncertainties.

Therefore, for practical systems, the performance of the Kalman estimator may suffer degradation. For this reason, we propose to investigate an alternative approach based on H_∞ estimation techniques [Has99] in the next section.

3.3 Relevance of H_∞ filtering for channel estimation

In this section, we will study the relevance of H_∞ filtering for channel estimation. The estimation criterion is to minimize the worst possible effects of the disturbances (i.e., the initial state, the driving process and the measurement noise) on the estimation error. This criterion requires no *a priori* knowledge about the noises, except that they have bounded energies. In that sense and according to Hassibi *et al.* [Has99], H_∞ filtering is more robust against the noise disturbances and modeling uncertainties than Kalman filtering.

3.3.1 State of the art

The H_∞ theory was initially developed in the framework of control [Zam81]. The first solution of the H_∞ estimation problem is based on polynomial decomposition techniques [Gri90]. However, they lead to formulas with high computational cost that cannot be used in practical cases. Besides, state-space based approaches have emerged and can be classified into two categories:

- The first one is based on the solution of a convex optimization problem under linear matrix inequality constraints [Ger99]. However, its computational cost is high.
- The second approach is based on the solution of a quadratic Riccati-type equation [Sha92]. The resulting algorithm is easy to implement and has lower computational cost than the above approaches.

Other approaches based on the so-called game theory have been proposed [Yae92] [She97]. According to the game theory, the H_∞ filter can be seen as a player prepared for the worst strategy that the other player can provide. This approach can also be viewed as a minimax problem, whose solution corresponds to an equilibrium point between the filter and the nature. It should be noted that the solution obtained by the game theory approaches is similar to that obtained by the Riccati-type equation. In particular, the game theory approach presented in [She97] shows that the H_∞ filter exists if there exits a stabilizing solution to a given Riccati-type equation.

Although the H_∞ theory has been extensively exploited in the framework of control, its applications in signal processing and more particularly in communications are still scarce. Thus, Shen *et al.* [She99] have proposed a speech enhancement approach, where the speech signal is modeled by an AR process. However, as the AR parameters are estimated directly from the noisy observations, this approach results in biased AR parameter estimates. In [Lab05], Labarre *et al.* have studied the relevance of H_∞ filtering for

speech enhancement. To avoid the problem of biased AR parameter estimates, they have developed a structure based on two mutually interactive H_∞ filters for the dual estimation of the speech signal and its AR parameters [Lab07]. In the framework of digital communications, Erdogan *et al.* [Erd00] have proposed to investigate the significance of the H_∞ approach to the linear equalization of communication channels. However, the authors did not consider the performance of their approach in realistic fading channels. In [Zhu99], an adaptive H_∞ filtering algorithm "similar" to the RLS algorithm is introduced to recursively update the tap-coefficient vector of a decision feedback equalizer for the purpose of adaptive equalization of time-varying fading channels. Nevertheless, this approach did not explicitly estimate the channel and, hence, cannot work in high Doppler rate environments. In [Cai04], Cai *et al.* have used the H_∞ filter proposed in [She97] to develop a channel estimation scheme for OFDM wireless communication systems, where the fading channels are modeled by AR processes. The scheme involves two-serially-connected H_∞ filters. The first one is used for AR parameter estimation and the second one for fading process estimation. Nevertheless, a biased estimation of the AR parameters is expected since the first H_∞ filter estimates the AR parameters directly from the noisy observations. This may lead to poor estimation of the fading process.

In this thesis, we propose to study the relevance of H_∞ filtering for the estimation of time-varying fading channels. More particularly, we will take advantage of the two mutually interactive H_∞ filter based approach [Lab07] to jointly estimate the fading channel and its AR parameters [Jam07b].

3.3.2 Estimation of the fading process based on H_∞ filtering

Given the fading channel state-space model (3.6), the H_∞ filtering makes it possible to focus on the estimation of a specific linear combination of the state vector components as follows:

$$z(n) = \boldsymbol{l}\mathbf{h}(n) \tag{3.10}$$

where $\boldsymbol{l}$ is a $1 \times p$ linear transformation operator. Here, as we aim at estimating the fading process $h(n)$, this operator is selected to be $\boldsymbol{l} = [\ 1 \quad 0 \quad \cdots \quad 0\ ]$.
Given (3.6), (3.10) and Figure 3.1, the H_∞ filtering provides the estimation of the fading process $\hat{h}(n) = \boldsymbol{l}\hat{\mathbf{h}}(n)$, by minimizing the H_∞ norm of the transfer operator $\mathcal{T}$ that maps the noise disturbances $u(n)$, $v(n)$ and the initial state error $\mathbf{e}_0 = \mathbf{h}(0) - \hat{\mathbf{h}}(0)$ to the

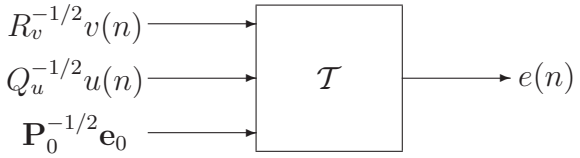

Figure 3.1: Transfer operator $\mathcal{T}$.

estimation error $e(n) = h(n) - \hat{h}(n) = \boldsymbol{l}(\mathbf{h}(n) - \hat{\mathbf{h}}(n))$, as follows:

$$J_\infty = \sup_{u(n),v(n),\mathbf{h}(0)} \frac{\sum_{n=0}^{N_s-1} |e(n)|^2}{\mathbf{e}_0^H \mathbf{P}_0^{-1} \mathbf{e}_0 + \sum_{n=0}^{N_s-1} \left(Q_u^{-1}|u(n)|^2 + R_v^{-1}|v(n)|^2\right)} \tag{3.11}$$

where N_s denotes the number of available data samples. In addition, $\mathbf{P}_0 > 0$, $Q_u > 0$ and $R_v > 0$ are weighting parameters which are tuned by the designer to achieve performance requirements.

However, as a closed-form solution to the above optimal H_∞ estimation problem does not always exist, the following suboptimal design strategy is usually considered:

$$J_\infty < \gamma^2 \tag{3.12}$$

where $\gamma > 0$ is a prescribed level of disturbance attenuation.

At that stage, there exists an H_∞ channel estimator $\hat{h}(n)$ for a given $\gamma > 0$ if there exists a stabilizing symmetric positive definite solution $\underline{\mathbf{P}}(n)$ to the following Riccati-type equation:

$$\underline{\mathbf{P}}(n+1) = \boldsymbol{\Phi}\underline{\mathbf{P}}(n)\mathbf{C}^{-1}(n)\boldsymbol{\Phi}^H + \mathbf{g}Q_u\mathbf{g}^T, \qquad \underline{\mathbf{P}}(0) = \mathbf{P}_0 \tag{3.13}$$

where:

$$\mathbf{C}(n) = \mathbf{I}_p - \gamma^{-2}\boldsymbol{l}^T\boldsymbol{l}\underline{\mathbf{P}}(n) + \mathbf{d}(n)R_v^{-1}\mathbf{d}^T(n)\underline{\mathbf{P}}(n) \tag{3.14}$$

This leads to the following constraint:

$$\underline{\mathbf{P}}(n)\mathbf{C}^{-1}(n) > 0 \tag{3.15}$$

If the condition (3.15) is fulfilled, the H_∞ channel estimator exists and is defined by:

$$\hat{h}(n) = \boldsymbol{l}\hat{\mathbf{h}}(n) \tag{3.16}$$

with:

$$\hat{\mathbf{h}}(n) = \boldsymbol{\Phi}\hat{\mathbf{h}}(n-1) + \underline{\mathbf{K}}(n)\nu(n), \qquad \hat{\mathbf{h}}(0) = \mathbf{0} \tag{3.17}$$

where the so-called innovation process $\nu(n)$ and the H_∞ filter gain $\underline{\mathbf{K}}(n)$ are respectively given by:

$$\nu(n) = r(n) - \mathbf{d}^T(n)\boldsymbol{\Phi}\hat{\mathbf{h}}(n-1) \tag{3.18}$$

and

$$\underline{\mathbf{K}}(n) = \underline{\mathbf{P}}(n)\mathbf{C}^{-1}(n)\mathbf{d}(n)R_v^{-1} \tag{3.19}$$

It should be noted that the matrix $\underline{\mathbf{P}}(n)$ can be seen as an upper bound of the error covariance matrix in the Kalman filter, i.e. $E[(\mathbf{h}(n)-\hat{\mathbf{h}}(n))(\mathbf{h}(n)-\hat{\mathbf{h}}(n))^H] \leq \underline{\mathbf{P}}(n)$ [Yae92]. Moreover, the H_∞ channel estimator (3.13)-(3.19) has similar observer structure as the Kalman's one. However, due to (3.14), the H_∞ channel estimator has a computational cost slightly higher than Kalman's one. If the weighting parameters Q_u, R_v and $\mathbf{P}_0$ are respectively chosen to be σ_u^2, σ_v^2 and the initial error covariance matrix of $\mathbf{h}(0)$, then as $\gamma \longrightarrow +\infty$ the H_∞ estimator reduces to a Kalman one.
It should be noted that the selection of the disturbance attenuation level γ is not an easy task. Here, it is carefully adjusted to satisfy the condition in (3.15).

Nevertheless, carrying out Kalman or H_∞ filtering to estimate $h(n)$ requires the AR parameters that are involved in the transition matrix $\mathbf{\Phi}$ and the variances of both the driving process σ_u^2 and the measurement noise σ_v^2 (or equivalently the weighting parameters Q_u and R_v in the case of H_∞ filtering). In subsection 1.3.4, the AR parameters and the driving process variance are obtained by solving the YW equations providing the maximum Doppler frequency f_d is available. However, f_d is not available in practical cases and should be estimated, which is not a trivial task (see, e.g., [Tep01] and references therein). Therefore, our goal in the next sections is to develop channel estimation techniques that make it possible to estimate the AR parameters and the variances of both the additive noise and driving process from the available noisy observations.

3.4 State of the art on AR parameter estimation from noisy data

In this section, we will present a brief[2] state of the art on the estimation of the AR parameters from noisy observations. More particularly, our purpose is to estimate the channel AR parameters from the received noisy signal (3.1), using a training based approach. Thus, in the time interval allocated to the transmission of the training sequence, the data modulation can be wiped out by multiplying the received signal samples with the training symbols, as follows:

$$y(n) = d^*(n)r(n) = h(n) + b(n) \tag{3.20}$$

where $b(n)$ is a zero-mean additive white noise whose variance satisfies $\sigma_b^2 = \sigma_v^2$.
By combining the AR model of the channel (1.30) with the observation equation (3.20), one can obtain:

$$y(n) = -\mathbf{y}_p^T(n-1)\boldsymbol{\theta} + \zeta(n) \tag{3.21}$$

where

$$\mathbf{y}_p(n-1) = \begin{bmatrix} y(n-1) & y(n-2) & \cdots & y(n-p) \end{bmatrix}^T \tag{3.22}$$

and

$$\zeta(n) = u(n) + b(n) + \sum_{i=1}^{p} a_i b(n-i) \tag{3.23}$$

As N_s observation samples are obtained during the transmission of a training sequence, equation (3.21) can be then written in a matrix form as follows:

$$\mathbf{y}_{N_s}(n) = \begin{bmatrix} -\mathbf{y}_p^T(n-1) \\ -\mathbf{y}_p^T(n-2) \\ \vdots \\ -\mathbf{y}_p^T(n-N_s) \end{bmatrix} \boldsymbol{\theta} + \begin{bmatrix} \zeta(n) \\ \zeta(n-1) \\ \vdots \\ \zeta(n-N_s+1) \end{bmatrix} = \mathbf{Y}_{N_s}(n)\boldsymbol{\theta} + \boldsymbol{\zeta}_{N_s}(n) \tag{3.24}$$

Therefore, the LS estimate $\hat{\boldsymbol{\theta}}_{LS}$ of $\boldsymbol{\theta}$ satisfies the following relationship:

$$\hat{\boldsymbol{\theta}}_{LS} = \left[\mathbf{Y}_{N_s}^H(n)\mathbf{Y}_{N_s}(n)\right]^{-1}\mathbf{Y}_{N_s}^H(n)\mathbf{y}_{N_s}(n) \tag{3.25}$$

and the corresponding LS estimation error is given by:

$$\hat{\boldsymbol{\theta}}_{LS} - \boldsymbol{\theta} = \left[\mathbf{Y}_{N_s}^H(n)\mathbf{Y}_{N_s}(n)\right]^{-1}\mathbf{Y}_{N_s}^H(n)\boldsymbol{\zeta}_{N_s}(n) \tag{3.26}$$

[2]For a more exhaustive state of the art on AR parameter estimation from noisy observations, the reader may refer to [Lab06a] [Naj06].

It should be noted that the LS solution (3.25) can be written in the form of the YW equations applied to the noisy observations, as follows:

$$\hat{\boldsymbol{\theta}}_{LS} = -\hat{\mathbf{R}}_{yy}^{-1}\hat{\mathbf{r}}_y \tag{3.27}$$

where $\hat{\mathbf{R}}_{yy}$ denotes the estimation of the $p \times p$ autocorrelation matrix $\mathbf{R}_{yy}$ of the observations $y(n)$ and $\hat{\mathbf{r}}_y$ is the estimation of the $p \times 1$ correlation vector $\mathbf{r}_y$ between $\mathbf{y}_p(n-1)$ and $y(n)$. However, as the expectation of the estimator (3.27) satisfies:

$$E\left[\hat{\boldsymbol{\theta}}_{LS}\right] = -\mathbf{R}_{yy}^{-1}\mathbf{r}_y \neq -\mathbf{R}_{hh}^{-1}\mathbf{r}_h = \boldsymbol{\theta} \tag{3.28}$$

the LS estimator of the AR parameters is biased. Indeed, the AR spectrum estimated from the noisy signal is flatter than the AR spectrum estimated from noise-free signal [Kay79]. In addition, since $y(n)$ is correlated with $\{\zeta(i)\}_{i=1,2,\cdots,n}$, the estimation error (3.26) does not go to zero when $N_s \longrightarrow \infty$. So, in that case, the LS estimator is not consistent.

The bias estimation problem of the channel AR parameters is noticeable in [Tsa96] [Cai04]. Indeed, in [Tsa96], Tsatsanis *et al.* suggest estimating the AR parameters from the channel covariance estimates by means of a YW estimator. In [Cai04], the authors have proposed a channel estimation scheme for OFDM systems based on two-serially-connected Kalman or H_∞ filters (see Figure 3.2). The first one is used for AR parameter estimation and the second one for fading process estimation. The AR parameters are directly estimated from the available noisy observations based on the following state-space representation:

$$\begin{cases} \boldsymbol{\theta}(n) = \boldsymbol{\theta}(n-1) \\ y(n) = -\mathbf{y}_p^T(n-1)\boldsymbol{\theta}(n) + \zeta(n) \end{cases} \tag{3.29}$$

In that case, the H_∞ filtering is more appropriate than the Kalman filtering since no *a priori* modeling of the colored noise process $\zeta(n)$ is required. Nevertheless, the AR parameter estimates in both cases are biased since the observation noise $\zeta(n)$ in the state-space representation of the system (3.29) is correlated with the AR parameters [Lab05].

To counteract the bias estimation problem, several approaches have been proposed, mostly in other fields than wireless communications. These approaches can be classified as on-line or off-line approaches. Let us first focus on off-line LS estimation approaches. Thus, Kay [Kay80] has proposed the so-called Noise-Compensated YW (NCYW) equations:

$$\hat{\boldsymbol{\theta}}_{LSC} = -\left(\mathbf{R}_{yy} - \sigma_b^2\mathbf{I}_p\right)^{-1}\mathbf{r}_y \tag{3.30}$$

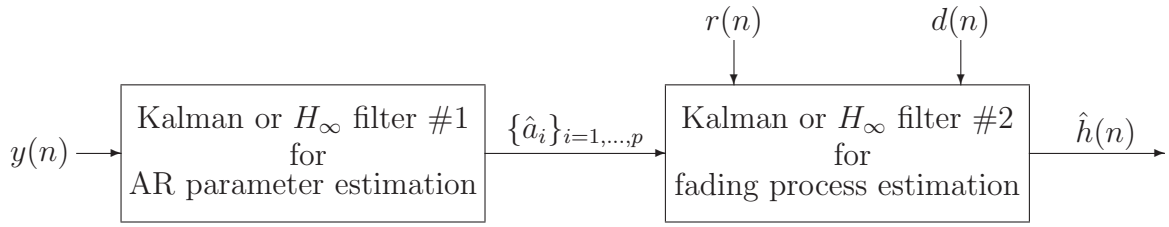

Figure 3.2: Two-serially-connected Kalman or H_∞ filters.

However, as the variance of the additive noise σ_b^2 has to estimated, the problem becomes nonlinear. Therefore, the joint estimation problem of the AR parameters and the additive noise variance was addressed by several authors. On the one hand, Zheng [Zhe99] [Zhe05] has proposed to estimate iteratively and alternatively the AR parameter vector $\boldsymbol{\theta}$ and the noise variance σ_b^2 using a bias correction LS scheme. On the other hand, Davila [Dav98a] has suggested solving the NCYW equations (3.30) by viewing this issue as a quadratic eigenvalue decomposition problem. Although the above schemes aim at compensating the noise influence, they may provide a set of AR parameter estimates which correspond to AR poles outside the unit circle in the z-plane [Lab06b].

On-line LS methods based on adaptive filters have also been developed. Thus, when using the so-called γ-LMS filter [Tre79], the updated tap-weight vector depends on the previous tap-weight vector multiplied by a factor γ defined from the variance of the additive noise and the LMS step-size. In [Wu97], the authors propose a method based on the so-called ρ-LMS filter. The idea is to update the AR parameters using the LMS filter on enhanced observations. Nevertheless, in the γ-LMS and ρ-LMS algorithms, the additive noise variance is assumed to be available. For this reason, Zhang *et al.* [Zha00] have proposed to estimate both the AR parameters and the noise variance based on the so-called β-LMS, resulting in unbiased estimation of the AR parameters. However, the convergence rate of these LMS based methods is low and the step-size should be carefully adjusted.

As an alternative, the EM algorithm, which is an iterative optimization algorithm producing ML estimates [Dem77], can be used [Der94]. It iterates between two steps: the expectation step (E-step) allows the computation of the expected log-likelihood function given current parameter estimates while the maximization step (M-step) makes it possible to update the estimates by maximizing the log-likelihood function. It often implies a Kalman smoothing. Nevertheless, since the EM algorithm operates repeatedly on a batch of data, it results in large storage requirements and high computational cost. In

addition, its success depends on the initial conditions. To overcome these disadvantages, two recursive filters (such as Kalman or RLS) can be cross-coupled to solve the so-called dual estimation issue [And79], i.e. the estimations of both the AR process and its parameters. Each time a new observation is available, the first filter uses the latest estimated AR parameters to estimate the signal, while the second filter uses the estimated signal to update the AR parameters. According to Gannot *et al.* [Gan98] [Gan03], this method can be viewed as a sequential version of the EM algorithm. In addition, it avoids a non-linear approach such as the Extended Kalman Filter (EKF). Coupling recursive filters was already developed for instance in the framework of speech enhancement [Dob98] and has also been used in [Dav98b] to complete the equalization of fast fading channels. Recently, in [Lab06b], a variant based on two interacting Kalman filters has been developed in which the variance of the innovation process in the first filter is used to define the gain of the second filter. Since this solution can be seen as a recursive IV technique, consistent estimates of the AR parameters are obtained [Lab06b]. This approach has been tested in the framework of speech enhancement [Lab04] [Lab06a].

3.5 Two-cross-coupled Kalman filter based estimator

In this section, we propose to adjust the two-cross-coupled Kalman filter based approach developed in [Lab06b] for the joint estimation of fading channels and their corresponding AR parameters [Jam05c] as shown in Figure 3.3.

Thus, at time instant n, the first Kalman filter uses the training sequence $d(n)$, the received noisy signal[3] $r(n)$ and the latest estimated AR parameters $\{\hat{a}_i\}_{i=1,\dots,p}$ to provide the estimation $\hat{h}(n)$ of the fading process $h(n)$ as in equation (3.7), while the second Kalman filter uses the estimated fading process $\hat{h}(n)$ to update the AR parameters. At the end of the training period, the receiver stores the estimated AR parameters and uses them in conjunction with the observation $r(n)$ and the decision $\hat{d}(n)$ (e.g., using equation (2.61) for instance) to predict the fading process $h(n+1)$ in a decision directed manner using equation (3.9).

It should be noted that the two Kalman filters are highly interactive since the variance of the innovation of the first filter is used to drive the gain of the second filter and to define the estimation of the driving process variance. This will be illustrated in the following subsections.

[3]Note that $r(n)$ corresponds to $y(n)$ when the training symbols are removed (see equation (3.20)).

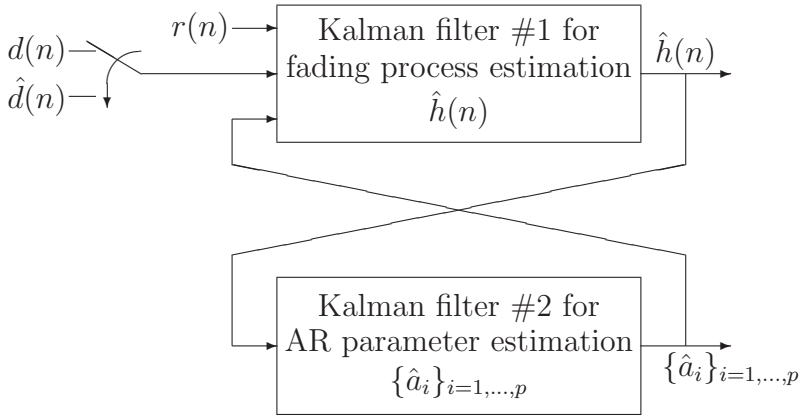

Figure 3.3: Proposed two-cross-coupled Kalman filter based channel estimator.

3.5.1 Estimation of the AR parameters from the estimated fading process

To estimate the AR parameters from the estimated fading process $\hat{h}(n)$, equations (3.7e) and (3.7f) are firstly combined to express the estimated fading process as a function of the AR parameters:

$$\begin{aligned}\hat{h}(n) &= \mathbf{g}^T\mathbf{\Phi}\hat{\mathbf{h}}(n-1) + \mathbf{g}^T\mathbf{K}(n)\nu(n) \\ &= -\hat{\mathbf{h}}^T(n-1)\boldsymbol{\theta}(n) + w(n) \\ &= \mathbf{d}_{\boldsymbol{\theta}}^T(n-1)\boldsymbol{\theta}(n) + w(n)\end{aligned} \tag{3.31}$$

where $\boldsymbol{\theta}(n) = [\ a_1 \quad a_2 \quad \cdots \quad a_p\ ]^T$, $\hat{\mathbf{h}}(n-1) = [\ \hat{h}(n-1) \quad \hat{h}(n-2) \quad \cdots \quad \hat{h}(n-p)\ ]^T$ and $\mathbf{d}_{\boldsymbol{\theta}}^T(n-1) = -\hat{\mathbf{h}}^T(n-1)$. In addition, the variance of the process $w(n) = \mathbf{g}^T\mathbf{K}(n)\nu(n)$ is given by:

$$\sigma_w^2(n) = \mathbf{g}^T\mathbf{K}(n)C(n)\mathbf{K}^H(n)\mathbf{g} \tag{3.32}$$

When the channel is assumed to be stationary, the AR parameters are time-invariant and satisfy the following relationship:

$$\boldsymbol{\theta}(n) = \boldsymbol{\theta}(n-1) \tag{3.33}$$

As relations (3.31) and (3.33) define a state-space representation for the estimation of the AR parameters, a second Kalman filter can be used to recursively estimate $\boldsymbol{\theta}(n)$ as follows:

$$\hat{\boldsymbol{\theta}}(n) = \hat{\boldsymbol{\theta}}(n-1) + \mathbf{K}_{\boldsymbol{\theta}}(n)w(n) \tag{3.34}$$

where the Kalman gain $\mathbf{K}_{\boldsymbol{\theta}}(n)$ and the update of the error covariance matrix $\mathbf{P}_{\boldsymbol{\theta}}(n)$ are respectively given by:

$$\mathbf{K}_{\boldsymbol{\theta}}(n) = \mathbf{P}_{\boldsymbol{\theta}}(n-1)\mathbf{d}^*_{\boldsymbol{\theta}}(n-1)\left(\mathbf{d}^H_{\boldsymbol{\theta}}(n-1)\mathbf{P}_{\boldsymbol{\theta}}(n-1)\mathbf{d}_{\boldsymbol{\theta}}(n-1) + \sigma^2_w(n)\right)^{-1} \tag{3.35}$$

and

$$\mathbf{P}_{\boldsymbol{\theta}}(n) = \mathbf{P}_{\boldsymbol{\theta}}(n-1) - \mathbf{K}_{\boldsymbol{\theta}}(n)\mathbf{d}^T_{\boldsymbol{\theta}}(n-1)\mathbf{P}_{\boldsymbol{\theta}}(n-1) \tag{3.36}$$

with initial conditions $\hat{\boldsymbol{\theta}}(0) = \mathbf{0}$ and $\mathbf{P}_{\boldsymbol{\theta}}(0) = \varsigma\mathbf{I}_p$.
The estimated AR parameters $\hat{\boldsymbol{\theta}}(n) = [\ \hat{a}_1 \quad \hat{a}_2 \quad \cdots \quad \hat{a}_p\ ]^T$ are then fed into the first Kalman filter (3.7) to estimate the fading process at time $n+1$ as shown in Figure 3.3.
According to (3.32) and (3.35), the two-cross-coupled Kalman filters are all the more mutually interactive as the variance of the innovation process of the first filter is used to drive the gain of the second.

Remark 1: The two-cross-coupled Kalman filter based channel estimator is a compact complex algorithm which estimates the complex fading process and its AR parameters. Instead of using the complex algorithm, an alternative approach would consist in decomposing the estimation of the complex fading process $h(n)$ into the separate estimation of its real part $h^{(r)}(n) = \mathrm{Re}(h(n))$ and its imaginary part $h^{(i)}(n) = \mathrm{Im}(h(n))$. Indeed, according to the fading process statistical properties given by equations (1.20) and (1.21), the real and imaginary parts of the complex fading process are uncorrelated and have the same ACF as the complex process. This implies that their AR parameters are the same. Thus, to estimate $h^{(r)}(n)$ and its AR parameters, we can apply a real version[4] of the proposed complex algorithm to the real part of the observations $r^{(r)}(n) = \mathrm{Re}(r(n))$ given by:

$$r^{(r)}(n) = h^{(r)}(n)d(n) + v^{(r)}(n) \tag{3.37}$$

where $v^{(r)}(n)$ is the real part of $v(n)$ with variance $\sigma^2_{v^{(r)}} = \frac{1}{2}\sigma^2_v$.
In the same manner, we can apply this approach to the imaginary part of the observations $r^{(i)}(n) = \mathrm{Im}(r(n))$ to estimate $h^{(i)}(n)$ and its AR parameters.
Therefore, while the complex algorithm has the advantage of estimating the complex fading process and its AR parameters in a compact manner, its real version can reduce the computational cost when estimating the AR parameters form either the real or the imaginary part of the complex fading process.

[4] A real version of the complex algorithm can be obtained by replacing the Hermitian operation $(\cdot)^H$ with the Transpose operation $(\cdot)^T$ and removing the complex conjugate operation $(\cdot)^*$.

3.5.2 Estimation of the driving process variance

To estimate the driving process variance σ_u^2, the Riccati equation is first obtained by inserting equation (3.7b) in (3.7g) as follows:

$$\mathbf{P}(n/n) = \mathbf{\Phi}\mathbf{P}(n-1/n-1)\mathbf{\Phi}^H + \mathbf{g}\sigma_u^2\mathbf{g}^T - \mathbf{K}(n)\mathbf{d}^T(n)\mathbf{P}(n/n-1) \tag{3.38}$$

Taking into account the variance of the innovation process (3.8) and the fact that $\mathbf{P}(n/n-1)$ is a symmetric hermitian matrix, one can rewrite the Kalman filter gain equation (3.7d) in the following manner:

$$\mathbf{d}^T(n)\mathbf{P}(n/n-1) = C(n)\mathbf{K}^H(n) \tag{3.39}$$

By combining equations (3.38) and (3.39), σ_u^2 can be expressed as follows:

$$\sigma_u^2 = \mathbf{f}\left[\mathbf{P}(n/n) - \mathbf{\Phi}\mathbf{P}(n-1/n-1)\mathbf{\Phi}^H + \mathbf{K}(n)C(n)\mathbf{K}^H(n)\right]\mathbf{f}^T \tag{3.40}$$

where $\mathbf{f} = \left[\mathbf{g}^T\mathbf{g}\right]^{-1}\mathbf{g}^T = \mathbf{g}^T$ is the pseudo-inverse of $\mathbf{g}$.
Thus, we propose to estimate σ_u^2 recursively as follows :

$$\hat{\sigma}_u^2(n) = \lambda\hat{\sigma}_u^2(n-1) + (1-\lambda)\mathbf{f}\mathbf{M}(n)\mathbf{f}^T \tag{3.41}$$

where $\mathbf{M}(n) = \mathbf{P}(n/n) - \mathbf{\Phi}\mathbf{P}(n-1/n-1)\mathbf{\Phi}^H + \mathbf{K}(n)|\nu(n)|^2\mathbf{K}^H(n)$, $|\nu(n)|^2$ is the instantaneous power of the innovation process that replaces its variance $C(n)$ and λ is the forgetting factor. It should be noted that λ can be either constant or time-varying (e.g., $\lambda(n) = (n-1)/n$).

3.5.3 Simulation results

In this subsection, we first provide preliminary experimental results to illustrate the performance of the proposed two-cross-coupled Kalman filter based channel estimator. A comparative simulation study is then carried out on AR parameter estimation between the proposed approach and two other approaches:

1. the two-serially-connected Kalman filters [Cai04] shown in Figure 3.2,
2. the YW estimator, used for instance in [Tsa96], which can be implemented by using the MATLAB function *aryule*.

In all of our simulations below, the fading process $h(n)$ is generated according to the autoregressive channel simulator [Bad05] with order varying from 2 to 20 and a given

Doppler rate f_dT_b. It is normalized to have a unit variance, i.e. $\sigma_h^2 = 1$. A zero-mean complex white Gaussian noise $v(n)$ with variance σ_v^2 is then added to $h(n)d(n)$ as in equation (3.1). Thus, the SNR is defined as follows:

$$\text{SNR} = 10\log_{10}\left(\frac{\sigma_h^2}{\sigma_v^2}\right) = 10\log_{10}\left(\frac{1}{\sigma_v^2}\right) \tag{3.42}$$

Here, it is assumed that the additive noise variance σ_v^2 is available.

According to the preliminary tests we have carried out, the performance of the proposed algorithm depends on the SNR, the number of available samples N_s, the Doppler rate f_dT_b and the AR model order p. In general, significant results are obtained when the SNR is not less than 5 dB while N_s is not less than 300 samples. The Doppler rate f_dT_b defines the locations of the AR model poles inside the unit circle in the z-plane. Thus, when dealing with high Doppler rates (i.e., $f_dT_b > 0.1$), the corresponding poles of the AR process are well separated and far from the unit circle (see, e.g., Figure 1.9). In these cases, our approach works very well. However, as the Doppler rate decreases, the corresponding poles become close to each other as well as to the unit circle. This results in AR parameters that are close to the boundary of the stability region in the z-plane. Therefore, the accurate estimation of these parameters becomes difficult. In addition, the convergence of the algorithm is slower.

Figure 3.4 and Figure 3.5 show the results obtained when the fading process $h(n)$ is generated from an AR(2) model with $f_dT_b = 0.25$, SNR=15 dB and $N_s = 300$. The AR(2) parameters are $a_1 = -0.7890$, $a_2 = 0.6770$ and $\sigma_u^2 = 0.4218$. The corresponding poles are at $0.8228e^{\pm j0.3408\pi}$. According to Figure 3.4, which shows the convergence characteristics of the proposed complex algorithm, the estimated AR(2) parameters converge close to the true values after approximately 200 symbols.

To compare the performance of the complex algorithm with its real version applied to the real or imaginary part of the observations, we present in Figure 3.5 the overlay plot of 10 realizations of the estimated AR(2) PSD and poles. One can notice that the estimates obtained from the real part, the imaginary part or the complex data are approximately the same. In addition, these estimates are very closed to the desired AR(2) spectrum and poles. The average estimated poles over 1000 realizations are $(0.8259\pm0.00071)e^{\pm j(0.3430\pm0.000081)\pi}$ from the real part, $(0.8247\pm0.00072)e^{\pm j(0.3435\pm0.000083)\pi}$ from the imaginary part and $(0.8252 \pm 0.00041)e^{\pm j(0.3426\pm0.000083)\pi}$ from the complex data. These estimates, as expected, are approximately the same.

In the following, we will only provide results obtained from the real version of the proposed complex algorithm applied to the real part of the observations.

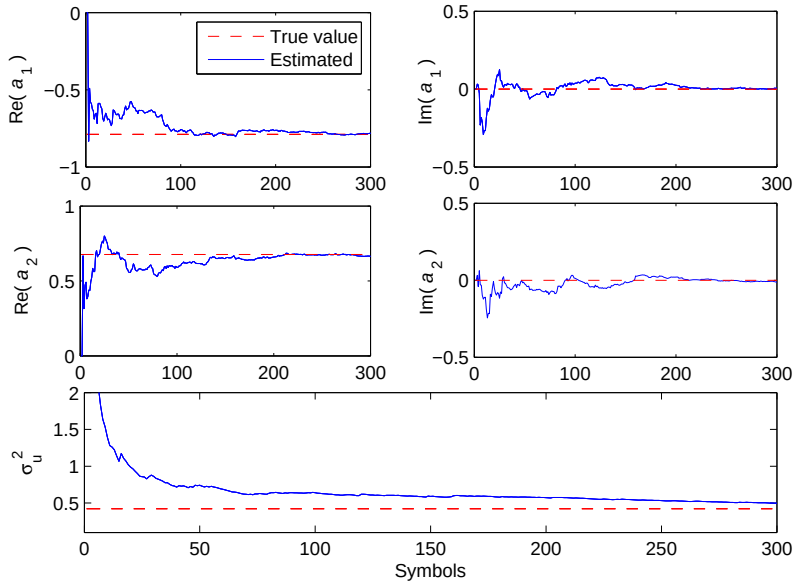

Figure 3.4: Estimation of the AR(2) parameters and the driving process variance using the complex algorithm. True values are $a_1 = -0.7890$, $a_2 = 0.6770$ and $\sigma_u^2 = 0.4218$. $f_d T_b = 0.25$, SNR=15dB and $N_s = 300$.

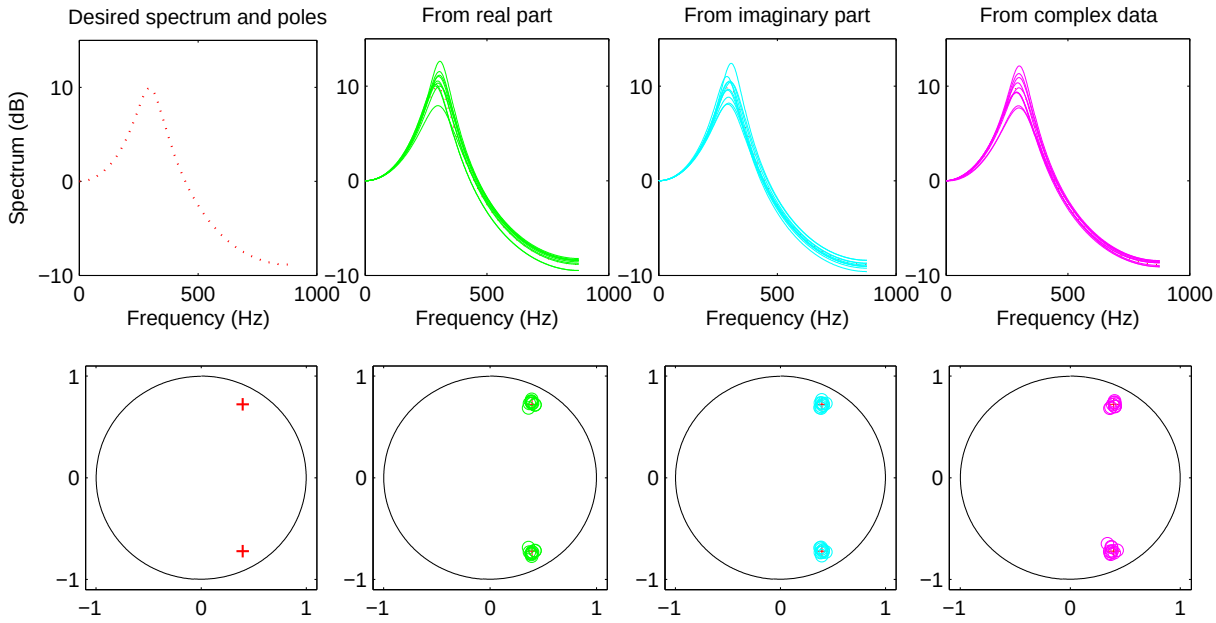

Figure 3.5: Estimation of AR(2) PSD and corresponding poles in the z-plane. 10 realizations are plotted. $f_d T_b = 0.25$, SNR=15dB and $N_s = 300$.

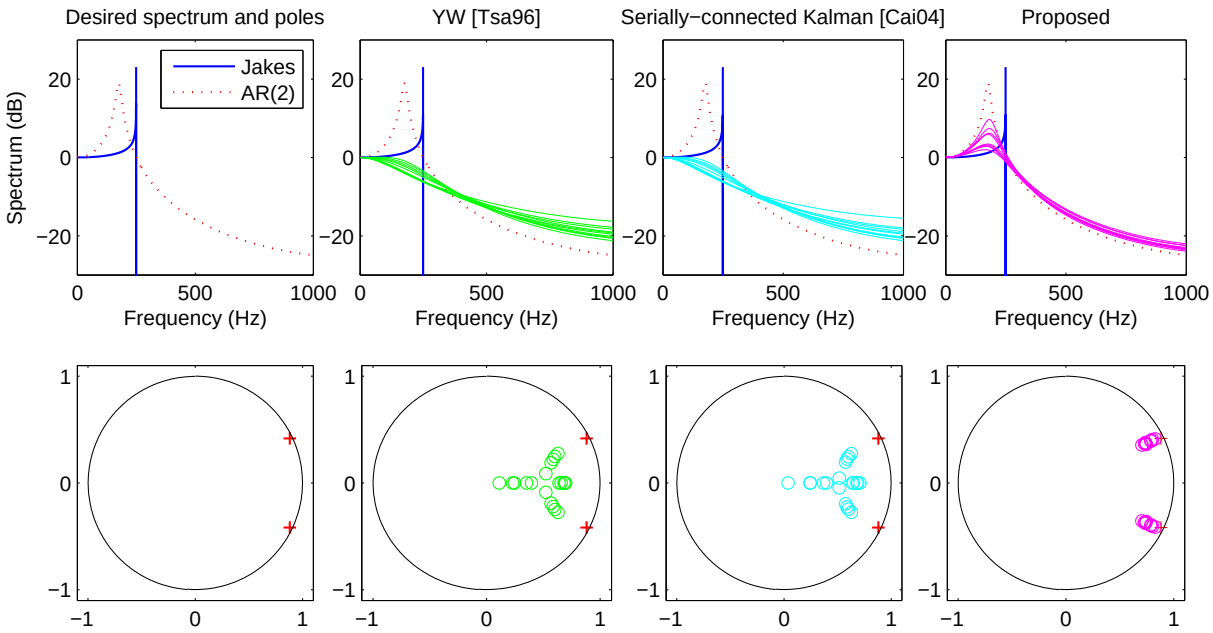

Figure 3.6: Estimations of AR(2) PSD and corresponding poles in the z-plane obtained by using the different methods. 10 realizations are plotted. $f_d T_b = 0.1$, SNR=10dB and $N_s = 500$.

According to Figure 3.6, Figure 3.7 and Figure 3.8 which respectively show the estimation of the PSD and poles of AR(2), AR(3) and AR(20) processes that model the Jakes spectrum, the proposed two-cross-coupled Kalman filter based method provides closer estimates to the desired AR spectrum and poles than the other approaches. In addition, the YW estimator [Tsa96] and the two-serially-connected Kalman filter based approach [Cai04] result in biased estimates and smoothed spectrum at low SNR (see Figures 3.6 and 3.7). Furthermore, the later approach may result in pole estimates outside the unit circle in the z-plane (see Figure 3.8). Moreover, increasing the AR model order yields a better fit between the spectra of the resulting process and the Jakes model. It should be noted that for every method and when the model order is getting higher (for instance $p = 20$), the accurate estimation of all the AR parameters becomes difficult even at high SNR and with a high number of observation samples (see Figure 3.8 where SNR=40dB and $N_s = 2000$ are used). This is due to the U-shaped low-pass band-limited nature of the channel spectrum or equivalently, to the positions of the corresponding AR poles which are close to the unit circle in the z-plane. Therefore, in these cases, the selection of the AR model order corresponds to a trade-off between the accuracy of the model and the difficulty in estimating its parameters.

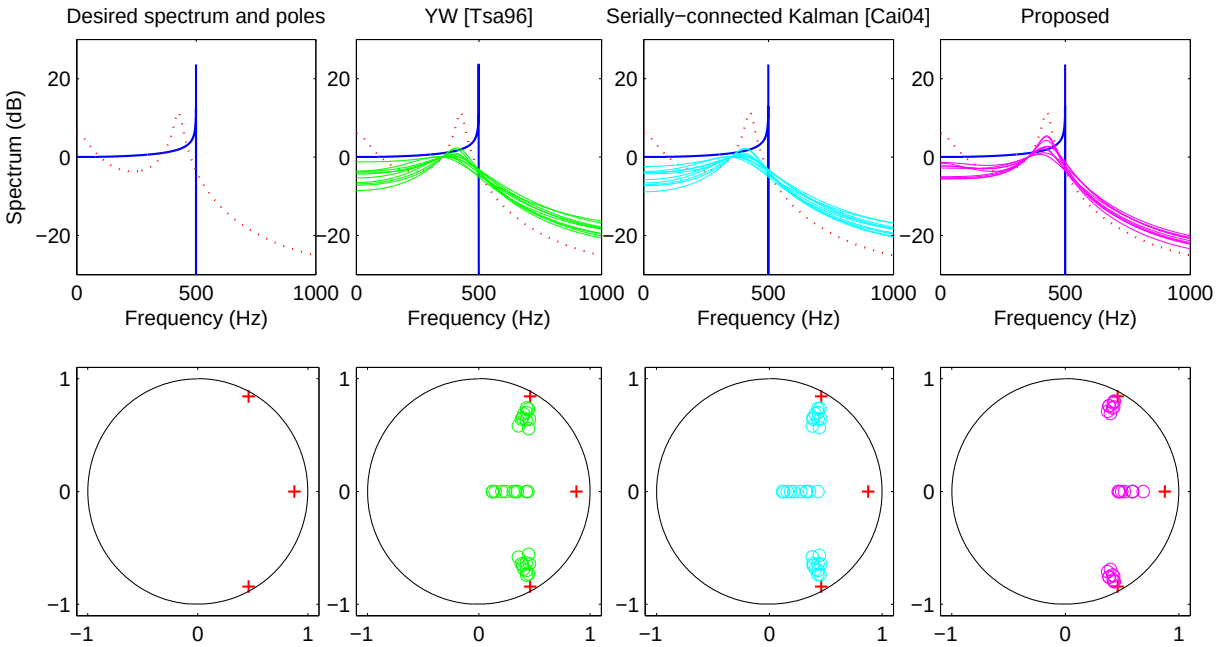

Figure 3.7: Estimations of AR(3) PSD and corresponding poles in the z-plane obtained by using the different methods. 10 realizations are plotted. $f_d T_b = 0.2$, SNR=12dB and $N_s = 500$.

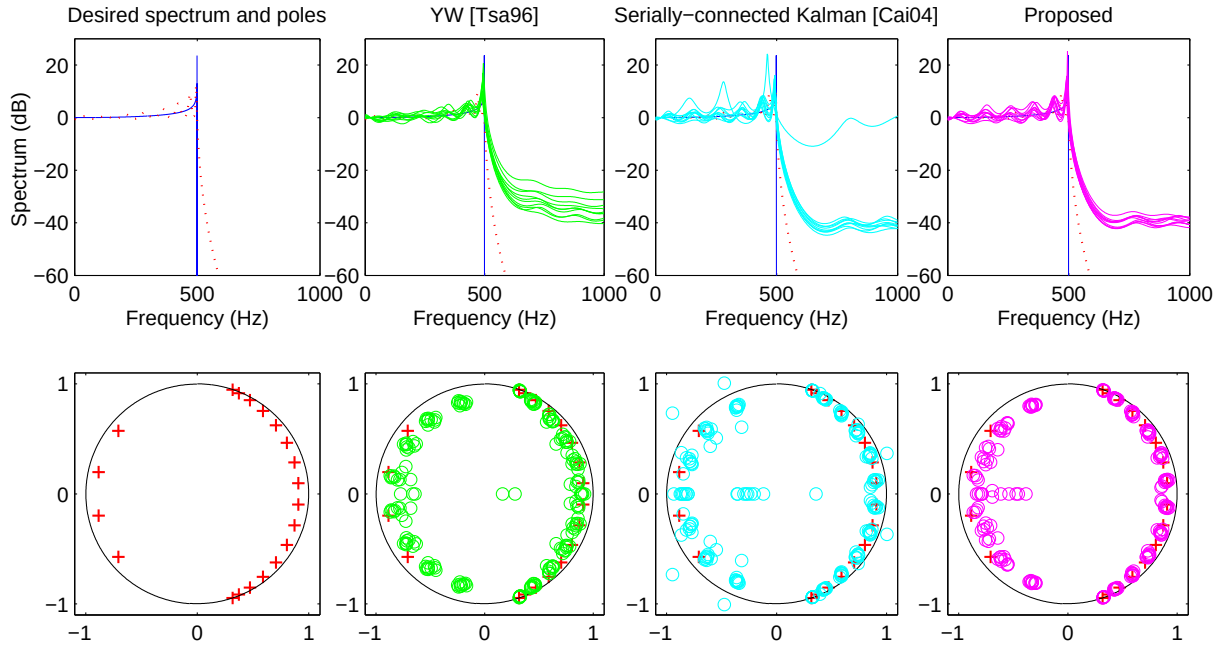

Figure 3.8: Estimations of AR(20) PSD and corresponding poles in the z-plane obtained by using the different methods. 10 realizations are plotted. $f_d T_b = 0.2$, SNR=40dB and $N_s = 2000$.

3.6 Two-cross-coupled H_∞ filter based estimator

In this section, we propose to take advantage of the two-cross-coupled H_∞ filter based structure recently developed in the framework of speech enhancement [Lab07] to design a channel estimation algorithm [Jam07b] as shown in Figure 3.9. One H_∞ filter is used to estimate the fading process as in equations (3.13)-(3.19), while the second one makes it possible to estimate the corresponding AR parameters from the estimated fading process as we will see in the next subsection.

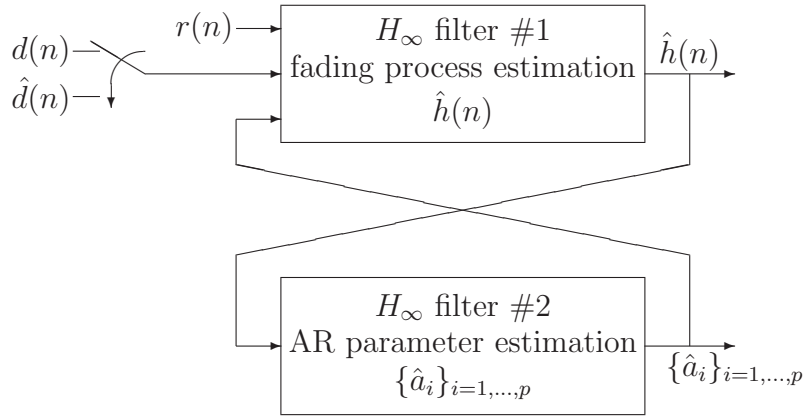

Figure 3.9: Proposed two-cross-coupled H_∞ filter based channel estimation scheme.

3.6.1 Estimation of the AR parameters from the estimated fading process

Here, we propose to estimate the AR parameters from the estimated fading process $\hat{h}(n)$ obtained by the first H_∞ filter (3.13)-(3.19). Thus, by following the same procedure as in subsection 3.5.1, the state-space representation for the estimation of the AR parameter vector $\boldsymbol{\theta}$ can be written as follows:

$$\begin{cases} \boldsymbol{\theta}(n) = \boldsymbol{\theta}(n-1) \\ \hat{h}(n) = \mathbf{d}_{\boldsymbol{\theta}}^T(n-1)\boldsymbol{\theta}(n) + \widetilde{w}(n) \end{cases} \tag{3.43}$$

where $\mathbf{d}_{\boldsymbol{\theta}}^T(n-1) = -[\ \hat{h}(n-1) \quad \hat{h}(n-2) \quad \cdots \quad \hat{h}(n-p)\ ]$ and $\widetilde{w}(n) = \boldsymbol{l}\underline{\mathbf{K}}(n)\nu(n)$.
By defining the estimation error due to the estimation of the AR parameters as $e_{\boldsymbol{\theta}} = \mathbf{d}_{\boldsymbol{\theta}}^T(n-1)\left(\boldsymbol{\theta}(n) - \hat{\boldsymbol{\theta}}(n)\right)$, a second H_∞ filter can therefore be used to recursively

estimate $\boldsymbol{\theta}$ as follows:

$$\hat{\boldsymbol{\theta}}(n) = \hat{\boldsymbol{\theta}}(n-1) + \underline{\mathbf{K}}_{\boldsymbol{\theta}}(n)\widetilde{w}(n), \quad \hat{\boldsymbol{\theta}}(0) = \mathbf{0} \tag{3.44a}$$

$$\underline{\mathbf{K}}_{\boldsymbol{\theta}}(n) = \underline{\mathbf{P}}_{\boldsymbol{\theta}}(n)\mathbf{C}_{\boldsymbol{\theta}}^{-1}(n)\mathbf{d}_{\boldsymbol{\theta}}(n-1)R_{\widetilde{w}}^{-1} \tag{3.44b}$$

$$\mathbf{C}_{\boldsymbol{\theta}}(n) = \mathbf{I}_p - \gamma_{\boldsymbol{\theta}}^{-2}\mathbf{d}_{\boldsymbol{\theta}}(n-1)\mathbf{d}_{\boldsymbol{\theta}}^H(n-1)\underline{\mathbf{P}}_{\boldsymbol{\theta}}(n) + \mathbf{d}_{\boldsymbol{\theta}}(n-1)R_{\widetilde{w}}^{-1}\mathbf{d}_{\boldsymbol{\theta}}^H(n-1)\underline{\mathbf{P}}_{\boldsymbol{\theta}}(n) \tag{3.44c}$$

$$\underline{\mathbf{P}}_{\boldsymbol{\theta}}(n+1) = \underline{\mathbf{P}}_{\boldsymbol{\theta}}(n)\mathbf{C}_{\boldsymbol{\theta}}^{-1}(n), \quad \underline{\mathbf{P}}_{\boldsymbol{\theta}}(0) = \mathbf{P}_{\boldsymbol{\theta}_0} \tag{3.44d}$$

where $\gamma_{\boldsymbol{\theta}} > 0$ is the disturbance attenuation level. In addition, $R_{\widetilde{w}} > 0$ and $\mathbf{P}_{\boldsymbol{\theta}_0} > 0$ are the weighting parameters.

It should be noted that our approach is different from the one in [Cai04] where two-serially-connected H_∞ filters are used to estimate the fading process and its AR parameters (see Figure 3.2). On the one hand, the approach in [Cai04] estimates the AR parameters directly from the noisy observations which yields biased values and may have a bad influence on the estimation of the fading process. On the other hand, our approach can provide reliable estimates by estimating the AR parameters from the estimated fading process.

3.6.2 Tuning the weighting parameters

The weighting parameters Q_u and R_v in the first H_∞ filtering algorithm (3.13)-(3.19) correspond respectively to the instantaneous power of the sequences $u(n)$ and $v(n)$. In [Cai04], Cai *et al.* have mentioned that for practical wireless communication systems the weighting parameters Q_u and R_v can be chosen respectively as the variance of the driving and additive sequences (i.e., $Q_u = \sigma_u^2$ and $R_v = \sigma_v^2$). Thus, by analogy with the Kalman filter theory, the weighting parameter Q_u can be recursively tuned by taking into account equation (3.41), as follows:

$$\hat{Q}_u(n) = \lambda\hat{Q}_u(n-1) + (1-\lambda)\mathbf{f}\underline{\mathbf{M}}(n)\mathbf{f}^T \tag{3.45}$$

where $\underline{\mathbf{M}}(n) = \underline{\mathbf{P}}(n) - \boldsymbol{\Phi}\underline{\mathbf{P}}(n-1)\boldsymbol{\Phi}^H + \underline{\mathbf{K}}(n)|\nu(n)|^2\underline{\mathbf{K}}^H(n)$, $\mathbf{f} = [\mathbf{g}^T\mathbf{g}]^{-1}\mathbf{g}^T = [\ 1 \quad 0 \quad \cdots \quad 0\ ]$ and λ is the forgetting factor.
In addition, the parameter R_v is assigned to σ_v^2. Furthermore, the parameter $R_{\widetilde{w}}$ in the second H_∞ filter (3.44) is tuned by taking into account equation (3.32), as follows:

$$R_{\widetilde{w}} = \boldsymbol{l}\underline{\mathbf{K}}(n)\left(\mathbf{d}^T(n)\underline{\mathbf{P}}(n)\mathbf{d}(n) + R_v\right)\underline{\mathbf{K}}^H(n)\boldsymbol{l}^T \tag{3.46}$$

Moreover, as we have no *a priori* knowledge about the initial state error, the weighting matrices $\mathbf{P}_0$ and $\mathbf{P}_{\boldsymbol{\theta}_0}$ are assigned to the identity matrix (i.e., $\mathbf{P}_0 = \mathbf{P}_{\boldsymbol{\theta}_0} = \mathbf{I}_p$).

It should be noted that, although the selected values of the weighting parameters might not correspond to the true values (instantaneous powers of the corresponding sequences), the H_∞ filtering by its nature is robust to these deviations [Has99].

3.6.3 Simulation results

In this subsection, we carry out a comparative simulation study on the estimation of the fading channel AR parameters between several methods:

1. the proposed two-cross-coupled H_∞ filters,
2. the proposed two-cross-coupled Kalman filters presented in section 3.5,
3. the two-serially-connected Kalman or H_∞ filters [Cai04] shown in Figure 3.2,
4. the YW estimator used for instance in [Tsa96].

Here, we consider the same simulation protocol as in subsection 3.5.3. In addition, the results are obtained by applying real versions of the proposed two-cross-coupled channel estimators to the real part of the observations (see remark 1 in section 3.5).

Table 3.1 shows the average AR(2) parameter estimates of the various approaches when $f_d T_b = 0.1$ and $N_s = 500$. From this table, the two-cross-coupled H_∞ filter based approach provides approximately the same results as the two-cross-coupled Kalman filter based one. In addition, both approaches yield much better estimates than the other approaches, especially at low SNR. In that case, the YW estimator and the two-serially-connected Kalman or H_∞ filter based estimators result in biased estimates. According to Figure 3.10, the two-cross-coupled H_∞ filter based approach yields much better estimates than the two-serially-connected H_∞ filter based one which results in smoothed spectrum. In addition, the two-cross-coupled H_∞ filter based estimator provides approximately the same estimates as the two-cross-coupled Kalman filter based one. Moreover, based on the various simulation tests we have carried out using high-order AR models, the two-cross-coupled Kalman and H_∞ filter based channel estimators yield approximately the same results. Therefore, although the two-cross-coupled H_∞ filter based approach does not provide better results than the two-cross-coupled Kalman filter based one, it has the advantage of relaxing the Gaussian assumptions required by Kalman filtering.

Nevertheless, in both two-cross-coupled Kalman and H_∞ filter based channel estimators, the additive noise variance is assumed to be known, which is not the case in practice and should be estimated. Therefore, as an alternative to the cross-coupled estimators, we propose to view the channel estimation as an EIV issue in the next section.

Table 3.1: Average AR(2) parameters and driving process variance estimates based on 1000 realizations. The true values are $a_1 = -1.7625$, $a_2 = 0.9503$ and $\sigma_u^2 = 0.0178$. $N_s = 500$ and $f_d T_b = 0.1$.

SNR		10 dB	15 dB	20 dB	40 dB
Proposed two-cross-coupled	$\hat{a}_1$	-1.4908	-1.6348	-1.7001	-1.7557
Kalman filters	$\hat{a}_2$	0.6991	0.8326	0.8926	0.9434
	$\hat{\sigma}_u^2$	0.0682	0.0344	0.0280	0.0167
Proposed two-cross-coupled	$\hat{a}_1$	-1.4878	-1.6746	-1.7400	-1.7576
H_∞ filters	$\hat{a}_2$	0.6975	0.8724	0.9336	0.9454
	$\hat{Q}_u$	0.0882	0.0192	0.0066	0.0031
Two-serially-connected	$\hat{a}_1$	-1.0274	-1.4018	-1.6184	-1.7567
H_∞ filters [Cai04]	$\hat{a}_2$	0.2601	0.6043	0.8107	0.9443
Two-serially-connected	$\hat{a}_1$	-1.0293	-1.4009	-1.6177	-1.7560
Kalman filters [Cai04]	$\hat{a}_2$	0.2616	0.6033	0.8100	0.9436
Yule-Walker [Tsa96]	$\hat{a}_1$	-1.0318	-1.3958	-1.6031	-1.7359
routine *aryule* of	$\hat{a}_2$	0.2647	0.5995	0.7970	0.9249
MATLAB 7.1	$\hat{\sigma}_u^2$	0.3284	0.1506	0.0704	0.0252

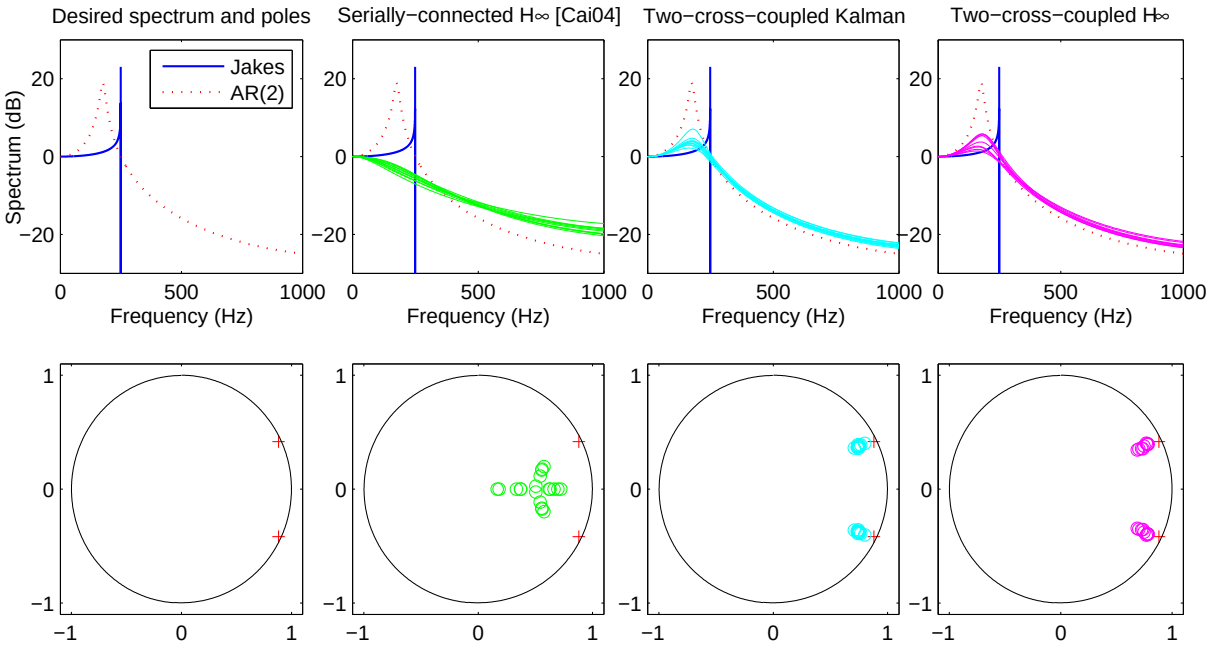

Figure 3.10: Estimations of AR(2) PSD and corresponding poles in the z-plane obtained by using the different methods. 10 realizations are plotted. $f_d T_b = 0.1$, SNR=10dB and $N_s = 500$.

3.7 Errors-in-variables approach for AR parameter estimation

In this section, we first provide the principles of the EIV models and the state of the art in that field. We then propose to identify the channel AR parameters and the variances of both the additive measurement noise and the driving process based on an EIV approach [Jam06] [Jam07a]. Finally, a comparative simulation study is carried out between the proposed method and other existing approaches.

3.7.1 Principles of EIV models

EIV is a modeling technique which assumes that every variable is disturbed by an additive error or noise term. The EIV models, originally developed in the framework of statistics, are now used in applications such as system identification, control, signal processing, etc. [Huf02] [Sod02] [Bob07].

Given a generic process described by κ variables $\{x_i\}_{i=1,\cdots,\kappa}$, the formulation of an EIV estimation problem consists in determining, on the only basis of noisy observations $\{y_i = x_i + b_i\}_{i=1,\cdots,\kappa}$, the set of κ-tuple $\{\xi_i\}_{i=1,\cdots,\kappa}$ that satisfies:

$$\begin{aligned} \xi_1 x_1 + \xi_2 x_2 + \cdots + \xi_\kappa x_\kappa &= 0 \\ [x_1 \quad x_2 \quad \cdots \quad x_\kappa][\xi_1 \quad \xi_2 \quad \cdots \quad \xi_\kappa]^T &= 0 \end{aligned} \tag{3.47}$$

or equivalently,

$$\mathbf{R_x} \begin{bmatrix} \xi_1 & \xi_2 & \cdots & \xi_\kappa \end{bmatrix}^T = \mathbf{0}_\kappa \tag{3.48}$$

where $\mathbf{R_x}$ is the covariance matrix of $\{x_i\}_{i=1,\cdots,\kappa}$.
When each noise term b_i is assumed to be zero-mean, independent of every other noise term and every variable x_i, one has:

$$\mathbf{R_x} = \mathbf{R_y} - \mathbf{R_b} \tag{3.49}$$

where $\mathbf{R_y}$ and $\mathbf{R_b}$ respectively denote the covariance matrix of $\{y_i\}_{i=1,\cdots,\kappa}$ and of $\{b_i\}_{i=1,\cdots,\kappa}$.
At that stage, the so-called Frisch scheme [Beg90] consists in searching for the diagonal matrices $\mathbf{R_b}$ which enable $\mathbf{R_y} - \mathbf{R_b}$ to be positive semidefinite:

$$\mathbf{R_y} - \mathbf{R_b} \geq \mathbf{0}_\kappa \tag{3.50}$$

Recently, Diversi *et al.* [Div05a] [Div05b] have proposed to take advantage of some theoretical results concerning the Frisch scheme [Beg90] to develop a new estimation

approaches for AR models in presence of noise. Their approaches consist in estimating the null space of specific autocorrelation matrices and have the advantage of providing estimates of the AR parameters and the variances of both the additive noise and the driving process in a congruent manner. Meanwhile, these approaches were analyzed and evaluated in the framework of speech dereverberation [Bob05] and speech enhancement [Bob06] [Bob07]. In [Jam06] [Jam07a], we have proposed to reformulate these approaches for the identification of time-varying Rayleigh fading channels.

In the next subsection, we will see how the channel AR parameter estimation can be mapped into an EIV problem.

3.7.2 EIV formulation of the channel AR parameter estimation

Given the channel AR model (1.30), our purpose is to estimate the channel AR parameters $\{a_i\}_{i=1,\ldots,p}$ and the noise variances (i.e., σ_b^2 and σ_u^2) from N_s observation samples, $\{y(n)\}_{n=1,\ldots,N_s}$ given by (3.20), obtained during the transmission of a training sequence. For this purpose, let us define the following four $(p+1)\times 1$ vectors:

$$\underline{\boldsymbol{\theta}}_{p+1} = \begin{bmatrix} a_p & \cdots & a_1 & 1 \end{bmatrix}^T \tag{3.51}$$

$$\underline{\mathbf{y}}(n) = \begin{bmatrix} y(n-p) & \cdots & y(n-1) & y(n) \end{bmatrix}^T \tag{3.52}$$

$$\underline{\mathbf{h}}(n) = \begin{bmatrix} h(n-p) & \cdots & h(n-1) & h(n) \end{bmatrix}^T \tag{3.53}$$

$$\underline{\mathbf{b}}(n) = \begin{bmatrix} b(n-p) & \cdots & b(n-1) & b(n) \end{bmatrix}^T \tag{3.54}$$

Thus, equations (1.30) and (3.20) can be respectively written in vector form as follows:

$$\begin{aligned} &\begin{bmatrix} h(n-p) & \cdots & h(n-1) & (h(n)-u(n)) \end{bmatrix} \underline{\boldsymbol{\theta}}_{p+1} \\ &= (\underline{\mathbf{h}}^T(n) - [\underbrace{0 \quad \cdots \quad 0}_{p} \quad u(n)\,])\underline{\boldsymbol{\theta}}_{p+1} = 0 \end{aligned} \tag{3.55}$$

and

$$\underline{\mathbf{y}}(n) = \underline{\mathbf{h}}(n) + \underline{\mathbf{b}}(n) \tag{3.56}$$

Given (3.56) and under the assumption of statistical independence between the additive noise and the fading process, the observation autocorrelation matrix satisfies:

$$\mathbf{R}_{yy}^{p+1} = E[\underline{\mathbf{y}}(n)\underline{\mathbf{y}}^H(n)] = \mathbf{R}_{hh}^{p+1} + \sigma_b^2\mathbf{I}_{p+1} \tag{3.57}$$

where $\mathbf{R}_{hh}^{p+1} = E[\underline{\mathbf{h}}(n)\underline{\mathbf{h}}^H(n)]$.
Then, pre-multiplying (3.55) by $\underline{\mathbf{h}}(n)$ and applying the expectation operator result in the

following equation:

$$(\mathbf{R}_{hh}^{p+1} - \text{diag}[\underbrace{0 \quad \cdots \quad 0}_{p} \quad \sigma_u^2\ ])\underline{\boldsymbol{\theta}}_{p+1} \triangleq \bar{\mathbf{R}}_{hh}^{p+1}\underline{\boldsymbol{\theta}}_{p+1} = \mathbf{0}_{p+1} \tag{3.58}$$

Hence, $\bar{\mathbf{R}}_{hh}^{p+1}$ is the positive semidefinite correlation matrix of the vector $[\ h(n-p) \quad \cdots \quad h(n-1) \quad (h(n)-u(n))\ ]^T$. Given (3.57) and the definition of $\bar{\mathbf{R}}_{hh}^{p+1}$ in (3.58), it is possible to write:

$$\bar{\mathbf{R}}_{hh}^{p+1} = \mathbf{R}_{yy}^{p+1} - \text{diag}\left[\sigma_b^2\mathbf{I}_p, \sigma_s^2\right] \geq \mathbf{0}_{p+1} \tag{3.59}$$

where

$$\sigma_s^2 = \sigma_b^2 + \sigma_u^2 \tag{3.60}$$

It should be noted that (3.55), (3.58) and (3.59) are respectively similar to (3.47), (3.48) and (3.50). Indeed, the κ-tuple $\{\xi_i\}_{i=1,\cdots,\kappa}$ in equation (3.47) correspond to the AR parameters $\underline{\boldsymbol{\theta}}_{p+1} = [a_p \quad \cdots \quad a_1 \quad 1]^T$. The EIV formulation of the channel AR parameter estimation is illustrated in Figure 3.11.

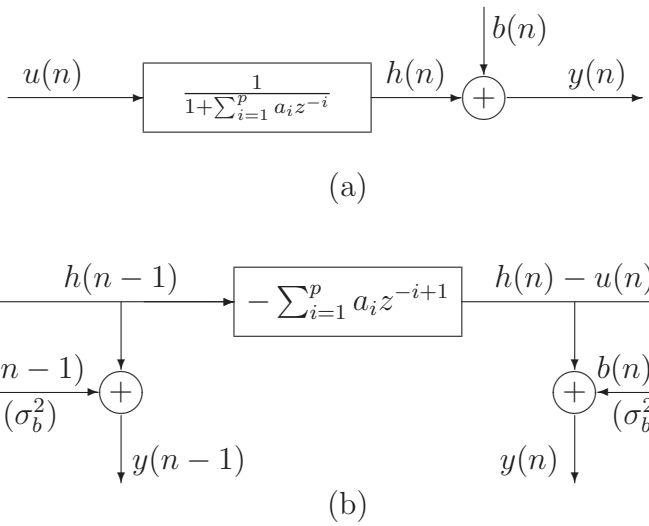

Figure 3.11: (a) AR channel model disturbed by AWGN. (b) corresponding EIV scheme.

By referring to the EIV based methods [Beg90] [Div05b], the actual point $O_a = (\sigma_s^2, \sigma_b^2)$ belongs to the set of solutions $O = (\alpha, \beta)$ making the following matrices positive semidefinite:

$$\bar{\mathbf{R}}_{hh}^{p+1}(O) = \mathbf{R}_{yy}^{p+1} - \text{diag}\left[\beta\mathbf{I}_p, \alpha\right] \geq \mathbf{0}_{p+1} \tag{3.61}$$

This set is the convex curve $S(\mathbf{R}_{yy}^{p+1})$ belonging to the first quadrant of the $(\alpha\beta)$-plane[5], and whose concavity faces the origin (see Figure 3.12). In addition, every point O can be

[5] α corresponds to σ_s^2 and stands for the abscissa, while β corresponds to σ_b^2 and stands for the ordinate.

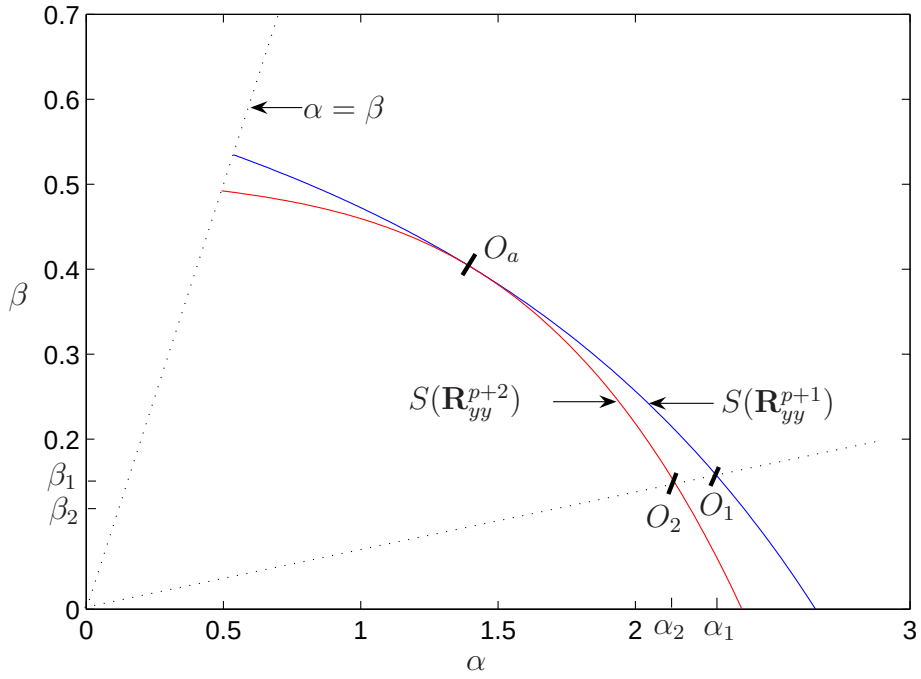

Figure 3.12: Typical shapes of $S(\mathbf{R}_{yy}^{p+1})$ and $S(\mathbf{R}_{yy}^{p+2})$.

associated with a parameter vector $\underline{\boldsymbol{\theta}}_{p+1}(O)$ satisfying (3.58) as follows:

$$\bar{\mathbf{R}}_{hh}^{p+1}(O)\underline{\boldsymbol{\theta}}_{p+1}(O) = \mathbf{0}_{p+1} \tag{3.62}$$

Therefore, the above procedure provides a family of solutions. To extract the true one, we carry out the same procedure using a $(p+1)^{th}$ order AR process. Thus, by extending the right hand side of the vectors in (3.52), (3.53) and (3.54) with a new value at time $n+1$, one obtains the $(p+2)\times 1$ vectors $\underline{\mathbf{y}}(n+1)$, $\underline{\mathbf{h}}(n+1)$ and $\underline{\mathbf{b}}(n+1)$. It follows that:

$$\bar{\mathbf{R}}_{hh}^{p+2}(O) = \mathbf{R}_{yy}^{p+2} - \mathrm{diag}\left[\beta\mathbf{I}_{p+1}, \alpha\right] \geq \mathbf{0}_{p+2} \tag{3.63}$$

and

$$\bar{\mathbf{R}}_{hh}^{p+2}(O)\underline{\boldsymbol{\theta}}_{p+2}(O) = \mathbf{0}_{p+2} \tag{3.64}$$

where the correlation matrices $\mathbf{R}_{yy}^{p+2}$ and $\bar{\mathbf{R}}_{hh}^{p+2}$ are now of size $(p+2)\times(p+2)$.
When $O = O_a$, one has more particularly:

$$\bar{\mathbf{R}}_{hh}^{p+2}(O_a)\begin{bmatrix} 0 \\ \underline{\boldsymbol{\theta}}_{p+1}(O_a) \end{bmatrix} = \mathbf{0}_{p+2} \tag{3.65}$$

Given (3.63) and (3.65), it can be verified that the convex curve $S(\mathbf{R}_{yy}^{p+2})$ lies under $S(\mathbf{R}_{yy}^{p+1})$ [Beg90]. In addition, the actual point O_a belongs to both $S(\mathbf{R}_{yy}^{p+1})$ and $S(\mathbf{R}_{yy}^{p+2})$

convex curves. Therefore, determining the point O_a and then extracting the parameter vector $\underline{\boldsymbol{\theta}}_{p+1}$ from the null space of $\bar{\mathbf{R}}_{hh}^{p+1}(O_a)$ using (3.62) result in a solution of the channel identification problem.

However, in all practical cases that rely on limited sequences of data, the EIV assumptions do not hold. Hence, no point O_a belongs to both $S(\mathbf{R}_{yy}^{p+1})$ and $S(\mathbf{R}_{yy}^{p+2})$. For this reason, several criteria have been proposed so that the EIV scheme can be applied to these cases [Div05a] [Div05b].

3.7.3 Application of the EIV scheme in practical cases

In this subsection, we will consider two criteria that allow the EIV scheme to be applied in practical cases.

3.7.3.1 Shift relation criterion

The Shift Relation (SR) criterion, proposed in [Div05b], is based on the shift-invariant property of dynamic systems described by (3.65). Thus, the search for $O_a = (\sigma_s^2, \sigma_b^2)$ along $S(\mathbf{R}_{yy}^{p+1})$ is based on minimizing the following SR criterion:

$$J_{SR}(O_1, O_2) = \begin{bmatrix} 0 \\ \underline{\boldsymbol{\theta}}_{p+1}(O_1) \end{bmatrix}^H \bar{\mathbf{R}}_{hh}^{p+2}(O_2) \begin{bmatrix} 0 \\ \underline{\boldsymbol{\theta}}_{p+1}(O_1) \end{bmatrix} \tag{3.66}$$

where $O_1 = (\alpha_1, \beta_1)$ and $O_2 = (\alpha_2, \beta_2)$ are defined as the intersections of the line from the origin with $S(\mathbf{R}_{yy}^{p+1})$ and $S(\mathbf{R}_{yy}^{p+2})$ (see Figure 3.12), such as:

$$\frac{\beta_1}{\alpha_1} = \frac{\beta_2}{\alpha_2} \tag{3.67}$$

The cost function defined in (3.66) exhibits the following properties:

1. $J_{SR}(O_1, O_2) \geq 0$
2. $J_{SR}(O_1, O_2) = 0 \Longleftrightarrow O_1 = O_2 = O_a$

Based on the SR criterion, the following identification algorithm can be considered.

Algorithm 1:

1. Compute the estimates of $\mathbf{R}_{yy}^{p+1}$ and $\mathbf{R}_{yy}^{p+2}$ as follows[6]:

$$\hat{\mathbf{R}}_{yy}^{p+1} = \frac{1}{N_s - p} \sum_{n=p+1}^{N_s} \underline{\mathbf{y}}(n)\underline{\mathbf{y}}^H(n) \tag{3.68}$$

$$\hat{\mathbf{R}}_{yy}^{p+2} = \frac{1}{N_s - p - 1} \sum_{n=p+1}^{N_s-1} \underline{\mathbf{y}}(n+1)\underline{\mathbf{y}}^H(n+1) \tag{3.69}$$

2. Start from generic points $O_1 = (\alpha_1, \beta_1)$ on $S(\hat{\mathbf{R}}_{yy}^{p+1})$ and $O_2 = (\alpha_2, \beta_2)$ on $S(\hat{\mathbf{R}}_{yy}^{p+2})$ such as $\frac{\beta_1}{\alpha_1} = \frac{\beta_2}{\alpha_2}$ (see Figure 3.12). Note that this is a solvable generalized eigenvalue problem [Gui95],

3. Compute $\bar{\mathbf{R}}_{hh}^{p+1}(O_1)$, $\bar{\mathbf{R}}_{hh}^{p+2}(O_2)$ and $\underline{\boldsymbol{\theta}}_{p+1}(O_1)$ by using relations (3.61), (3.63) and (3.62) respectively,

4. Compute the SR cost function $J_{SR}(O_1, O_2)$ from (3.66),

5. Search on $S(\hat{\mathbf{R}}_{yy}^{p+1})$ for the variances of both the additive noise and the driving process which minimize $J_{SR}(O_1, O_2)$.

3.7.3.2 HOYW equations based criterion

The second criterion, based on the so-called HOYW equations, was recently proposed in [Div05a]. To obtain this criterion, let us first define the following two $q \times 1$ vectors:

$$\underline{\mathbf{y}}_q(n) = \begin{bmatrix} y(n-p-q) & \cdots & y(n-p-2) & y(n-p-1) \end{bmatrix}^T \tag{3.70}$$

$$\underline{\mathbf{h}}_q(n) = \begin{bmatrix} h(n-p-q) & \cdots & h(n-p-2) & h(n-p-1) \end{bmatrix}^T \tag{3.71}$$

where $q > p$. It follows that:

$$\boldsymbol{\Sigma}_{hh}^q = E[\underline{\mathbf{h}}_q(n)\underline{\mathbf{h}}^H(n)] = \begin{bmatrix} R_{hh}(q) & R_{hh}(q+1) & \cdots & R_{hh}(q+p) \\ R_{hh}(q-1) & R_{hh}(q) & \cdots & R_{hh}(q+p-1) \\ \vdots & \vdots & \ddots & \vdots \\ R_{hh}(1) & R_{hh}(2) & \cdots & R_{hh}(p+1) \end{bmatrix} \tag{3.72}$$

[6]It should be noted that, due to the finite length computations and the imperfect channel simulations, the estimated autocorrelation matrices may be complex with very small imaginary parts. To guarantee that the AR parameters are real, we propose to replace the estimated matrices with their real parts (i.e., $\hat{\mathbf{R}}_{yy}^{p+1} = \mathrm{Re}(\hat{\mathbf{R}}_{yy}^{p+1})$ and $\hat{\mathbf{R}}_{yy}^{p+2} = \mathrm{Re}(\hat{\mathbf{R}}_{yy}^{p+2})$).

Since the matrix $\mathbf{\Sigma}_{hh}^{q}$ does not contain the zero lag term $R_{hh}(0)$ and hence does not involve the additive noise variance σ_b^2 , one can write:

$$\mathbf{\Sigma}_{yy}^{q} = E[\underline{\mathbf{y}}_q(n)\underline{\mathbf{y}}^H(n)] = \mathbf{\Sigma}_{hh}^{q} \tag{3.73}$$

Thus, the set of q HOYW equations can be written in the following manner:

$$\mathbf{\Sigma}_{hh}^{q}\underline{\boldsymbol{\theta}}_{p+1} = \mathbf{\Sigma}_{yy}^{q}\underline{\boldsymbol{\theta}}_{p+1} = \mathbf{0}_q \tag{3.74}$$

The HOYW criterion is hence defined as the square norm of $\mathbf{\Sigma}_{yy}^{q}\underline{\boldsymbol{\theta}}_{p+1}$ as follows:

$$J_{HOYW}(O_1) = \|\mathbf{\Sigma}_{yy}^{q}\underline{\boldsymbol{\theta}}_{p+1}(O_1)\|^2 = \underline{\boldsymbol{\theta}}_{p+1}^{H}(O_1)(\mathbf{\Sigma}_{yy}^{q})^H\mathbf{\Sigma}_{yy}^{q}\underline{\boldsymbol{\theta}}_{p+1}(O_1) \tag{3.75}$$

By taking $q > p$, $J_{HOYW}(O_1)$ will exhibits the following properties:

1. $J_{HOYW}(O_1) \geq 0$
2. $J_{HOYW}(O_1) = 0 \Longleftrightarrow O_1 = O_a$

Therefore, the second identification algorithm can be formulated as follows.

Algorithm 2:

1. Compute the estimate of $\mathbf{R}_{yy}^{p+1}$ from (3.68) and the estimate of $\mathbf{\Sigma}_{yy}^{q}$ as follows[7]:

$$\hat{\mathbf{\Sigma}}_{yy}^{q} = \frac{1}{N_s - p - q}\sum_{n=p+q+1}^{N_s}\underline{\mathbf{y}}_q(n)\underline{\mathbf{y}}^H(n), \tag{3.76}$$

2. Start from a generic point $O_1 = (\alpha_1, \beta_1)$ on $S(\hat{\mathbf{R}}_{yy}^{p+1})$. Note that this is a solvable generalized eigenvalue problem [Gui95],
3. Compute $\bar{\mathbf{R}}_{hh}^{p+1}(O_1)$ and $\underline{\boldsymbol{\theta}}_{p+1}(O_1)$ by using relations (3.61) and (3.62) respectively,
4. Compute the cost function $J_{HOYW}(O_1)$ from (3.75),
5. Search on $S(\hat{\mathbf{R}}_{yy}^{p+1})$ for the variances of both the additive noise and the driving process which minimize $J_{HOYW}(O_1)$.

[7]To guarantee that the AR parameters are real, we propose to replace the estimated matrices with their real parts (i.e., $\hat{\mathbf{R}}_{yy}^{p+1} = \mathrm{Re}(\hat{\mathbf{R}}_{yy}^{p+1})$ and $\hat{\mathbf{\Sigma}}_{yy}^{q} = \mathrm{Re}(\hat{\mathbf{\Sigma}}_{yy}^{q})$).

3.7.4 Fading process estimation combining EIV with Kalman or H_∞ filter

Once the channel AR parameters $\{a_i\}_{i=1,\ldots,p}$ and the variances of both the additive measurement noise σ_u^2 and the driving process σ_u^2 are estimated by using the EIV based approach, the estimation of the fading process $h(n)$ can be carried out by means of the Kalman filtering algorithm (3.7). To avoid the restrictive Gaussian assumptions imposed by Kalman filtering, H_∞ filtering can be used instead (3.13)-(3.19). The combination of the EIV based approach with either Kalman or H_∞ filtering for the estimation of the fading process and its AR parameters is shown in Figure 3.13. This structure operates as follows. During the training mode, the EIV based approach estimates the channel AR parameters and the noise variances from N_s data samples $\{y(n)\}_{n=1,\cdots,N_s}$. Once the training mode is over, the estimated parameters are stored and used in conjunction with the observations $r(n)$ and the decision $\hat{d}(n)$ (e.g., using (2.61) for instance) to predict the fading process in a decision directed manner.

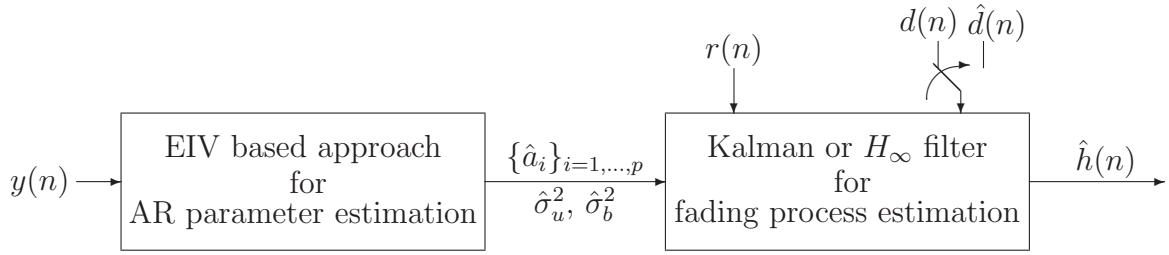

Figure 3.13: Combining EIV based approach with either Kalman or H_∞ filtering for channel estimation.

3.7.5 Simulation results

In this subsection, we carry out a comparative simulation study on the identification of AR fading channels between several methods:

1. the proposed EIV based approach using either the SR or HOYW criterion,
2. the proposed two-cross-coupled H_∞ filters presented in section 3.6,
3. the proposed two-cross-coupled Kalman filters presented in section 3.5,
4. the two-serially-connected Kalman or H_∞ filters [Cai04] shown in Figure 3.2,
5. the standard YW estimator used for instance in [Tsa96].

The fading process $h(n)$ is generated according to the autoregressive channel simulator [Bad05] with order vary from 2 to 20 and a given Doppler rate f_dT_b.
In all simulations, real versions of the proposed algorithms are applied to the real part of the observations to obtain the results.

According to our preliminary simulation results, the proposed EIV based approach provides reliable estimates of the AR parameters even at low SNR (e.g., SNR=5dB) and/or when the number of samples are limited (e.g., $N_s = 200$), which are not the cases when dealing with the other approaches. In addition, it was noticed that the EIV based approach is less sensitive to the variations in the Doppler rate f_dT_b and the AR model order p than the other approaches. Moreover, the EIV based approach can provide an estimation of the measurement noise variance, which is not the case for the other methods.

Table 3.2 shows the average AR(2) parameters and noise variances estimates of the various approaches when $f_dT_b = 0.14$ and $N_s = 200$. From this table, the proposed EIV based approach with the SR criterion provides approximately the same results as that using the HOYW criterion. In addition, the EIV based approaches outperform the other approaches, especially at low SNR ratios. Furthermore, they have the advantage of providing reliable estimates of the additive noise variance. On the other hand, the two-cross-coupled estimators yield better estimates than the serially-connected ones which result in biased estimates at low SNR ratios.
In the following, as the SR criterion yields approximately the same results as the HOYW criterion, we will only consider the SR criterion in the EIV based approach.

According to Figures 3.14, 3.15 and 3.16, which respectively show the estimation of the PSD and poles of AR(2), AR(5) and AR(20) processes that model the Jakes spectrum,

Table 3.2: Average AR(2) parameters and noise variances estimates based on 1000 realizations. The true values are $a_1 = -1.5513$, $a_2 = 0.9018$ and $\sigma_u^2 = 0.0625$. $N_s = 200$ and $f_d T_b = 0.14$.

SNR		5 dB $\sigma_b^2 = 0.3162$	10 dB $\sigma_b^2 = 0.1$	15 dB $\sigma_b^2 = 0.0316$	20 dB $\sigma_b^2 = 0.01$
Proposed EIV based approach	$\hat{a}_1$	-1.5360	-1.5421	-1.5443	-1.5440
(HOYW criterion with $q = 4$)	$\hat{a}_2$	0.8855	0.8925	0.8938	0.8945
	$\hat{\sigma}_u^2$	0.0666	0.0629	0.0615	0.0621
	$\hat{\sigma}_b^2$	0.3139	0.0996	0.0319	0.0099
Proposed EIV based approach	$\hat{a}_1$	-1.5229	-1.5437	-1.5446	-1.5435
(SR criterion)	$\hat{a}_2$	0.8738	0.8941	0.8941	0.8941
	$\hat{\sigma}_u^2$	0.0793	0.0624	0.0615	0.0625
	$\hat{\sigma}_b^2$	0.3098	0.0995	0.0319	0.0098
Proposed two-cross-coupled	$\hat{a}_1$	-1.1977	-1.3565	-1.4549	-1.5030
Kalman filters	$\hat{a}_2$	0.5979	0.7330	0.8174	0.8595
	$\hat{\sigma}_u^2$	0.2545	0.1406	0.1046	0.0988
Proposed two-cross-coupled	$\hat{a}_1$	-1.1615	-1.3181	-1.4561	-1.5133
H_∞ filters	$\hat{a}_2$	0.5706	0.7002	0.8221	0.8729
	$\hat{Q}_u$	0.5395	0.2637	0.1075	0.0660
Two-serially-connected	$\hat{a}_1$	-0.7099	-1.0759	-1.3396	-1.4691
H_∞ filters [Cai04]	$\hat{a}_2$	0.1668	0.4643	0.7017	0.8238
Two-serially-connected	$\hat{a}_1$	-0.7125	-1.0789	-1.3406	-1.4702
Kalman filters [Cai04]	$\hat{a}_2$	0.1678	0.4667	0.7026	0.8248
Yule-Walker [Tsa96]	$\hat{a}_1$	-0.7059	-1.0726	-1.3248	-1.4489
routine *aryule* of	$\hat{a}_2$	0.1632	0.4626	0.6896	0.8064
MATLAB 7.1	$\hat{\sigma}_u^2$	0.7717	0.3798	0.1941	0.1182

the EIV based approach provides closer estimates to the true spectrum and poles than the two-cross-coupled Kalman filter based method. In addition, increasing the AR model order allows for a better fit between the PSD of the resulting process and the theoretical Jakes one. Furthermore, due to the U-shaped low-pass band-limited nature of the channel Doppler spectrum, high SNR is required to better estimate high-order AR model parameters (see Figure 3.16 where SNR=40dB is used).

Based on the various tests we have carried out, the proposed EIV approach is a promising technique for the estimation of the fading channel AR parameters and the additive noise variance.

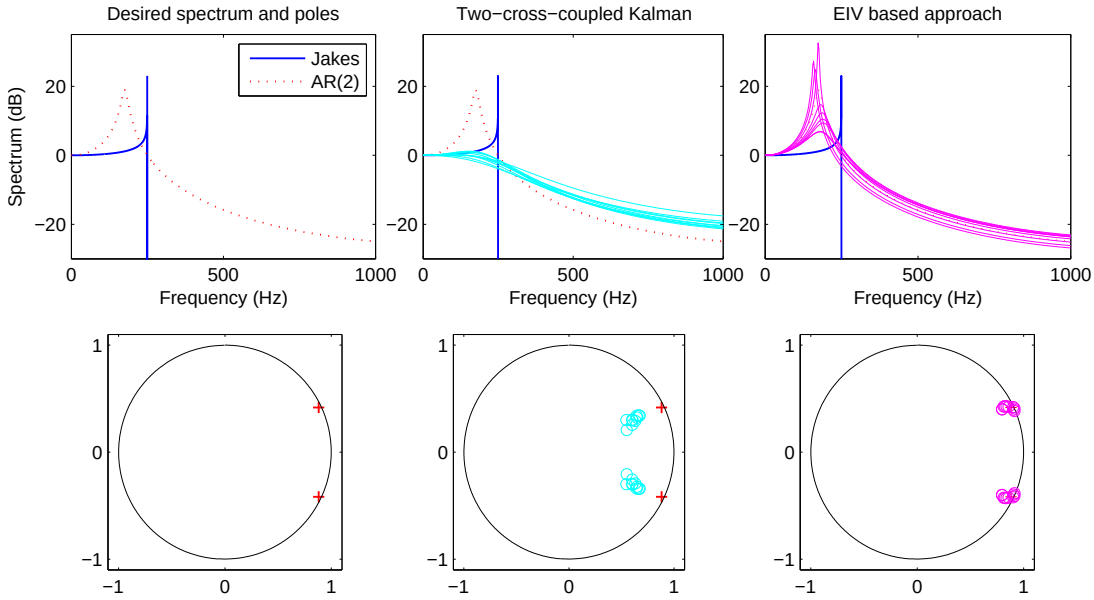

Figure 3.14: 10 overlay plots of the estimation of AR(2) PSD and corresponding poles in the z-plane. $f_d T_b = 0.1$, SNR=5dB and $N_s = 300$.

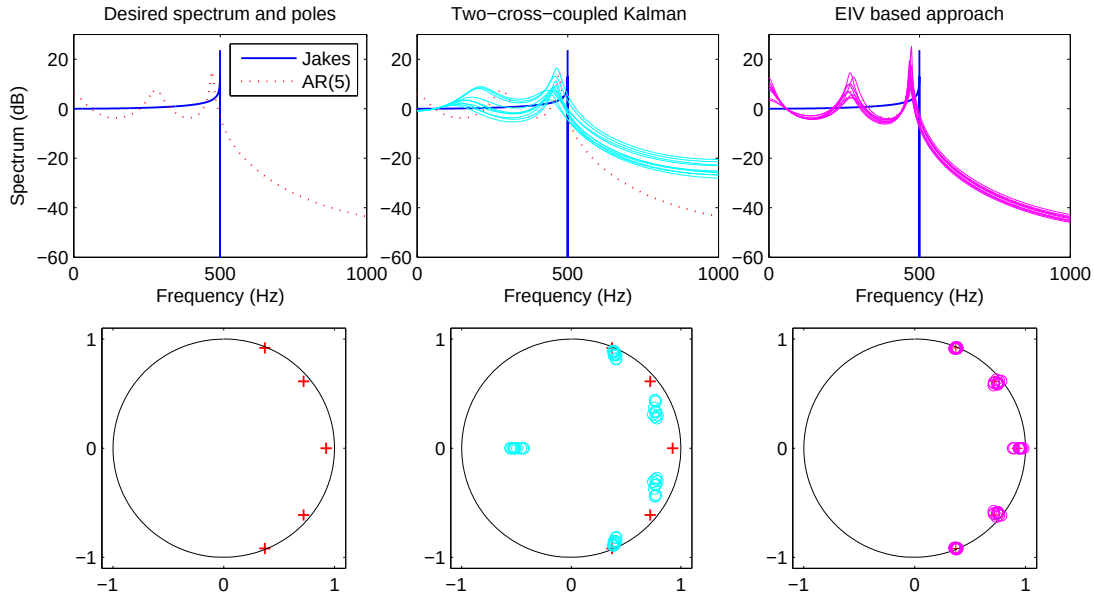

Figure 3.15: 10 overlay plots of the estimation of AR(5) PSD and corresponding poles in the z-plane. $f_d T_b = 0.2$, SNR=25dB and $N_s = 300$.

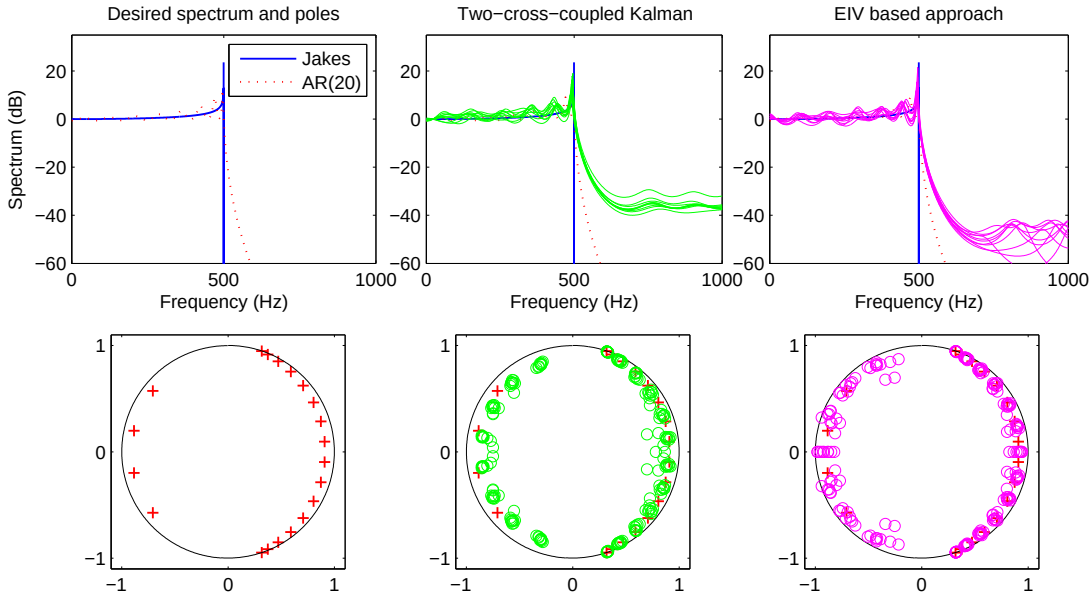

Figure 3.16: 10 overlay plots of the estimation of AR(20) PSD and corresponding poles in the z-plane. $f_dT_b = 0.2$, SNR=40dB and $N_s = 1000$.

3.8 Application to the estimation of MC-DS-CDMA channels

In this section, we consider the estimation and equalization of MC-DS-CDMA[8] fading channels based on the receiver structure introduced in section 2.4. This receiver, shown in Figure 2.14, consists of a decorrelating detector along each carrier followed by a MRC. The decorrelating detector is used to eliminate the MAI caused by other users leading to an observation similar to (3.1). The MRC is used to compensate for the effect of fading by using channel estimates from the channel estimators proposed in the previous sections.

A down-link MC-DS-CDMA system with BPSK modulation, M carriers and $K = 10$ active users is considered. The spreading sequences of all users are gold codes of length $N = 31$. The MC-DS-CDMA fading processes $\{h_m(n)\}_{m=1,\cdots,M}$ are generated according to the modified Jakes model given by equation (1.29) with $L_o = 16$ oscillators and a predetermined value of the Doppler rate f_dT_b. In all of our simulations, the training period for channel estimation is limited to $N_s = 300$ symbols[9]. Besides, like in [Kal03],

[8] Although we focuss our attention on the estimation of MC-DS-CDMA fading channels, the proposed channel estimation techniques can also be applied for other systems such as OFDM.

[9] This long training period is necessary to estimate the channel dynamics. It is usually available at the start of the transmission [Tsa96].

correct decisions are assumed to be used to derive the various channel estimators in the decision directed mode, i.e. $\hat{d}(n) = d(n)$.

We carry out a comparative simulation study on channel estimation and equalization between the following channel estimators:

1. the proposed EIV based approach combined with either Kalman or H_∞ filters,
2. the proposed two-cross-coupled H_∞ filters presented in section 3.6,
3. the proposed two-cross-coupled Kalman filters presented in section 3.5,
4. the two-serially-connected H_∞ filters proposed in [Cai04] and shown in Figure 3.2,
5. the LMS and RLS channel estimators used for instance in [Kal03].

In all simulations, the proposed complex algorithms are applied to the complex data to obtain the results.

According to Figure 3.17, which shows the estimated real and imaginary parts of the fading process $h_1(n)$ over the first carrier, the two-cross-coupled Kalman filter based estimator with AR(5) model provides much better channel estimates than the LMS and RLS estimators.

Figures 3.18 and 3.19 show the BER performance versus either the SNR or the Doppler rate of the two-cross-coupled Kalman filter based estimator with various order AR models. Thus, exploiting the channel statistics by using AR models in the proposed estimator results in significant performance improvement over the LMS and RLS based ones which tend to an error floor at high SNR. In addition, increasing the AR model order will improve the BER performance with the amount of improvement decreases as the model order increases. Although high-order AR models (e.g., AR(20)) can provide better modeling approximation than low-order AR models (see Figure 1.11), the amount of BER improvement in that case is small compared with the resulting computational cost $O(p^3)$ of the estimation algorithm. Therefore, to reduce the computational cost, an AR(5) is recommended.

In Figure 3.19, for very low Doppler rates (e.g., $f_d T_b = 0.001$), comparable BER performances can be noticed for the various estimators. However, for high Doppler rates $f_d T_b > 0.01$, the proposed estimator performs much better than the others especially for high-order AR models. Therefore, the proposed estimator is appealing for high Doppler rate environments.

According to Figure 3.20, the two-cross-coupled H_∞ filter based estimator provides approximately the same BER results as the Kalman based one. Nevertheless, the H_∞ filtering has the advantage of relaxing the restrictive Gaussian assumptions imposed by

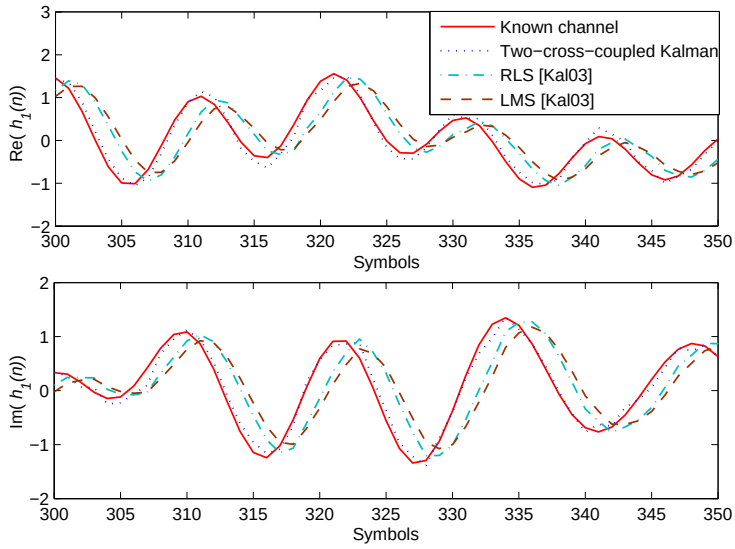

Figure 3.17: Estimation of the real and imaginary parts of the fading process $h_1(n)$ over the first carrier. $f_d T_b = 0.1$, SNR=20dB.

Kalman filtering. In addition, a significant frequency diversity gain is obtained when increasing the number of carriers from $M = 1$ to $M = 3$. In Figure 3.21, the proposed two-cross-coupled H_∞ filter based estimator outperforms the two-serially-connected H_∞ filter based one. This is due to the fact that the later approach results in biased AR parameter estimates which has a bad influence on the estimation of the fading process.

The BER performance of the MC-DS-CDMA system when considering the combination of the EIV based approach with Kalman filtering is illustrated in Figure 3.22 and Figure 3.23. Thus, according to Figure 3.22, this combination outperforms the LMS and RLS estimators, especially for high-order AR models and high Doppler rates. In addition, increasing the AR model order beyond 5 will not improve much the BER performance. Thus, an AR(5) process can provide a trade-off between the accuracy of the model, the computational cost of the estimation algorithm and the subsequent BER. According to Figure 3.23, the EIV approach combined with a Kalman filter yields slightly lower BER than the two-cross-coupled Kalman filter estimator. In addition, the former approach can provide an estimation of the additive noise variance which is not the case for the later approach. Besides, the combination of the EIV approach with either Kalman or H_∞ filtering yield approximately the same BER results.

According to the various simulations we have carried out, the EIV approach combined with either Kalman or H_∞ filtering is more recommended than the other channel estimation techniques.

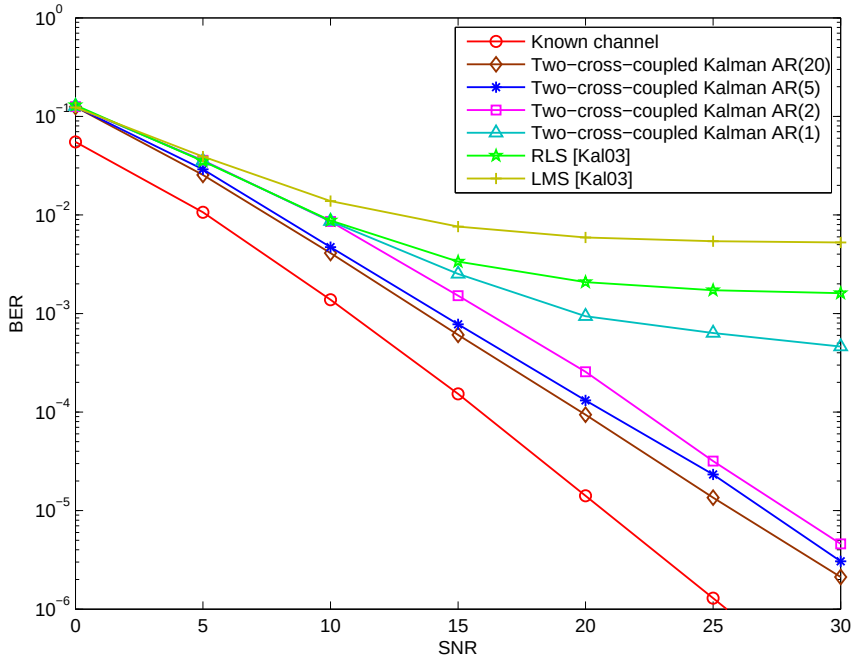

Figure 3.18: BER versus SNR for the MC-DS-CDMA system with the various channel estimators. $f_dT_b = 0.05$ and $M = 2$.

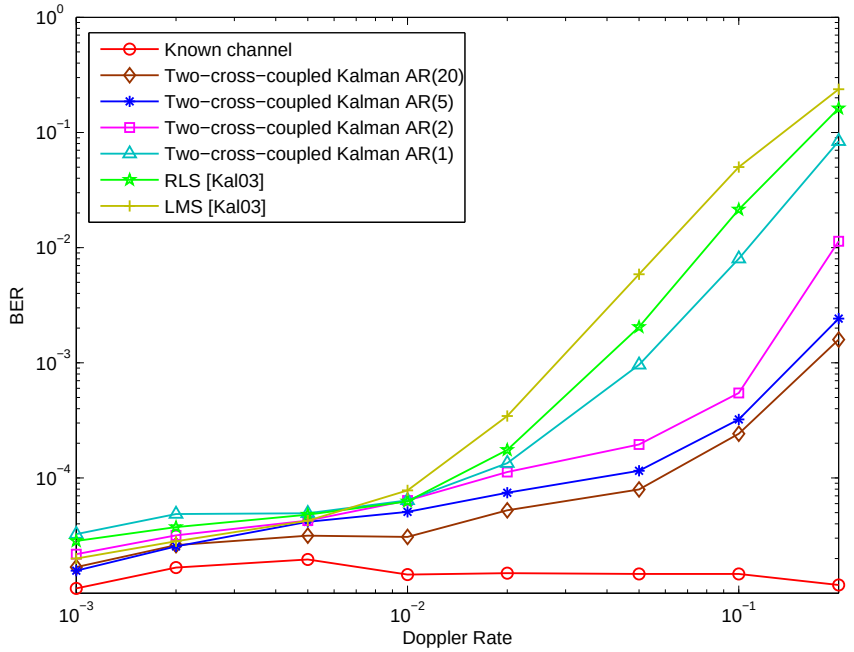

Figure 3.19: BER versus Doppler rate f_dT_b for the MC-DS-CDMA system with the various channel estimators. SNR=20dB and $M = 2$.

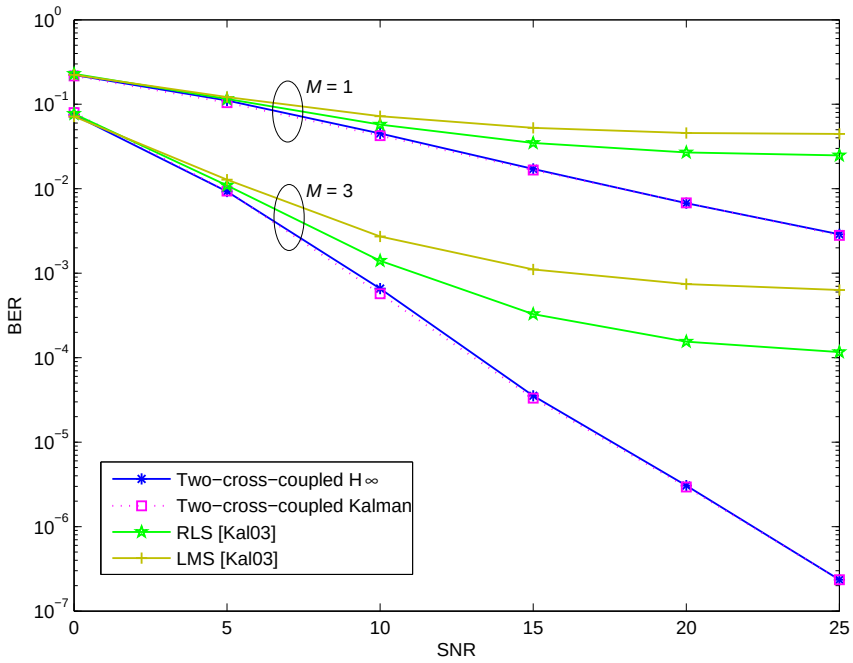

Figure 3.20: BER performance of the two-cross-coupled Kalman and H_∞ channel estimators with AR(5) model. Number of carriers considered are $M = 1$ and $M = 3$. $f_d T_b = 0.05$.

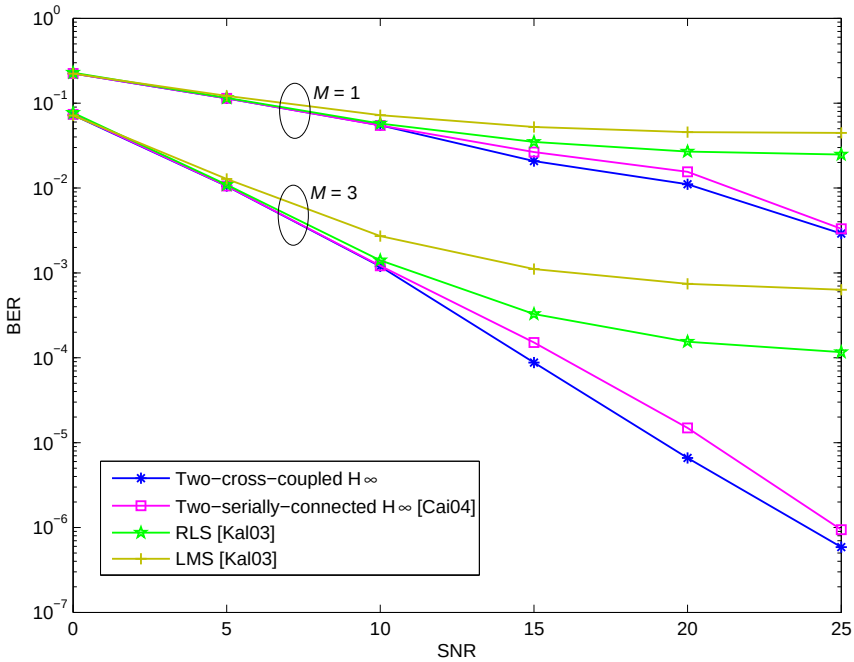

Figure 3.21: BER performance of the two-cross-coupled and the two-serially-connected H_∞ filter based channel estimators with AR(2) model. Number of carriers considered are $M = 1$ and $M = 3$. $f_d T_b = 0.05$.

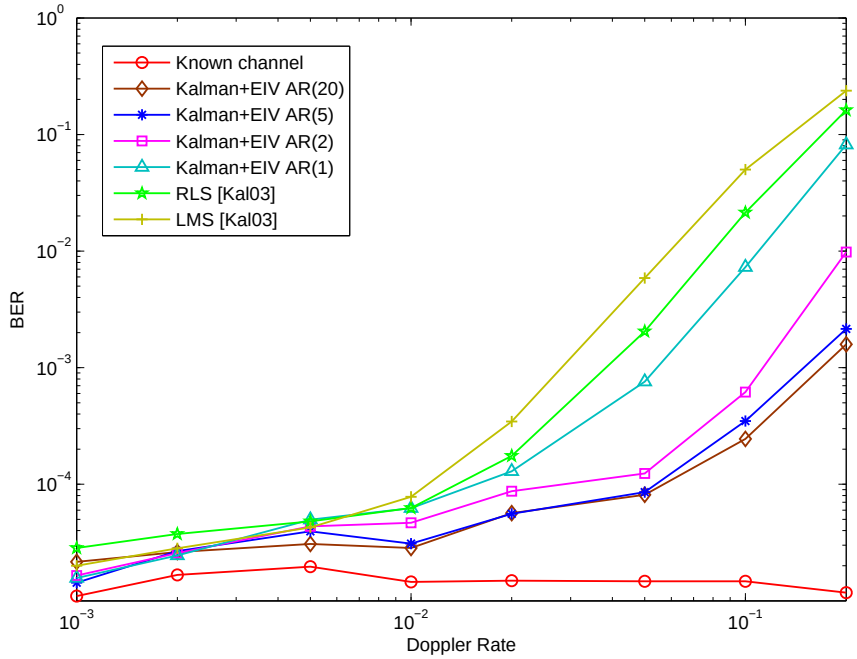

Figure 3.22: BER performance versus Doppler rate of the Kalman filter + EIV channel estimator with various order AR models. SNR=20dB and $M = 2$.

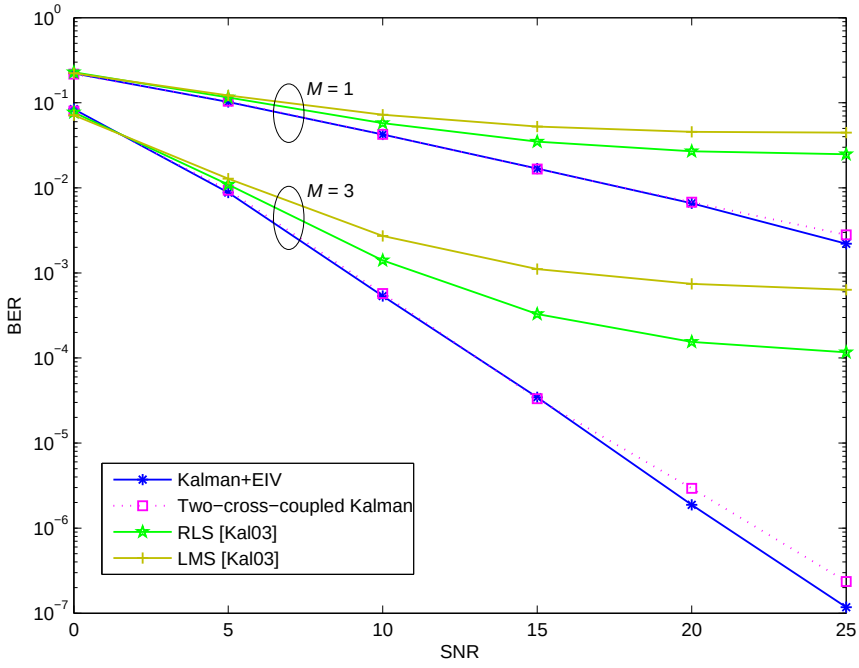

Figure 3.23: BER performance of the Kalman filter + EIV channel estimator and the two-cross-coupled Kalman filter based one with AR(5) model. Number of carriers considered are $M = 1$ and $M = 3$. $f_d T_b = 0.05$.

Conclusions and Perspectives

In this thesis, we have proposed five receiver structures for MC-DS-CDMA systems in Rayleigh fading channels [Jam04] [Jam05a] [Jam05b]. In addition, as receiver design usually requires the explicit estimation of the channel fading processes, we have proposed new training-aided channel estimation techniques based on *a priori* AR modeling of fading channels [Jam05c] [Jam07b] [Jam06] [Jam07a].

In the first chapter, we have motivated the selection of MC-DS-CDMA system and pointed out its relevance for the future 4G mobile wireless systems, where one of the major challenges is to provide high data rates to high speed mobile terminals. High mobility results in Doppler shifts and time-varying fading over each carrier. The time-variation of fading processes are approximated by AR models. As low-order AR models result in poor approximation, we have studied the relevance of high-order AR models. In that case, due to the band-limited nature of Doppler fading processes, a deterministic model should be considered. To avoid this problem, we follow Baddour's work [Bad05], initially developed in the framework of channel simulation, where they have "slightly" modified the properties of the channel by considering the sum of the theoretical fading process and a zero-mean white process whose variance is very small. This enables us to consider AR models whose order is high enough to better approximate the channel.

When considering the conventional MC-DS-CDMA receiver [Kon96], the fading processes are assumed to be available at the receiver. In addition, the BER performance of this receiver is shown to be limited by the MAI and the near-far problem. To avoid these drawbacks, we have proposed five receivers in chapter 2. Thus, to reduce the computational cost of the MMSE receiver [Mil00b], two adaptive MMSE receiver structures based on the APA are first introduced [Jam04]. The SD structure consists of a particular adaptive filter for each carrier, whereas the JD structure is defined by the concatenation of the adaptive filter weights dedicated to each carrier. Simulation results show that the JD structure outperforms the SD one. Moreover, the two structures have the same order of complexity when considering the APA, but this is not the case for the RLS filter where

the JD structure has higher complexity than the SD one. Hence, APA in the JD structure corresponds to a trade-off between performance and complexity.

To avoid the use of a training sequence for every active user, we have then proposed two blind adaptive MOE receivers based on APA-like multiuser detector [Jam05a], where only the spreading code and the timing of the desired user are required. The post-detection combining based receiver consists of a blind adaptive detector along each carrier followed by a post-detection combiner, whereas the pre-detection combining based receiver consists of a MRC followed by a single blind adaptive detector. According to the simulation study we have carried out, the pre-detection combining based receiver provides slightly lower BER results than the post-detection combining based one. In addition, the comparative simulation study we have carried out with existing blind LMS and Kalman filter based detectors [Hon95] [Zha02] shows that the proposed APA-like detector in the pre-detection combining based receiver can provide a trade-off between performance and complexity. Moreover, the proposed blind APA-like detector is shown to outperform the training based APA in high MAI environments, in terms of SINR improvement and BER.

When the spreading sequences of all active users are assumed to be available, we have proposed a receiver structure which consists of a decorrelating detector, a Kalman channel estimator and a MRC [Jam05b]. Simulation results show that the proposed receiver can completely eliminate the MAI and is insensitive to the near-far problem. In addition, it provides approximatly the same BER performance as the adaptive receivers without the need of any training period.

In chapter 3, we have proposed several channel estimation schemes based on *a priori* AR modeling for time-varying fading channels. The first scheme makes it possible to jointly estimate the fading process and its AR parameters based on two-cross-coupled Kalman filters [Jam05c]. One Kalman filter is used to estimate the fading process while the second one makes it possible to estimate the corresponding AR parameters from the estimated fading process. The two Kalman filters are all the more mutually interactive as the variance of the innovation of the first filter is used to drive the gain of the second. Simulation results show that the proposed approach can provide reliable estimates of the AR parameters, especially when the Doppler rate is high $f_d T_b \geq 0.1$.

Nevertheless, Kalman filtering is optimal in the MMSE sense providing the initial state, the driving process and the measurement noise in the state-space representation of the system are independent, white and Gaussian. However, these assumptions do not always hold in practice. For this reason, we have proposed to investigate an alternative approach based on H_∞ estimation techniques, where no statistical assumption are required.

The estimation criterion is to minimize the worst possible effects of the noise disturbances on the estimation error. More particularly, the method we have proposed is based on two-cross-coupled H_∞ filters which allow the fading process and its AR parameters to be jointly estimated [Jam07b]. Simulation results show that the proposed two-cross-coupled Kalman and H_∞ filter based approaches provide approximately the same results. In addition, these approaches outperform the approaches based on two-serially-connected Kalman or H_∞ filters proposed in [Cai04] which result in biased estimates of the AR parameters.

As an alternative to the two-cross-coupled Kalman or H_∞ filter based estimators, we have proposed to view the channel AR parameter estimation as an EIV issue [Jam06] [Jam07a]. The proposed approach consists in estimating the null space of specific autocorrelation matrices and has the advantage of providing the estimation of the channel AR parameters and variances of both the additive noise and driving process in the state-space representation of the fading channel system. The proposed EIV based approach is combined with either Kalman or H_∞ filters to estimate the channel fading process. The comparative simulation study we have carried out on AR parameter estimation shows that the proposed EIV based approach outperforms the other approaches ([Tsa96], [Cai04], [Jam05c], [Jam07b]), especially in the presence of high amount of noise (e.g., SNR=5 dB). In addition, unlike the other approaches, it has also the advantage of providing an estimation of the measurement noise variance.

Furthermore, for all the channel estimation techniques we have proposed, increasing the AR model order allows a better fit between the PSD of the resulting process and the PSD of the Jakes model. However, when the model order is getting higher (for instance $p = 20$), the accurate estimation of all the AR parameters becomes difficult even at high SNR and with a high number of observation samples. This is due to the U-shaped low-pass band-limited nature of the channel spectrum or equivalently, to the positions of the corresponding AR poles which are close to the unit circle in the z-plane. Therefore, in these cases, the selection of the AR model order corresponds to a trade-off between the accuracy of the model and the difficulty in estimating its parameters.

The comparative simulation study we have carried out on the estimation of MC-DS-CDMA fading channels shows that the proposed channel estimators provide much lower BER than the LMS and RLS based ones, especially in high Doppler rate environments. In addition, the two-cross-coupled Kalman and H_∞ filter based channel estimators yields approximately the same BER results. Furthermore, the EIV approach combined with Kalman or H_∞ filters provide slightly better BER results than the two-cross-coupled

Kalman or H_∞ filter based estimators. Moreover, an AR(5) model corresponds to a trade-off between the BER performance and the computational cost of the estimation algorithm.

It should be noted that some assumptions have been made in this thesis. To avoid them, the following suggestions for future work can be pointed out:

- Firstly, we have assumed that the fading processes over all carriers are uncorrelated and, hence, they are estimated separately. However, correlation among multi-carrier fading processes might arise due to the existence of a significant Doppler spread for instance. To exploit these correlations, the joint estimation of the fading processes can be addressed based on a vector (multi-channel) AR model. Therefore, the extension of the proposed channel estimation techniques to account for a vector AR model is a possible direction for future work.

- Secondly, the separate estimation of the transmitted data symbol and the fading channel is studied based on a decision directed approach where we have assumed that the decisions of previous data symbols are all correct. Nevertheless, this approach might result in bursts of opposite decisions in the cases of deep fades. To avoid this problem, the joint estimation of the transmitted symbol and the fading channel can be addressed based on a nonlinear filtering approach such as particle filtering. In particular, the relevance of the so-called Rao-Blackwellized particle filtering techniques can be investigated. Indeed, cross-coupling these techniques with Kalman filtering to jointly estimate the transmitted symbols and both the channel and its AR parameters is currently under investigation by one of the PhD students in our group.

- Finally, when designing receivers, we have assumed that they are synchronized with the desired user and/or all users. One might relax this assumption by developing estimation techniques to estimate the delays of all user signals.

In addition, the relevance of the channel estimation techniques we have proposed in chapter 3 can be investigated for other systems than MC-DS-CDMA. Indeed, the estimation of OFDM fading channels is currently under investigation by one of the master students at Al-Quds University who is actually under the joint supervision of myself and Dr. H. Abdel Nour.

Acronyms and Abbreviations

1G	First Generation Mobile Wireless Systems
2G	Second Generation Mobile Wireless Systems
3G	Third Generation Mobile Wireless Systems
4G	Fourth Generation Mobile Wireless Systems
ACF	AutoCorrelation Function
APA	Affine Projection Algorithm
AR	AutoRegressive
ARMA	AutoRegressive Moving Average
AWGN	Additive White Gaussian Noise
B3G	Beyond 3G
BER	Bit Error Rate
BPSK	Binary Phase Shift Keying
CDMA	Code Division Multiple Access
DS	Direct-Sequence
DS-CDMA	Direct-Sequence Code Division Multiple Access
EDGE	Enhanced Data rates for GSM Evolution
EIV	Errors-In-Variables
EKF	Extended Kalman Filter
EM	Expectation Maximization
FDMA	Time Division Multiple Access
FFT	Fast Fourier Transform
GPRS	General Packet Radio Service
GSM	Global System for Mobile communication
HOYW	High Order Yule-Walker
IFFT	Inverse Fast Fourier Transform
IMT-2000	International Mobile Telecommunications - 2000
IS-95	Interim Standard - 95
ISI	Inter-Symbol Interference
ISR	Interference to Signal Ratio
IV	Instrumental Variables

JD	Joint Detection
LMS	Least Mean Square
LS	Least Square
MAI	Multiple Access Interference
MC	Multi-Carrier
MC-CDMA	Multi-Carrier Code Division Multiple Access
MC-DS-CDMA	Multi-Carrier Direct-Sequence Code Division Multiple Access
ML	Maximum Likelihood
MMSE	Minimum Mean Square Error
MOE	Mean Output Energy
MRC	Maximal Ratio Combining
MSE	Mean Square Error
MT-CDMA	Multi-Tone Code Division Multiple Access
MYW	Modified Yule-Walker
NCYW	Noise Compensated Yule-Walker
NLMS	Normalized Least Mean Square
OFDM	Orthogonal Frequency Division Multiplexing
PIC	Parallel Interference Cancellation
PSD	Power Spectral Density
RLS	Recursive Least Square
SD	Separate Detection
SINR	Signal to Interference-plus-Noise Ratio
SNR	Signal to Noise Ratio
SR	Shift Relation
TDMA	Time Division Multiple Access
TF	Time-Frequency
UMTS	Universal Mobile Telecommunications System
WCDMA	Wide-band CDMA
WLAN	Wireless Local Area Network
YW	Yule-Walker

Notations

$E[\cdot]$	expectation operator
diag$[\cdot]$	diagonal matrix
det$[\cdot]$	determinant
sgn$(\cdot)$	signum function
Re$(\cdot)$	real part
Im$(\cdot)$	imaginary part
exp$(\cdot)$	exponential function
ln$(\cdot)$	natural logarithm
$\log_{10}(\cdot)$	logarithm of base 10
$J_0(\cdot)$	zero-order Bessel function of the first kind
$\delta(\cdot)$	dirac delta function
$\|\cdot\|$	Euclidean norm
$\lvert\cdot\rvert$	absolute value
$O(\cdot)$	order of multiplication complexity
min$(\cdot)$	minimum
sup	supremum
$(\cdot)^*$	complex conjugate
$(\cdot)^T$	transpose
$(\cdot)^H$	hermitian (complex conjugate transpose)
$(\cdot)^{-1}$	inverse
$\lfloor x \rfloor$	largest integer smaller or equal to x
∇	gradient
j	$\sqrt{-1}$
$\hat{x}$	estimate of x
σ_x^2	variance of x
$\mathbf{x}$	vector $\mathbf{x}$
$\mathbf{X}$	matrix $\mathbf{X}$
$\mathbf{0}_p$	zero vector of size $p \times 1$
$\mathbf{I}_p$	identity matrix of size $p \times p$
$r_m(t)$	received signal at the m^{th} carrier

$\mathbf{x}_m(n)$	received vector at the m^{th} carrier in the n^{th} bit interval
$\underline{\mathbf{x}}_m(n)$	received vector after channel compensation
$\boldsymbol{\eta}_m(n)$	AWGN vector at the m^{th} carrier in the n^{th} bit interval
$h_m(n)$	complex fading process at the m^{th} carrier in the n^{th} bit interval
$h_m^{(r)}(n)$	real part of the fading process
$h_m^{(i)}(n)$	imaginary part of the fading process
g_{ml}	random amplitude associated with the l^{th} scatterer and the m^{th} carrier
φ_{ml}	random angle of arrival associated with the l^{th} scatterer and the m^{th} carrier
φ_{ml}	random initial phase associated with the l^{th} scatterer and the m^{th} carrier
$\mathbf{q}_m$	the m^{th} Walsh-Hadamard codeword
$d_k(n)$	the n^{th} data bit of the k^{th} user
$\mathbf{c}_k$	spreading code of the k^{th} user
$\mathbf{f}_k$	left cyclic shift of the k^{th} user spreading code $\mathbf{c}_k$
$\mathbf{g}_k$	right cyclic shift of the k^{th} user spreading code $\mathbf{c}_k$
$\mathbf{R}$	cross-correlation matrix of the spreading codes $\{\mathbf{c}_k\}_{k=1,\cdots,K}$
$[\mathbf{R}]_{ij}$	the $(i,j)^{th}$ element of the matrix $\mathbf{R}$
P_k	power of the k^{th} user signal
τ_k	time delay of the k^{th} user signal
$\mathbf{w}(n)$	adaptive filter weights at time n
$\mathbf{a}(n)$	adaptive part of the blind multiuser detector at time n
μ	step-size in the LMS algorithm
μ_{N}	normalized step-size in the NLMS and APA
λ	forgetting factor in the RLS algorithm
δ	regularization constant in the NLMS and APA
ϵ	very small positive constant
ς	positive constant (large value: lack of knowledge, small value: confidence)
γ	disturbance attenuation level in the H_∞ algorithm
L	block length in the APA
M	number of carriers in a MC-DS-CDMA system
K	number of active users in a MC-DS-CDMA system
N_s	number of available data samples

T_b	bit duration
T_c	chip duration of wide-band single-carrier DS-CDMA system
MT_c	chip duration of MC-DS-CDMA system
N	processing gain (code length) for each carrier in a MC-DS-CDMA system
N_0	processing gain (code length) of wide-band single-carrier DS-CDMA system
W	signal bandwidth
W_M	bandwidth of each carrier signal in MC-DS-CDMA system
W_0	bandwidth of wide-band single-carrier DS-CDMA system
L_p	number of resolvable paths in multi-path fading channel
L_s	number of scatterers in frequency-flat fading channel
B_c	channel coherence bandwidth
T_0	channel coherence time
T_m	channel maximum delay spread
f_d	maximum Doppler frequency
f_c	central carrier frequency
f_m	m^{th} carrier frequency
f_dT_b	Doppler rate
υ	mobile speed
c	light speed
$r(n)$	received noisy signal from time-varying frequency-flat fading channel
$y(n)$	received noisy observations after removing the training symbols
p	AR model order
$\{a_i\}_{i=1,\cdots,p}$	AR model parameters
$\boldsymbol{\theta}$	AR parameter vector
$\underline{\boldsymbol{\theta}}_{p+1}$	AR parameter vector of size $(p+1)\times 1$
$\boldsymbol{\Phi}$	Companion matrix containing the AR parameters
$\hat{\mathbf{h}}(n/n-1)$	*a priori* estimate of $\mathbf{h}(n)$ given $n-1$ observations
$\hat{\mathbf{h}}(n/n)$	*a posteriori* estimate of $\mathbf{h}(n)$ given n observations
$\mathbf{K}(n)$	Kalman filter gain at time n
$\mathbf{P}(n/n-1)$	*a priori* covariance matrix of the state vector error
$\mathbf{P}(n/n)$	*a posteriori* covariance matrix of the state vector error

$\underline{\mathbf{K}}(n)$	H_∞ filter gain at time n
$\underline{\mathbf{P}}(n)$	positive definite matrix in the H_∞ filter
$\nu(n)$	innovation process
$\sigma_b^2 = \sigma_v^2$	measurement noise variance
σ_u^2	driving process variance
σ_h^2	fading process variance
R_v	power of the measurement noise
Q_u	power of the driving process
$R_{hh}(n)$	ACF of the channel
$\Psi(f)$	PSD of the channel
$\Psi_{AR}(f)$	PSD of the AR process
$\mathbf{R}_{hh}$	channel autocorrelation matrix
$\mathbf{R}_{yy}^{p+1}$	observation autocorrelation matrix of size $(p+1) \times (p+1)$
$\bar{\mathbf{R}}_{hh}^{p+1}$	positive semidefinite correlation matrix of size $(p+1) \times (p+1)$

Bibliography

[AM97] K. Abed-Meraim, W. Qiu, Y. Hua. – Blind system identification. *Proceedings of the IEEE*, vol. 85, August 1997, pp. 1310–1322.

[And79] B. D. O. Anderson, J. B. Moore. – *Optimal Filtering*, Prentice Hall, Englewood Cliffs, NJ, 1979.

[Bad05] K. E. Baddour, N. C. Beaulieu. – Autoregressive modeling for fading channel simulation. *IEEE Trans. on Wireless Communications*, vol. 4, July 2005, pp. 1650–1662.

[Bai96] P. W. Baier. – A critical review of CDMA. *Proceedings of IEEE-VTC*, pp. 6–10, Atlanta, USA, April 1996.

[Beg90] S. Beghelli, R. Guidorzi, U. Soverini. – The Frisch scheme in dynamic system identification. *Automatica*, vol. 26, 1990, pp. 171–176.

[Bel63] P. A. Bello. – Characterization of randomly time-variant linear channels. *IEEE Trans. on Communications*, vol. 13, December 1963, pp. 360–393.

[Bin90] J. Bingham. – Multicarrier modulation for data transmission: an idea whose time has come. *IEEE Communication Magazine*, vol. 28, May 1990, pp. 5–14.

[Bob05] W. Bobillet, E. Grivel, R. Guidorzi, M. Najim. – Noisy speech dereverberation as a SIMO system identification issue. *Proceedings of IEEE-SSP*, Bordeaux, France, 17–20, 2005.

[Bob06] W. Bobillet, E. Grivel, M. Najim, R. Diversi, R. Guidorzi, U. Soverini. – Errors-in-variables based identification of autoregressive parameters for speech enhancement using one microphone. *Proceedings of ISCCSP*, Marrakech, Morocco, March 13–15, 2006.

[Bob07] W. Bobillet, R. Diversi, E. Grivel, R. Guidorzi, M. Najim, U. Soverini. – Speech enhancement combining optimal smoothing and errors-in-variables identification of noisy AR processes. *Accepted to IEEE Trans. on Signal Processing*, 2007.

[Cai02] G. Caire, P. A. Humblet, G. Montalbano, A. Nordio. – Initial synchronization of DS-CDMA via bursty pilot signals. *IEEE Trans. on Communications*, vol. 50, April 2002, pp. 677–685.

[Cai04] J. Cai, X. Shen, J. W. Mark. – Robust channel estimation for OFDM wireless communication systems - an H_∞ approach. *IEEE Trans. on Wireless Communications*, vol. 3, November 2004, pp. 2060–2071.

[CDM01] CDMA2000. – *Physical Layer Standard for CDMA2000 Spread Spectrum Systems*, 2001.

[Che92] J. H. Chen, R. V. Cox, Y. C. Lin, N. Jayant, M. J. Melchner. – A low-delay CELP coder for the CCITT 16 kb/s speech coding standard. *IEEE Journal on Selected Areas in Communications*, vol. 10, June 1992, pp. 830–849.

[Che01] L. Chen, B. Chen, W. Hou. – Adaptive multiuser DFE with Kalman channel estimation for DS-CDMA systems in multipath fading channels. *Signal Processing*, vol. 81, April 2001, pp. 713–733.

[Cho93] A. Chouly, A. Brajal, S. Jourdan. – Orthogonal multicarrier techniques applied to direct sequence spread spectrum CDMA systems. *Proceedings of IEEE-GLOBECOM*, pp. 1723–1728, Houston, USA, November 1993.

[Cla68] R. H. Clarke. – A statistical theory of mobile-radio reception. *Bell Syst. Tech. J.*, July 1968, pp. 957–1000.

[Das93] V. M. Dasilva, E. S. Sousa. – Performance of orthogonal CDMA codes for quasi-synchrounous communication systems. *Proceedings of IEEE-ICUPC*, pp. 995–999, Ottawa, Canada, October 1993.

[Das94] V. M. Dasilva, E. S. Sousa. – Multicarrier orthogonal CDMA signals for quasi-synchrounous communication systems. *IEEE Journal on Selected Areas in Communications*, vol. 12, June 1994, pp. 842–852.

[Dav98a] C. E. Davila. – A subspace approach to estimation of autoregressive parameters from noisy measurements. *IEEE Trans. on Signal Processing*, vol. 46, February 1998, pp. 531–534.

[Dav98b] L. Davis, I. Collings, R. Evans. – Coupled estimators for equalization of fast-fading mobile channels. *IEEE Trans. on Communications*, vol. 46, October 1998, pp. 1262–1265.

[Dem77] A. P. Dempster, N. M. Laird, D. B. Rubin. – Maximum likelihood from incomplete data via the EM algorithm. *Journal of the Royal Statistical Society*, vol. 39, 1977, pp. 1–38.

[Den93] P. Dent, G. Bottomley, T. Croft. – Jakes fading model revisited. *IEE Electronics Letters*, vol. 29, June 1993, pp. 1162–1163.

[Der94] M. Deriche. – AR parameter estimation from noisy data using the EM algorithm. *Proceedings of IEEE-ICASSP*, pp. 69–72, Adelaide, Australia, 19–22, 1994.

[Din98] E. H. Dinan, B. Jabbari. – Spreading codes for direct sequence CDMA and wideband CDMA cellular networks. *IEEE Communication Magazine*, vol. 36, September 1998, pp. 48–54.

[Div05a] R. Diversi, R. Guidorzi, U. Soverini. – A noise-compensated estimation scheme for AR processes. *Proceedings of IEEE-CDC*, Seville, Spain, December 12–15, 2005.

[Div05b] R. Diversi, U. Soverini, R. Guidorzi. – A new estimation approach for AR models in presence of noise. *Proceedings of the 16th IFAC World Congress*, Prague, Czech Republic, July 3–8, 2005.

[Dob98] G. Doblinger. – Smoothing of noisy AR signals using an adaptive Kalman filter. *Proceedings of EURASIP-EUSIPCO*, pp. 781–784, Rhodes, Greece, September 8–11, 1998.

[Erd00] A. T. Erdogan, B. Hassibi, T. Kailath. – On linear H_∞ equalization of communication channels. *IEEE Trans. on Signal Processing*, vol. 48, November 2000, pp. 3227–3231.

[Ewe94] E. Eweda. – Comparisons of RLS, LMS, and sign algorithms for tracking randomly time-varying channels. *IEEE Trans. on Signal Processing*, vol. 42, November 1994, pp. 2937–2944.

[Faz93a] K. Fazel. – Performance of CDMA/OFDM for mobile communication systems. *Proceedings of IEEE-ICUPC*, pp. 975–979, Ottawa, Canada, October 12–15, 1993.

[Faz93b] K. Fazel, L. Papke. – On the performance of convolutionally-coded CDMA/OFDM for mobile communication systems. *Proceedings of IEEE-PIMRC*, pp. 468–472, Yokohama, Japan, October 1993.

[Faz03] K. Fazel, S. Kaiser. – *Multi-Carrier and Spread Spectrum Systems*, Wiley, 2003.

[Gan98] S. Gannot, D. Burshtein, E. Weinstein. – Iterative and sequential Kalman filter-based speech enhancement algorithms. *IEEE Trans. on Speech and Audio Processing*, vol. 6, July 1998, pp. 373–385.

[Gan03] S. Gannot, M. Moonen. – On the application of the unscented Kalman filter to speech processing. *Proceedings of the International Workshop on Acoustic Echo and Noise Control (IWAENC)*, Kyoto, Japan, September 8–11, 2003.

[Gay95] S. L. Gay, S. Tavathia. – The fast affine projection algorithm. *Proceedings of IEEE-ICASSP*, Michigan, USA, May 9–12, 1995.

[Ger99] J. C. Geromel. – Optimal linear filtering under parameter uncertainty. *IEEE Trans. on Signal Processing*, vol. 47, January 1999, pp. 168–175.

[Gia98] G. B. Giannakis, C. Tepedelenlioglu. – Basis expansion models and diversity techniques for blind identification and equalization of time-varying channels. *Proceedings of the IEEE*, vol. 86, October 1998, pp. 1969–1986.

[Gri90] M. J. Grimble, A. E. Sayed. – Solution of the H_∞ optimal linear filtering problem for discrete-time systems. *IEEE Trans. on Acoustics, Speech, and Signal Processing*, vol. 38, July 1990, pp. 1092–1104.

[Gri02] E. Grivel, M. Gabrea, M. Najim. – Speech enhancement as a realization issue. *Signal Processing*, vol. 82, December 2002, pp. 1963–1978.

[Gro06] J. Grolleau, E. Grivel, M. Najim. – Relevance of the asymptotic reduced-rank MMSE detector in MC-DS-CDMA system. *Proceedings of ISCCSP*, Marrakech, Morocco, March 13–15, 2006.

[Gui95] R. Guidorzi, M. Pierantoni. – A new parametrization of Frisch scheme solutions. *Proceedings of the XII International Conference on Systems Science*, Wroclaw, Poland, September 1995.

[Han98] L. Hanzo. – Bandwidth-efficient wireless multimedia communications. *Proceedings of the IEEE*, vol. 86, July 1998, pp. 1342–382.

[Han03] L. Hanzo, L. Yang, E. Kuan, K. Yen. – *Single and Multi-carrier* DS-CDMA*, Multiuser Detection, Space-Time Spreading, Synchronization and Standard*, IEEE Press-Wiley, England, 2003.

[Har97] S. Hara, R. Prasad. – Overview of multicarrier CDMA. *IEEE Communication Magazine*, vol. 35, December 1997, pp. 126–133.

[Has99] B. Hassibi, A. H. Sayed, T. Kailath. – *Indefinite Quadratic Estimation and Control: A Unified Approach to an H_2 and H_∞ Theories*, SIAM, Philadelphia, PA, 1999.

[Has06] W. Hassasneh, A. Jamoos, E. Grivel, H. Abdel Nour. – Estimation of MC-DS-CDMA fading channels based on Kalman filtering with high order autoregressive models. *Proceedings of IEEE-MCWC*, Amman, Jordan, September 17–20, 2006.

[Hay02] S. Haykin. – *Adaptive Filter Theory*, Prentice Hall, 2002.

[Hay03] S. Haykin, B. Widrow. – *Least-Mean-Square Adaptive Filters*, Wiley, 2003.

[Hon95] M. Honig, U. Madhow, S. Verdú. – Blind adaptive multiuser detection. *IEEE Trans. on Information Theory*, vol. 41, July 1995, pp. 944–960.

[Hon00] M. Honig, M. K. Tsatsanis. – Adaptive techniques for multiuser CDMA receivers. *IEEE Signal Processing Magazine*, vol. 17, May 2000, pp. 49–61.

[Huf02] S. Van Huffel, P. Lemmerling. – *Total Least Squares and Errors-In-Variables Modeling*, Kluwer Academic Publisher, Dordrecht, Netherlands, 2002.

[IS-95] IS-95. – *Mobile station - base station compatibility standard for dual mode wideband spread spectrum cellular system*, 1995.

[Jak74] W. C. Jakes. – *Microwave Mobile Communications*, Wiley, New York, 1974.

[Jam04] A. Jamoos, E. Grivel, M. Najim. – Designing adaptive filters-based MMSE receivers for asynchronous multicarrier DS-CDMA systems. *Proceedings of IEEE-PIMRC*, pp. 2930–2934, Barcelona, Spain, September 5–8, 2004.

[Jam05a] A. Jamoos, E. Grivel, M. Najim. – Blind adaptive multi-user detection for multi-carrier DS-CDMA systems in frequency selective fading channels. *Proceedings of IEEE-ICASSP*, pp. 925–928, Philadelphia, USA, March 18–23, 2005.

[Jam05b] A. Jamoos, E. Grivel, H. Abdel Nour. – Kalman filtering based channel prediction and decorrelation multiuser detection for MC-DS-CDMA systems. *Proceedings of the 8th COST 276 workshop*, Trondheim, Norway, May 26–28, 2005.

[Jam05c] A. Jamoos, D. Labarre, E. Grivel, M. Najim. – Two cross coupled Kalman filters for joint estimation of MC-DS-CDMA fading channels and their corresponding autoregressive parameters. *Proceedings of EURASIP-EUSIPCO*, Antalya, Turkey, September 4–8, 2005.

[Jam06] A. Jamoos, W. Bobillet, E. Grivel, H. Abdel Nour, M. Najim. – Identification of time-varying frequency-flat Rayleigh fading channels based on errors-in-variables approach. *Proceedings of IEEE-SPAWC*, Cannes, France, July 2–5, 2006.

[Jam07a] A. Jamoos, E. Grivel, W. Bobillet, R. Guidorzi. – Errors-in-variables based approach for the identification of AR time-varying fading channels. *Accepted to IEEE Signal Processing Letters*, April 2007.

[Jam07b] A. Jamoos, J. Grolleau, E. Grivel, H. Abdel Nour, M. Najim. – Kalman vs H_∞ algorithms for MC-DS-CDMA channel estimation with or without a priori AR modeling. *IEEE Multi-Carrier Spread-Spectrum (MC-SS), Herrsching, Germany. Lecture Notes in Electrical Engineering*, Springer Verlag, 2007.

[Jma05] A. Jmalipour, T. Wada, T. Yamazato. – A tutorial on multiple access technologies for beyond 3G mobile networks. *IEEE Communications Magazine*, vol. 43, February 2005, pp. 110–117.

[Kal03] D. N. Kalofonos, M. Stojanovic, J. G. Proakis. – Performance of adaptive MC-CDMA detectors in rapidly fading Rayleigh channels. *IEEE Trans. on Wireless Communications*, vol. 2, March 2003, pp. 229–239.

[Kaw95] T. Kawahara, T. Matsumoto. – Joint decorrelating multiuser detection and channel estimation in asynchronous CDMA mobile communications channels. *IEEE Trans. on Vehicular Technology*, vol. 44, August 1995, pp. 506–515.

[Kay79] S. M. Kay. – The effects of noise on the autoregressive spectral estimator. *IEEE Trans. on Acoustics, Speech, and Signal Processing*, vol. ASSP-27, October 1979, pp. 478–485.

[Kay80] S. M. Kay. – Noise compensation for autoregressive spectral estimates. *IEEE Trans. on Acoustics, Speech, and Signal Processing*, vol. ASSP-28, June 1980, pp. 292–303.

[Kay88] S. M. Kay. – *Modern Spectral Estimation*, Prentice Hall, Englewood Cliffs, NJ, 1988.

[Kom02] C. Komninakis, C. Fragouli, A. H. Sayed, R. D. Wesel. – Multi-input multi-output fading channel tracking and equalization using Kalman estimation. *IEEE Trans. on Signal Processing*, vol. 50, May 2002, pp. 1065–1076.

[Kon93] S. Kondo, L. Milstein. – On the use of multicarrier direct sequence spread spectrum systems. *Proceedings of IEEE-MILCOM*, pp. 52–56, Boston, USA, October 11–14, 1993.

[Kon96] S. Kondo, L. Milstein. – Performance of multicarrier DS-CDMA systems. *IEEE Trans. on Communications*, vol. 44, February 1996, pp. 238–246.

[Lab04] D. Labarre, E. Grivel, M. Najim, E. Todini. – Two-Kalman filters based instrumental variable techniques for speech enhancement. *Proceedings of IEEE-MMSP*, pp. 375–378, Siena, Italy, September 2004.

[Lab05] D. Labarre, E. Grivel, M. Najim, N. Christov. – Relevance of H_∞ filtering for speech enhancement. *Proceedings of IEEE-ICASSP*, pp. 169–172, Philadelphia, USA, March 18–21, 2005.

[Lab06a] D. Labarre. – *Du filtrage de Kalman aux techniques H_∞ et particulaires: Application au traitement du signal de parole et à l'analyse de signaux biomédicaux*,

PHD dissertation under the supervision of M. Najim and E. Grivel, Equipe Signal et Image, UMR 5131 LAPS, Université Bordeaux I, Bordeaux, France, 2006.

[Lab06b] D. Labarre, E. Grivel, Y. Berthoumieu, E. Todini, M. Najim. – Consistent estimation of autoregressive parameters from noisy observations based on two interacting Kalman filters. *Signal Processing*, vol. 86, October 2006, pp. 2863–2876.

[Lab07] D. Labarre, E. Grivel, M. Najim. – Dual H_∞ algorithms for signal processing, application to speech enhancement. *Accepted to IEEE Trans. on Signal Processing*, 2007.

[Las03] S. Lasaulce, P. Loubaton, E. Moulines. – A semi-blind channel estimation technique based on second-order blind method for CDMA systems. *IEEE Trans. on Signal Processing*, vol. 51, July 2003, pp. 1894–1904.

[Lin95] L. Lindbom. – *A Wiener filtering approach to the design of tracking algorithms with applications in mobile radio communications*, PHD dissertation, Department of Technology, Uppsala University, Uppsala, Sweden, 1995.

[Lin02] L. Lindbom, A. Ahlen, M. Sternad, M. Falkenstrom. – Tracking of time-varying mobile radio channels. II: a case study. *IEEE Trans. on Communications*, vol. 50, January 2002, pp. 156–167.

[Liu01] H. Liu, H. Yin. – Receiver design in multicarrier direct-sequence CDMA communications. *IEEE Trans. on Communications*, vol. 49, August 2001, pp. 1479–1487.

[Lok99] T. Lok, T. Wong, J. Lehnert. – Blind adaptive signal reception for MC-CDMA systems in Rayleigh fading channels. *IEEE Trans. on Communications*, vol. 47, March 1999, pp. 464–471.

[Lou00] P. Loubaton, E. Moulines. – On blind multiuser forward link channel estimation by the subspace method: identifiability results. *IEEE Trans. on Signal Processing*, vol. 48, August 2000, pp. 2366–2376.

[Lup89] R. Lupas, S. Verdú. – Linear multiuser detectors for synchronous code-division multiple-access channels. *IEEE Trans. on Information Theory*, vol. 35, January 1989, pp. 123–136.

[Lup90] R. Lupas, S. Verdú. – Near-far resistance of multiuser detectors in asynchronous channels. *IEEE Trans. on Communications*, vol. 38, April 1990, pp. 496–508.

[Mad94] U. Madhow, M. Honig. – MMSE interference suppression for direct-sequence spread-spectrum CDMA. *IEEE Trans. on Communications*, vol. 42, December 1994, pp. 3178–3188.

[Mad98] U. Madhow. – Blind adaptive interference suppression for direct-sequence CDMA. *Proceedings of the IEEE*, vol. 86, October 1998, pp. 2049–2069.

[Mil95] S. Miller. – An adaptive direct-sequence code-division multiple-access receiver for multiuser interference rejection. *IEEE Trans. on Communications*, vol. 43, April 1995, pp. 1556–1565.

[Mil00a] S. Miller, M. Honig, L. Milstein. – Performance analysis of MMSE receivers for DS-CDMA in frequency-selective fading channels. *IEEE Trans. on Communications*, vol. 48, November 2000, pp. 1919–1929.

[Mil00b] S. Miller, B. Rainbolt. – MMSE detection of multicarrier CDMA. *IEEE Journal on Selected Areas in Communications*, vol. 18, November 2000, pp. 2356–2362.

[Mor96] D. R. Morgan, S. G. Kratzer. – On a class of computationally efficient, rapidly converging, generalized NLMS algorithms. *IEEE Signal Processing Letters*, vol. 3, August 1996, pp. 245–247.

[Mos96] S. Moshavi. – Multi-user detection for DS-CDMA communications. *IEEE Communication Magazine*, vol. 34, October 1996, pp. 124–136.

[Mou95] E. Moulines, P. Duhamel, J. F. Cardoso, S. Mayrargue. – Subspace methods for the blind identification of multichannel FIR filters. *IEEE Trans. on Signal Processing*, vol. 43, February 1995, pp. 516–525.

[Muc04] L. Mucchi, S. Morosi, E. Del Re, R. Fantacci. – A new algorithm for blind adaptive multiuser detection in frequency selective multipath fading channel. *IEEE Trans. on Wireless Communications*, vol. 3, January 2004, pp. 235–247.

[Naj06] M. Najim. – *Modélisation, Estimation et Filtrage Optimal en Traitement du Signal*, Hermes Science Publications, (in French), 2006.

[Nam00] J. Namgoong, T. F. Wong, J. S. Lehnert. – Subspace multiuser detection for multicarrier DS-CDMA. *IEEE Trans. on Communications*, vol. 48, November 2000, pp. 1897–1908.

[Nog98] J. L. Noge. – *Bayesian state-space modelling of spatio-temporal non-Gaussian radar returns*, PHD dissertation under the supervision of Dr. W. J. Fitzgerald, Department of Engineering, University of Cambridge, 1998.

[Pap02] A. Papoulis, S. U. Pillai. – *Probability, Random Variables and Stochastic Processes*, McGraw-Hill, New York, 2002.

[Poo97] H. V. Poor, X. Wang. – Code-aided interference suppression for DS/CDMA communications-part II: parallel blind adaptive implementations. *IEEE Trans. on Communications*, vol. 45, September 1997, pp. 1112–1122.

[Pop01] M. F. Pop, N. C. Beaulieu. – Limitations of sum-of-sinusoids fading channel simulators. *IEEE Trans. on Communications*, vol. 49, April 2001, pp. 699–708.

[Pro95] J. G. Proakis. – *Digital Communications*, McGraw-Hill, New York, 1995.

[Rap01] T. S. Rappaport. – *Wireless Communications: Principles and Practice*, Prentice Hall, 2001.

[Rhe03] J. Rhee, M. Woo, D. Kim. – Multichannel joint detection of multicarrier 16-QAM DS/CDMA system for high-speed data transmission. *IEEE Trans. on Vehicular Technology*, vol. 52, January 2003, pp. 37–47.

[Ruw06] H. Ruweished, A. Jamoos, H. Abdel Nour. – Variable step-size adaptive filter based MMSE receivers for MC-DS-CDMA mobile systems. *Proceedings of the international Arab Conference on Information Technology (ACIT)*, Yarmouk University, Jordan, December 19–21, 2006.

[Sad06] P. Sadeghi, P. Rapajic, R. Kennedy, T. Abhayapala. – Autoregressive time-varying flat-fading channels: model order and information rate bounds. *Proceedings of IEEE-ISIT*, Washington, USA, July 9–14, 2006.

[Sch01] D. Schafhuber, G. Matz, F. Hlawatsch. – Simulation of wideband mobile radio channels using subsampled ARMA models and multistage interpolation. *Proceedings of IEEE-SSP*, pp. 571–574, Singapore, August 6–8, 2001.

[Sha92] U. Shaked, Y. Theodor. – H_∞ - optimal estimation: a tutorial. *Proceedings of IEEE-CDC*, Tucson, Arizona, 1992.

[She97] X. Shen, L. Deng. – Game theory approach to discrete H_∞ filter design. *IEEE Trans. on Signal Processing*, vol. 45, April 1997, pp. 1092–1095.

[She99] X. Shen, L. Deng. – A Dynamic system approach to speech enhancement using the H_∞ filtering algorithm. *IEEE Trans. on Speech and Audio Processing*, vol. 7, July 1999, pp. 391–399.

[Shi04] H. Shin, A. H. Sayed, W. Song. – Variable step-size NLMS and affine projection algorithms. *IEEE Signal Processing Letters*, vol. 11, February 2004, pp. 132–135.

[Sod02] T. Soderstrom, U. Soverini, K. Mahata. – Perspectives on errors-in-variables estimation for dynamic systems. *Signal Processing*, vol. 82, October 2002, pp. 1139–1154.

[Sou96] E. A. Sourour, M. Nakagawa. – Performance of orthogonal multicarrier CDMA in a multipath fading channel. *IEEE Trans. on Communications*, vol. 44, March 1996, pp. 356–367.

[Sto99] M. Stojanovic, Z. Zvonar. – Performance of multiuser detection with adaptive channel estimation. *IEEE Trans. on Communications*, vol. 47, August 1999, pp. 1129–1132.

[Str96] E. G. Strom, S. Parkvall, S. L. Miller, B. E. Ottersten. – DS-CDMA synchronization in time-varying fading channels. *IEEE Journal on Selected Areas in Communications*, vol. 14, October 1996, pp. 1636–1642.

[Stu01] G. L. Stuber. – *Principles of Mobile Communication*, MA: Kluwer, Norwell, 2001.

[Tac03] K. Tachikawa. – A perspective on the evolution of mobile communications. *IEEE Communication Magazine*, vol. 41, October 2003, pp. 66–73.

[Tep01] C. Tepedelenlioglu, A. Abdi, G. B. Giannakis, M. Kaveh. – Estimation of Doppler spread and signal strength in mobile communications with applications to handoff and adaptive transmission. *Wireless Communications and Mobile Computing*, vol. 1, June 2001, pp. 221–242.

[The92] C. W. Therrien. – *Discrete Random Signals and Statistical Signal Processing*, Prentice Hall, Englewood Cliffs, NJ, 1992.

[Ton04] L. Tong, B. M. Sadler, M. Dong. – Pilot-assisted wireless communications. *IEEE Signal Processing Magazine*, vol. 21, November 2004, pp. 12–25.

[Tre79] J. R. Treichler. – Transient and convergent behavior of the adaptive line enhancer. *IEEE Trans. on Acoustics, Speech, and Signal Processing*, vol. ASSP-27, February 1979, p. 5362.

[Tri03] A. Trivedi, D. Mehra. – Affine projection adaptive algorithm for multiuser MMSE receivers in frequency-selective fading channels for asynchronous W-CDMA systems. *Proceedings of IEEE-WCNC*, Louisiana, USA, March 16–20, 2003.

[Tsa96] M. Tsatsanis, G. B. Giannakis, G. Zhou. – Estimation and equalization of fading channels with random coefficients. *Signal Processing*, vol. 53, September 1996, pp. 211–229.

[Tug00] J. K. Tugnait, Lang Tong, Zhi Ding. – Single-user channel estimation and equalization. *IEEE Signal Processing Magazine*, vol. 17, May 2000, pp. 17–28.

[Van93] L. Vandendorpe. – Multi-tone direct sequence CDMA system in an indoor wireless environment. *Proceedings of IEEE first symposium of communications and vehicular technology in the Benelux*, pp. 4.1–1–4.1–8, Delft, Netherlands, October 1993.

[Ver86] S. Verdú. – Minimum probability of error for asynchronous Gaussian multiple-access channels. *IEEE Trans. on Information Theory*, vol. 32, January 1986, pp. 85–96.

[Ver98] S. Verdú. – *Multiuser Detection*, Cambridge University press, Cambridge, U.K., 1998.

[Vit95] A. I. Viterbi. – *CDMA: Principles of Spread Spectrum Communications*, Addison-Wesley, 1995.

[Wan98] X. Wang, H. V. Poor. – Blind multiuser detection: a subspace approach. *IEEE Trans. on Information Theory*, vol. 44, March 1998, pp. 677–690.

[Wan00] Z. Wang, G. B. Giannakis. – Wireless multicarrier communications: where Fourier meets Shannon. *IEEE Signal Processing Magazine*, vol. 17, May 2000, pp. 29–48.

[Wan04] H. Wang, K. Yen, K. W. Ang, Y. H. Chew. – Performance analysis of an adaptive PIC receiver with diversity combining for multicarrier DS-CDMA system. *Proceedings of IEEE-VTC*, pp. 1371–1375, Milan, Italy, May 17–19, 2004.

[Wen01] J. F. Weng, T. Le-Ngoc. – RAKE receiver using blind adaptive minimum output energy detection for DS/CDMA over multipath fading channels. *IEE Proceedings Communications*, vol. 148, December 2001, pp. 385–392.

[Woo98] G. Woodward, B. Vucetic. – Adaptive detection for DS-CDMA. *Proceedings of the IEEE*, vol. 86, July 1998, pp. 1413–1434.

[Wu97] W. R. Wu, P. C. Chen. – Adaptive AR modeling in white Gaussian noise. *IEEE Trans. on Signal Processing*, vol. 45, May 1997, pp. 1184–1192.

[Wu00] H. Y. Wu, A. Duel-Hallen. – Multiuser detectors with disjoint Kalman channel estimators for synchronous CDMA mobile radio channels. *IEEE Trans. on Communications*, vol. 48, May 2000, pp. 752–756.

[Xu01] W. Xu, L. Milstein. – On the performance of multicarrier RAKE systems. *IEEE Trans. on Communications*, vol. 49, October 2001, pp. 1812–1823.

[Yae92] I. Yaesh, U. Shaked. – Game theory approach to optimal linear state estimation and its relation to the minimum H_∞ - norm estimation. *IEEE Trans. on Automatic Control*, vol. 37, June 1992, pp. 828–831.

[Yan03a] L. Yang, L. Hanzo. – Multicarrier DS-CDMA: a multiple access scheme for ubiquitous broadband wireless communications. *IEEE Communication Magazine*, October 2003, pp. 116–124.

[Yan03b] L. Yang, W. Hua, L. Hanzo. – A multicarrier DS-CDMA system using both time-domain and frequency-domain spreading. *Proceedings of IEEE-VTC*, pp. 2426–2430, Florida, USA, October 6–9, 2003.

[Yan06] L. Yang, W. Hua, L. Hanzo. – Multiuser detection assisted time- and frequency-domain spread multicarrier code-division multiple-access. *IEEE Trans. on Vehicular Technology*, vol. 55, January 2006, pp. 397–404.

[Yee93] N. Yee, J. Linnartz, G. Fettweis. – Multi-carrier CDMA in indoor wireless radio networks. *Proceedings of IEEE-PIMRC*, pp. 109–113, Yokohama, Japan, September 1993.

[Zam81] G. Zames. – Feedback and optimal sensitivity: model reference transformations, multiplicative seminorms, and approximate inverses. *IEEE Trans. on Automatic Control*, vol. 26, April 1981, pp. 301–320.

[Zha00] Y. Zhang, C. Wen, Y. C. Soh. – Unbiased LMS filtering in the presence of white measurement noise with unknown power. *IEEE Trans. on Circuits and Systems-II: Analog and Digital Signal Processing*, vol. 47, September 2000, pp. 968–972.

[Zha02] X. Zhang, W. Wei. – Blind Adaptive multiuser detection based on Kalman filtering. *IEEE Trans. on Signal Processing*, vol. 50, January 2002, pp. 87–95.

[Zhe99] W. X. Zheng. – A least-squares based method for autoregressive signals in presence of noise. *IEEE Trans. on Circuits and Systems-II: Analog and Digital Signal Processing*, vol. 46, January 1999, pp. 81–85.

[Zhe03] Y. R. Zheng, C. Xiao. – Simulation models with correct statistical properties for Rayleigh fading channels. *IEEE Trans. on Communications*, vol. 51, June 2003, pp. 920–928.

[Zhe05] W. X. Zheng. – Fast identification of autoregressive signals from noisy observations. *IEEE Trans. on Circuits and Systems-II: Express Briefs*, vol. 52, January 2005, pp. 43–48.

[Zhu99] W. Zhuang. – Adaptive H_∞ channel equalization for wireless personal communications. *IEEE Trans. on Vehicular Technology*, vol. 48, January 1999, pp. 126–136.

[Zvo94] Z. Zvonar, D. Brady. – Multiuser detection in single-path fading channels. *IEEE Trans. on Communications*, vol. 42, April 1994, pp. 1729–1739.